Technologies and Processes for the Advancement of Materials

Thermal processing

ISSUE FOCUS ///

THERMOCOUPLES / MEDICAL APPLICATIONS

OPTIMAL FABRICATION OF A THIN-FILM THERMOCOUPLE

COMPANY PROFILE ///

Algas-SDI

MAY 2024
thermalprocessing.com

aichelin group

AFC HOLCROFT

industrial furnace solutions

Green Technology

Innovative Universal Batch Quench Austemper [UBQA] Salt Quench Systems

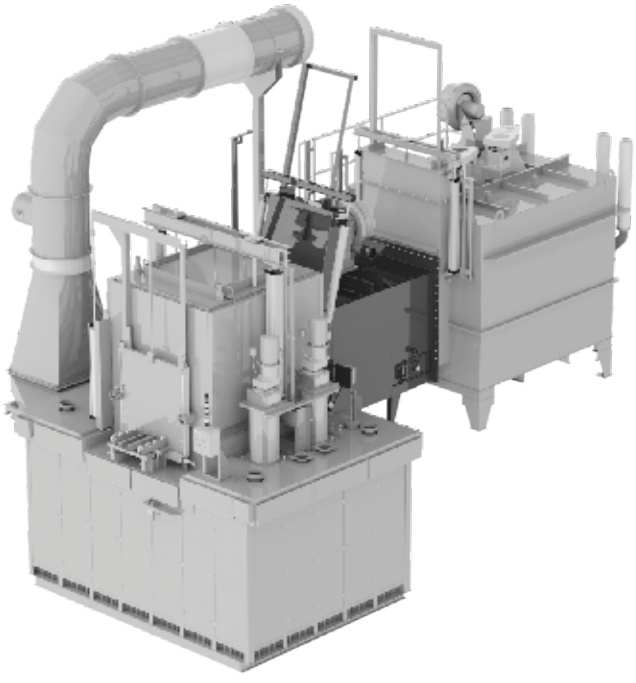

www.afc-holcroft.com

248.624.8191

THERMOCOUPLE TECHNOLOGY

CUSTOM SENSOR MANUFACTURER

Proudly Made in the USA

ACCURACY. RELIABILITY. SOLUTIONS.

PRODUCTS

- THERMOCOUPLES & RTD ASSEMBLIES
- THERMOWELLS
- PROTECTION TUBES
- THERMOCOUPLE WIRE / MULTI CABLE
- THERMOCOUPLES & RTD ACCESSORIES
- ALLOY PIPE & TUBING

SERVICES / CAPABILITIES

- ENGINEERED SOLUTIONS FOR YOUR PROCESS
- ALLOY APPLICATION ENGINEERING
- GTAW CERTIFIED TECHNICIANS
- CALIBRATION & CERTIFICATION

TTEC®

WWW.TTECONLINE.COM • SALES@TTECONLINE.COM
215-529-9394

CONTENTS ///

COVER PHOTO: RdF CORPORATION, SHUTTERSTOCK / ILLUSTRATION BY RICK FRENNEA

SECO/WARWICK

INVENTION MEETS RELIABILITY

THE SECRET TO SLASHING FURNACE ENERGY CONSUMPTION BY UP TO 50%

SECO/WARWICK Aftermarket Services is ready to help you save energy.

Our detailed energy audit identifies energy consumption, inefficiencies, and losses, then retrofits your atmosphere furnace using the latest energy-saving insulation, controls, and waste-heat recuperation.

Don't send money up the chimney, let SECO/WARWICK put it back in your pocket.

For the best process savings for your application, consult our SECO/VISORY team:

info-usa@secowarwick.com / 814-332-8475

www.SecoWarwick.com

DEPARTMENTS ///

MAY 2024 VOLUME 13 / NUMBER 5

UPDATE ///

New Products, Trends, Services & Developments

Q&A ///

JAMES P. ADAMS

EXECUTIVE DIRECTOR/CEO ///
METAL POWDER INDUSTRIES FEDERATION
AND APMI INTERNATIONAL

RESOURCES ///

International Federation for Heat Treatment (IFHTSE)

The international association whose primary interest is heat treatment and surface engineering shares news of its activities to promote collaboration on issues affecting the industry. **18**

Industrial Heating Equipment Association (IHEA)

The national trade association representing the major segments of the industrial heat processing equipment industry shares news of its activities, training, and key developments in the industry. **20**

METAL URGENCY ///

Modeling cyclic loading and the Bauschinger effect to understand plastic deformation in steel. **22**

HOT SEAT ///

Polymer quenchants are useful for reducing distortion and residual stress in quenched aluminum components. **24**

QUALITY COUNTS ///

Successful heat treating requires all hands on deck – and a well-thought-out process that considers the needs of both production and quality. **26**

Thermal Processing is published monthly by Media Solutions, Inc., 266D Yeager Parkway Pelham, AL 35124. Phone (205) 380-1573 Fax (205) 380-1580 International subscription rates: $105.00 per year. Postage Paid at Pelham AL and at additional mailing offices. Printed in the USA. POSTMASTER: Send address changes to *Thermal Processing* magazine, P.O. Box 1210 Pelham AL 35124. Return undeliverable Canadian addresses to P.O. Box 503 RPO West Beaver Creek Richmond Hill, ON L4B4R6.

Powder Met2024 : AMPM 2024

JUNE 16–19 • PITTSBURGH

Americas' Leading Conferences on Powder Metallurgy and Metal Additive Manufacturing are Coming to the Steel City!

- PM, MIM, and Metal AM Tutorials
- Carbide Technical Track
- Daily Light Registration
- Keynote Speaker: Damon West— *"Be the Coffee Bean"*

For details, visit
PowderMet2024.org or AMPM2024.org

Metal Powder Industries Federation
APMI International

FROM THE EDITOR ///

Monitoring precise temps takes precise equipment

Thermocouples may seem like routine pieces of equipment for a heat-treating operation, and it might be easy to dismiss them, but not using the proper thermocouple could mean a huge dent in your company's bottom line.

But just because something isn't flashy, doesn't mean you should take it for granted.

This month's cover story takes a deep dive into the optimal fabrication of a thin-film thermocouple using Alumel/Chromel junctions. This TFTC sensor technique can detect temperatures in a unique environment in many cases, and it has potential for measuring cutting temperature.

For the past few years, *Thermal Processing* has added a medical-applications Focus topic because, like aerospace, heat-treating is also a big part of products that not only keep us alive, but also help make living more comfortable.

To that end, our next story takes a high-tech leap into reducing the time and cost of the heat treatment post of Ti6Al4V, a titanium alloy used in the medical sector.

In addition to those two articles, be sure and check out our company profile on Algas-SDI. In the article, I talked with Ad De Pijper, Algas-SDI's director of the combustion products value stream division. In the profile, he laid out his company's fascinating story of how supply chain issues from the COVID pandemic changed the course of Algas-SDI's product catalog for the betterment of the industry.

But the May issue's thermal-processing coverage is just getting started. Be sure to check out our monthly columnists as they tackle a variety of subjects vital to heat treating.

I hope you enjoy this month's content, and if you'd like to contribute to a future issue, please don't hesitate to contact me. I'm always on the lookout for expert advice that furthers the advancement of the heat-treat industry.

Yes, May is finally here with — hopefully — a relaxing summer close on its heels.

So, grab our latest issue and take it to the deck. It may not keep you cool, but the information inside certainly is.

As always, thanks for reading!

KENNETH CARTER, EDITOR
editor@thermalprocessing.com
(800) 366-2185 x204

CALL FOR ARTICLES Have a technical paper or other work with an educational angle? Let Thermal Processing publish it. Contact the editor, Kenneth Carter, at *editor@thermalprocessing.com* for how you can share your expertise with our readers.

Thermal processing

David C. Cooper
PUBLISHER

EDITORIAL

Kenneth Carter
EDITOR

Jennifer Jacobson
ASSOCIATE EDITOR

Joe Crowe
ASSOCIATE EDITOR | SOCIAL MEDIA

SALES

Dave Gomez
VICE PRESIDENT I SALES & MARKETING

Kendall DeVane
NATIONAL SALES MANAGER

Susan Heinauer
REGIONAL SALES MANAGER

CIRCULATION

Teresa Cooper
MANAGER

Jamie Willett
ASSISTANT

DESIGN

Rick Frennea
CREATIVE DIRECTOR

Michele Hall
GRAPHIC DESIGNER

CONTRIBUTING WRITERS

DONG MIN KIM
JUN YOUNG KIM
DEAN KOUPRIANOFF
HEE JUNG KWAK
D. SCOTT MACKENZIE
JASON MEYER
JIN HO PARK
WILLIE DU PREEZ
DONG YEOL SHIN
TONY TENAGLIER

media solutions

PUBLISHED BY MEDIA SOLUTIONS, INC.
P. O. BOX 1987 • PELHAM, AL 35124
(800) 366-2185 • (205) 380-1580 FAX

David C. Cooper
PRESIDENT

Teresa Cooper
OPERATIONS

CUSTOM DESIGN HEAT RESISTANT CASTINGS AND FABRICATIONS

Wirco has been trusted for over 60 years to develop and manufacture high-temperature heat treatment tooling for numerous industries in the form of both castings and fabrications.

Wirco has capabilities to create any custom designed tooling of any shape and size along with specific fabrication techniques to help meet the needs for your process.

Wirco's serpentine trays are built to stay flat while providing ample strength under heavy loads. Our construction techniques allow for expansion and contraction during the heating and cooling process. Utilizing light weight construction, Wirco's serpentine trays will increase your part allowance by decreasing tooling weight. Wirco can custom design a tray of any size to fit your application.

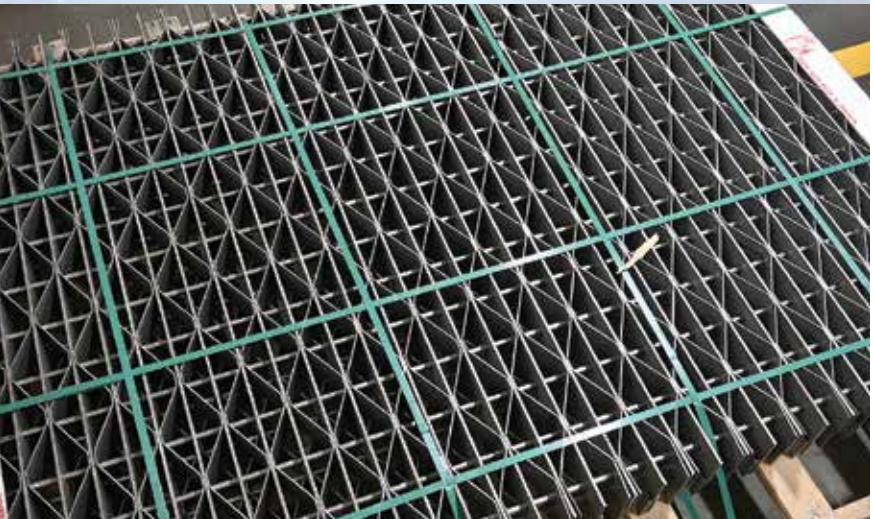

OUR GOAL

CREATE EXCELLENT PRODUCTS AND PARTNERSHIPS

- Fabricated Heat Treating Work Carriers
- Cast Heat Treating Work Carriers
- Heat Treatment Furnace Parts
- Steel Production Support
- Hyper Alloys Fabricated Products

CONTACT US

Sales@Wirco.com
800.348.2880

Partner with Wirco, your American-made engineered alloy solution.

All five Solar Atmospheres facilities are now an option for customers with Lockheed Martin requirements for thermal processing services. (Courtesy: Solar Atmospheres)

Solar Atmospheres S.C. earns Lockheed Space Systems OK

Solar Atmospheres Greenville, South Carolina, facility has been awarded Lockheed Martin Space Systems approval. With this approval, now all five Solar Atmospheres facilities are an option for customers with Lockheed Martin requirements for thermal processing services.

"We are proud to once again provide our customers in the Southeastern U.S. with another regional option for aerospace and defense thermal processes, saving them time and money while continuing to deliver the high level of quality required," said Steve Prout, president of Solar Atmospheres' Greenville facility.

With the ability to support vacuum thermal processing needs ranging from development cycles to 50,000-pound loads at temperatures of up to 2,400°F, Solar Atmospheres provides AS9100 and Nadcap quality accredited heat treatments, providing its customers with the confidence their product is being processed as specified.

MORE INFO www.solaratm.com

Kuźnia Jawor elevates forging expertise with Nitrex

Kuźnia Jawor S.A., a European company specializing in the production of hot forged and CNC machined components for the automotive, machinery, mining, and piping industries, has enhanced its manufacturing capabilities through a substantial plant modernization. Located in the southwestern region of Poland, Kuźnia Jawor has solidified its position as a leading provider of forged and CNC automotive parts within Poland, as well as mining parts in international markets such as Czechia and Tűrkiye.

Kuźnia Jawor leverages its in-house capabilities to design and manufacture forging tools, a crucial element of the production process. This is necessary for obtaining repeatable strength parameters in steel and ensuring their resistance to geometric changes or abrasive wear, factors that are addressed through heat treatment. Building on this foundation, the company recently revamped its heat-treating operations by introducing cutting-edge equipment and technologies, aiming to streamline operations for improved efficiency and to elevate the quality of its forged and machined products. The investment encompassed the replacement of the entire production line, based on an oil-hardening furnace and two outdated nitriding furnaces. The decision to upgrade was prompted by the need to eliminate archaic technology, address inadequate controls, and ensure that the company remains at the forefront of innovation, sustainability, and excellence in the forging industry. The current production line has been designed using a Nitrex nitriding system and a vacuum hardening furnace.

The company's forging and CNC processes are marked by meticulous precision, with dies initially undergoing treatment in the vacuum furnace before proceeding to the nitriding phase. This multi-step approach is essential for achieving a zero-white layer, effectively preventing surface cracking in the H11, H13, and WNL hot work steel dies subjected to high-pressure hammer forging. A crucial part of this initiative was the installation of a new Nitrex horizontal-loading system, featuring the furnace model NXH-9912, a custom solution designed to facilitate the seamless automatic transfers of loads between operations.

The turnkey system is equipped with Nitreg® nitriding technology, which significantly enhances the wear and corrosion resistance of treated tooling. This innovative technology not only improves die durability and performance but also facilitates efficiency gains, leading to savings in process

SEND US YOUR NEWS Companies wishing to submit materials for inclusion in Thermal Processing's Update section should contact the editor, Kenneth Carter, at editor@thermalprocessing.com. Releases accompanied by color images will be given first consideration.

Kuźnia Jawor S.A. installed a Nitrex horizontal-loading system, featuring the furnace model NXH-9912, a custom solution designed to facilitate the seamless automatic transfers of loads between operations. (Courtesy: Nitrex)

time and resources, including electricity and process gases. Furthermore, the system adheres to industry standard 2759/10 controlled nitriding, ensuring the highest quality and precision in the heat-treating process. Interestingly, Kuźnia Jawor is also engaged in an ongoing collaborative research and development project with a local university, exploring hybrid coatings that combine Nitreg nitriding technology with PVD and CVD processes, with the aim of further enhancing tool performance.

Kuźnia Jawor's core values prioritize a sustainable future, and this strategic investment seamlessly aligns with its mission to protect the natural environment. This enables them to actively reduce CO emissions, decrease energy consumption, and more. This holistic approach harmonizes operations with Kuźnia Jawor sustainability objectives, making it an optimal fit for their business.

"Kuźnia Jawor's choice to partner with Nitrex was driven by the need to replace outdated equipment, modernize, and expand their production facility," said Marcin Stoklosa, Nitrex technical sales manager who oversaw the project. "The result? Improved quality, enhanced performance, and a stronger position in the forging industry. Nitrex's extensive experience and track record of success in delivering the right technology for forging dies, along with our proven history of over 30 installations in Poland, played a pivotal role in securing the partnership."

MORE INFO www.nitrex.com

L&L delivers electric dual-chamber box furnace

L&L Special Furnace Co. has shipped a model QDD29 economical dual-chamber heat-treating and tempering oven to an equipment provider located in the Midwest. The furnace will ultimately be installed in a Snap On production facility servicing tool and die support within the company's production line.

The smallest of L&L's dual-chamber furnaces, the QDD series is ideal for various thermal applications. Its compact over/under design saves floor space and provides dependable and reliable heat-treating without the delays of third-party vendors, shipping costs, and transit holdups.

The top chamber is primarily deployed for heat-treating tool steels at temperatures up to 2,200°F; the tempering chamber is suited to temperatures up to 1,250°F and has a recirculation baffle that makes it suitable for small aluminum work as well. The hardening and tempering chambers have interior dimensions of 12" wide by 8" high by 24" deep, with total external dimensions of 55" wide by 70" tall by 56" deep.

The QDD29 is controlled with digital single setpoint controls along with overtemperature protection. Solid-state relays drive the heating elements in a simple, robust control circuit.

All L&L Special Furnace machines can be

L&L Special Furnace Company's Model QDD over/under heat-treating system. (Courtesy: L&L Special Furnace Company)

configured with various options and be specifically tailored to solve your thermal needs. We also offer furnaces equipped with pyrometry packages to meet the latest ASM2750 specifications.

Options include a variety of control and recorder configurations. An optional three-day, all-inclusive startup service is available with each system in the continental United States and Canada. International startup and training service is available by factory quote.

MORE INFO www.llfurnace.com

Delta H builds on record of excellence, unveils growth plan

Delta H®, known for precision in the design and manufacturing of industrial ovens and furnaces, celebrates a year of significant achievements and sets a strategic path for growth and innovation. Proven as a hallmark of quality and service, Delta H is positioned at the cusp of another expansion phase, marking its presence more prominently in both military initiatives and commercial ventures, particularly in high-demand aerospace applications.

2023 achievements include:

» Surpassed 450 lifetime oven and furnace installations, firmly establishing Delta H as a trusted leader in the industry.

» Conducted hundreds of technical service and preventative maintenance projects, ensuring products' optimal performance and reliability.

» Invested in a substantial inventory of official OEM spare parts, ready for overnight shipping, significantly minimizing downtime for clientele.

» Strengthened military alliances and developed new commercial partnerships, notably within challenging aerospace frameworks.

As Delta H ventures into 2024, it eyes fruitful expansions across production capabilities and customer support enhancements, aiming to solidify its place in industrial thermal processing technology. Key focus areas include:

» Introducing advanced new products designed to meet burgeoning market needs.

» Expanding its spare parts inventory to promise immediate delivery of crucial components, curtailing operational halts.

» Harnessing field service expertise to fortify preventative maintenance programs and technical enhancements.

» Forging invaluable commercial connections in promising sectors, extending its footprint beyond aviation and aerospace into medical and automotive industries.

"Our decades of engineering and design expertise, supported by advanced 3D modeling and manufacturing excellence, have been pivotal to our growth," said Richard Conway, director/CTO of Delta H. "As a turnkey solution provider, from concept design to delivery and commissioning, we remain committed to precision manufacturing and comprehensive customer service."

With robust business acumen and a vision deeply rooted in customer satisfaction, Delta H is well-prepared for sustained growth and continued leadership in technology innovation.

MORE INFO www.delta-h.com

Automotive company orders 2nd EndoFlex generator

An automotive company in South America has recently placed a follow-up order for a second EndoFlex generator from UPC-Marathon, a Nitrex company. Following the successful installation of a 200 m^3/h EndoFlex unit last

In 2023, Delta H® surpassed 450 lifetime oven and furnace installations, establishing the company as a trusted leader in the industry. (Courtesy: Delta H)

Technical Education. Career Development. International Networking.

Log on to **www.stle.org/annualmeeting** for registration and hotel information.

Early Birds! Register by **March 22** and save $100 on your meeting fee.

78th STLE Annual Meeting & Exhibition

May 19-23
Minneapolis Convention Center
Minneapolis, Minnesota (USA)

MINNEAPOLIS

78th STLE ANNUAL MEETING & EXHIBITION | **MAY 19-23, 2024**

Whether you work in the field or lab–in industry, academia or government–STLE's Annual Meeting has programming designed specifically for you. Please join your peers from around the globe for five unique days of technical training and industry education that could change your career.

Program Highlights:

- 500 Technical Presentations and Posters
- 13 Lubrication-Specific Education Courses
- Sustainable Power Generation Track including Fossil Fuels, Hydropower, Nuclear, Solar and Wind
- Discussion Round Tables – An Idea Exchange Event
- Electric Vehicles Track and Course
- Trade Show
- Commercial Marketing Forum
- Business Networking

stle
• connect • learn • achieve

Society of Tribologists and Lubrication Engineers
840 Busse Highway, Park Ridge, Illinois 60068 (USA)
P: (847) 825-5536 | F: (847) 825-1456 | www.stle.org | information@stle.org
Follow us on:

A South American automotive company has ordered a second EndoFlex generator from UPC-Marathon, a Nitrex Company. (Courtesy: Nitrex)

year, the new generator, boasting a similar capacity, aims to enhance stability, ensure consistent composition and gas flows, and prioritize top-tier quality of automotive gear boxes while achieving efficiencies in heat-treatment operations.

Prior to adopting the EndoFlex solution, the manufacturer relied on four outdated generator units, each with a capacity of 70 m^3/h and consuming 80 kW of power. Remarkably, with the same 80 kW of power consumption, the EndoFlex generator delivers an impressive 200 m^3/h capacity, marking a substantial increase in efficiency and cost-effectiveness for the customer.

This transition to EndoFlex represents not only a remarkable 75 percent reduction in power consumption but also a significant contribution to operational efficiency and sustainability efforts. Furthermore, the new generator streamlines maintenance procedures, adheres to stringent quality standards, and reduces CO_2 emissions. EndoFlex's precision control over gas quality and production for the neutral hardening furnace enhances product quality, reduces operating costs, and optimizes energy consumption. By automatically adjusting gas production to match real-time furnace demand, EndoFlex effectively eliminates overproduction and waste.

"We're proud to continue our partnership with this automotive customer," said Marcio Boragini, UPC-Marathon's sales director for Brazil. "This latest investment builds on the success of our first EndoFlex installation, establishing a benchmark for excellence. Moreover, EndoFlex offers a compelling return on investment, empowering the manufacturer to achieve their business objectives fast, while reinforcing our commitment to driving success together."

UPC-Marathon, a Nitrex company, pioneers industrial process control, automation, and digitalization for heat treatment and combustion markets. The mission is to support furnace OEMs and equipment end-users with innovative solutions, enhancing profitability and reliability while optimizing operational efficiency. End-to-end control solutions encompass probes, analyzers, controllers, flow control systems, upgrades/retrofits, SCADA, and engineered solutions for various heat-treat processes. Leveraging digitalization platform QMULUS, customers gain a deeper understanding of their assets and production processes.

MORE INFO www.nitrex.com

Tenova joins RINA's Hydra project fueled by 100% hydrogen

Tenova, a leading developer and provider of sustainable solutions for the green transition of the metals industry, is partnering with RINA, a multinational engineering consultancy, inspection, and certification company, on the ambitious European Commission-backed Hydra project.

The 88-million-euro project is funded by the European Commission's NextGenerationEU and backed by the Italian Ministry of Enterprises and Made in Italy. It aims to drive 100 percent hydrogen-fueled steel production and allow all steelmakers to test it, using the results to drive future investment plans toward sustainable production of steel.

Recognized for its expertise in innovative green technologies that facilitate the decarbonization of the steel sector, Tenova has been contracted to supply a 30m tall Direct Reduction Iron ore (DRI) tower which will use hydrogen as a reducing agent, and an electric arc furnace (EAF). The DRI plant, based on the cutting-edge ENERGIRON® Direct Reduction technology, jointly developed by Tenova and Danieli, together with the Tenova EAF will produce up to seven tons per hour at its full production capability within 2025.

Thanks to this pilot mini mill, European steelmakers will therefore have the opportunity to test steel production with several different combinations: the DRI plant can use different percentages of natural gases and hydrogen as well as process a wide range of iron ores that will be tested in Tenova EAF providing thus concrete results and analysis for future investment and applications. In addition, plastics or other waste materials can also be injected into the EAF steel bath as an alternative to carbon.

"I am very proud of this project with RINA as it provides all European steelmakers the first open-source facility that will enable them to test the process with our pilot plant and drive their future investments to drastically reduce their emissions," said Roberto Pancaldi, Tenova CEO. "Our cooperation with RINA dates back to the nineties with several

projects successfully developed."

"Hydra aims at decarbonizing the steel production process through hydrogen-based technologies," said Carlo Luzzatto, CEO and general manager of RINA. "Thanks to the help of our partners, we will build a pilot plant to experiment with steel production, emitting a marginal fraction of the carbon emissions currently released by the world steel industry. Hydra is available to the entire supply chain for research and development on the production of clean steel."

MORE INFO www.tenova.com

First Seco/Warwick Indian CAB line goes to Narain Cooling

Seco/Warwick's first made-in-India CAB line will go to Narain Cooling Technologies. (Courtesy: Seco/Warwick)

Seco/Warwick will soon produce a CAB line in India. The solution's recipient is an Indian company producing heat exchangers. The furnace will help Narain Cooling Technologies maintain high efficiency production while meeting strict energy consumption requirements.

The CAB line on order is a furnace with a 1,300 mm wide conveyor belt, which will be used to produce medium-sized heat exchangers. This is the first CAB line sold by

Seco/Warwick entirely made in India in the Group's new factory. The production site was important to Narain Cooling Technologies.

"Starting continuous brazing line production in India is a milestone in Seco/Warwick history," said Binoy Koshy, managing director of Seco/Warwick India. "This allows us as a Group to optimize production and significantly reduce delivery costs and related emissions. India is a world leader in the production of heat exchangers, including those intended for the automotive market. Seco/Warwick will provide significant support to companies from this region, thanks to the possibility of supplying high-class metal heat-treatment furnaces, manufactured entirely in this region of the world."

"The key to success in this market is not only local production, but also ensuring competent on-site service," said Piotr Skarbiński, vice president of the aluminum and CAB Segment of the Seco/Warwick Group. "Seco/Warwick has a professional team of engineers in this part of the world who provide support to our partners."

"Last year was a breakthrough for us because we started production in India," said Sławomir Woźniak, CEO of the Seco/Warwick Group. "Already this year, the first CAB lines will roll off the Indian assembly line and reach new customers. The first made-in-India CAB line will go to Narain Cooling Technologies. I believe that this will be the beginning of our long-term cooperation and a clear signal to the market about the Group's readiness to provide first-choice solutions."

Seco/Warwick's CAB lines manufactured in India are the first choice in this region.

The CAB line ordered by the partner is equipped with a 1.3 m wide belt. The furnace chamber design ensures perfect temperature uniformity, and the furnace has an innovative continuous atmosphere control system as well as a PLC control system.

CAB lines are an excellent solution for continuous brazing of products with similar dimensions and features. The temperature is distributed evenly over the entire width and length of the conveyor belt, thanks to several independent heating zones. The line ordered by Narain Cooling Technologies was adapted to its specific needs. The idea was to obtain sufficiently high efficiency within the constraints associated with limited access to power supply.

The new Ipsen Connect customer service portal simplifies access to essential resources, including order history, service requests, and furnace documentation. (Courtesy: Ipsen USA)

"This is our first cooperation with Seco/Warwick," said Deepesh Goyal, managing director from Narain Cooling Technologies. "We set high and specific requirements for this furnace, which Seco/Warwick met. The fact that the solution is manufactured in India is of great importance to Narain Cooling Technologies. It is not only a matter of reducing costs or better logistics, but also subsequent service issues and global support for the domestic market development."

MORE INFO www.secowarwick.com

Solar Atmospheres successfully relocates to Chesterfield

Solar Atmospheres of Michigan has successfully relocated from the old Fraser and Warren facilities to a new, state-of-the-art location in Chesterfield, Michigan.

All 10 furnaces (both new and existing) are fully operational at the Chesterfield plant, heralding a new era of efficiency and productivity. This spring, construction will begin on a 15,000-square-foot expansion on an adjacent lot. The expansion will allow for the investment in cutting-edge vacuum furnaces from Solar Manufacturing.

"Our future is very bright in Michigan," said Bob Hill, president of Solar Atmospheres of Michigan. "The consolidation and expansion will allow us to elevate our service standards and meet the evolving demands of our clientele across Michigan and the surrounding states. Solar of Michigan remains steadfast in its dedication to innovation, service excellence, and customer satisfaction as it ventures into this new chapter of growth and expansion."

MORE INFO www.solaratm.com

Ipsen launches digital platform to assist customers

Ipsen prioritizes customer assistance with its new Ipsen Connect. The customer service portal simplifies access to essential resources, including order history, service requests, and furnace documentation.

Key features of the new digital gateway include:

›› Convenient part management: Request or reorder parts, view order history, and access furnace documentation seamlessly.

›› Streamlined service requests: Schedule maintenance, troubleshooting, or calibration appointments in just a few clicks.

›› Best practices and expert insights: Access troubleshooting guides, online training videos, and answers to frequently asked questions.

›› Real-time updates: Keep your operations informed and on track with live updates, including order status, active quotes,

planned maintenance, and scheduled service appointments.

Ipsen's Digital Technologies team worked with internal and external stakeholders over the last several years, leveraging their insights to develop and evaluate the portal before its launch.

"By aligning our digital initiatives with our customers' needs, our goal is to provide cutting-edge solutions that enhance efficiency, productivity, and customer satisfaction," said Aymeric Goldsteinas, Ipsen's vice president of digital technologies.

Following a successful beta test with 40 customers, Ipsen Connect is now available to all existing U.S. customers with vacuum furnace equipment. (Some features may not be available for older furnace models.) The service doesn't require any software installation and can be accessed through any internet-connected PC or mobile browser.

MORE INFO www.ipsenusa.com

Argentine heat treater commissions Nitrex system

Sudosilo S.A., a leading commercial heat treatment service provider in South America, is bringing premier nitriding to the Argentine industrial sector with the recent commissioning of a Nitrex turnkey installation. This newly operational nitriding system, acknowledged as a best-in-class nitriding solution, represents a significant milestone as the first of its kind in Argentina, offering third-party heat treatment services to the region.

At the forefront of technological advancement, Sudosilo has embraced cutting-edge technologies to cater to various sectors, including aluminum injection, aluminum extrusion, forging, and oil applications. The integration of a Nitrex system into its operations is set to establish a new benchmark for quality and precision in nitriding treatments.

"The competitive edge of this installation lies in its meticulous control and automation capabilities, ensuring process stability and the ability to generate specialized processes and recipes tailored to unique requirements of each application," said Jerónimo Alberto Colazo, production manager at Sudosilo. "This high level of customization and precision guarantees superior quality, meeting the intricate demands of industries served by Sudosilo."

The new Nitrex system adheres to CQI-9 guidelines for automotive heat-treatment processes and NADCAP requirements for aerospace applications. This aligns Sudosilo with international standards, positioning the company to meet the exacting demands of both Argentine and South American markets for quality, innovation, and unparalleled service.

The successful commissioning of the turnkey system, featuring a pit-type furnace model NX-1015 with Nitreg® controlled nitriding, Nitreg®-C controlled nitrocarburizing, and ONC® post-oxidation process technologies, was completed in November 2023. These advanced technologies ensure a uniform case depth and precise management of nitriding/nitrocarburizing/oxidation layer formation, optimizing the mechanical properties of tooling and dies. Nitreg and Nitreg-C contribute to enhancing surface hardness and fatigue resistance, while ONC improves corrosion resistance. Notably, the system eliminates the need for post-finishing operations and boasts a substantial load capacity of 4,400 pounds (2000 kg). Marathon Systems Control, serving as a Nitrex representative for Latin America, played a pivotal role in executing the system installation and finalizing the process validation.

"We sincerely appreciate Sudosilo for choosing Nitrex as their preferred partner," Jack Kalucki, technical advisor at Nitrex. "The installation at Sudosilo not only signifies a leap in technological innovation but is also a commitment to manufacturing excellence. This adoption of advanced heat-treatment technologies, such as Nitreg, will not only enhance product performance and improve manufacturing but will also set new benchmarks that exceed the demands of industries across the region."

MORE INFO www.nitrex.com

Delta H surpasses 50 heat systems to armed forces

Delta H® has provided more than 50 heat-treating system installations to multiple military facilities around the world along with training and on-site qualifying assistance.

The military facilities include Air National Guard bases; USAF bases stateside, Guam, Alaska, and Hawaii; air bases in Japan, Germany, United Kingdom — Royal Air Force, Middle East; the U.S. Navy, U.S. Coast Guard, and U.S. Army facilities.

The systems included either single, dual, or triple chamber designs of both the heavy-duty commercial aviation standard models DCAHT®/SCAHT® Series, Delta H's innovative Defender Series — developed for the armed forces, and aircraft composite walk-in ovens.

All systems are in full compliance to NAVAIR Tech Order 1-1A-9, and meet AMS2750 accountability standards for accuracy, temperature uniformity, calibration, and secure batch records.

Military personnel are provided full operator and heat-treating training, as well as on-site qualifying assistance to meet and maintain the stringent pyrometry standards, and maintenance training. Successful trainees receive certificates of training as qualified to use their Delta H furnace for heat treatment of aircraft parts.

"It is a deep honor and humbling for the Delta H team to support our armed forces," said Delta H director/CTO Richard Conway. "We take the utmost care to ensure the best of our craftsmanship and abilities are utilized to deliver the finest heat-treating equipment for aircraft maintenance to our warfighters."

MORE INFO www.delta-h.com

Can-Eng honors Donofrio for 25 years of service

Can-Eng Furnaces InternationaL LTD announced Tim Donofrio, vice president of sales, has reached his 25-year milestone with the company.

Tim Donofrio

Donofrio joined Can-Eng in 1999 in an outside sales capacity, eventually leading the company's aluminum products group, which captured a significant portion of the ICE and aluminum structural casting component heat-treatment equipment market.

In 2009, Donofrio took on additional responsibilities for the sales and marketing of Can-Eng's flagship mesh belt furnace technology resulting in sales around the globe. Since 2016, he has been vice president of sales, including all marketing activities.

Prior to joining Can-Eng, Donofrio held a senior management position in commercial heat treating and began his career in the closed die forging business. He is a graduate of the Manufacturing Engineering Technology Program at Niagara College and has a degree in business from Brock University.

With the launch of Evergreen Kiln Technologies, LLC in 2024, Donofrio has the added sales and marketing responsibilities for kilns used in the processing of anode and cathode materials for the emerging EV BEV (battery electric vehicle) market.

MORE INFO www.can-eng.com

Motorcycle maker selects Nitrex for sustainability

Guangdong Tayo Motorcycle Technology Co. Ltd. has invested in a nitriding/nitrocarburizing system for its new production facility in Jiangmen City, in southern China's Guangdong province.

Heat-treat solutions company Nitrex was commissioned to deliver a comprehensive turnkey system, geared toward enhancing the performance and durability of multiple components within Guangdong Tayo Motorcycle including those for the brands Haojiang, Daye, Shengshi, and Qidian.

As part of their development strategy, Guangdong Tayo Motorcycle — a renowned Chinese manufacturer of motorcycles and bicycles — has placed sustainability, product quality, service excellence, and market expansion at the heart of their mission. Paving the way for superior motorcycles and bicycles, the company evaluated various options and ultimately selected Nitrex for its precision-controlled processes, process stability and repeatability, equipment longevity and reliability, and commitment to environmental friendliness.

The turnkey system comprises a large pit-type furnace, model NX-1225, boosting a 4,000-kg load capacity and incorporating two cutting-edge process technologies – Nitreg® controlled nitriding and Nitreg®-C nitrocarburizing. These value-added surface treatments augment the properties of motorcycle and bicycle metal components, significantly enhancing wear resistance and providing protection against rust and corrosion. Additionally, the system features an ammonia dryer and accelerated cooling system, facilitating the delivery of high-purity ammonia and faster cycle times to optimize production efficiency.

"Our partnership with Guangdong Tayo Motorcycle Technology Co. Ltd. will help them in fulfilling their mission of delivering top-notch, highly durable, and reliable motorcycles and bicycles to their global customer base," said Nikola Dzepina, Nitrex account executive. "With precision control and guaranteed results, the Nitrex system will empower Guangdong Tayo Motorcycle to consistently achieve excellence, setting their products apart in the competitive two-wheeler market."

"This system's exceptional reliability, engineered for longevity with minimal maintenance requirements and low utility and production media consumption costs, aligns perfectly with Guangdong Tayo Motorcycle's vision for a sustainable future," said Tao Liu, sales manager at Nitrex China.

MORE INFO www.nitrex.com

FIND THE INFORMATION YOU NEED AT THERMAL PROCESSING

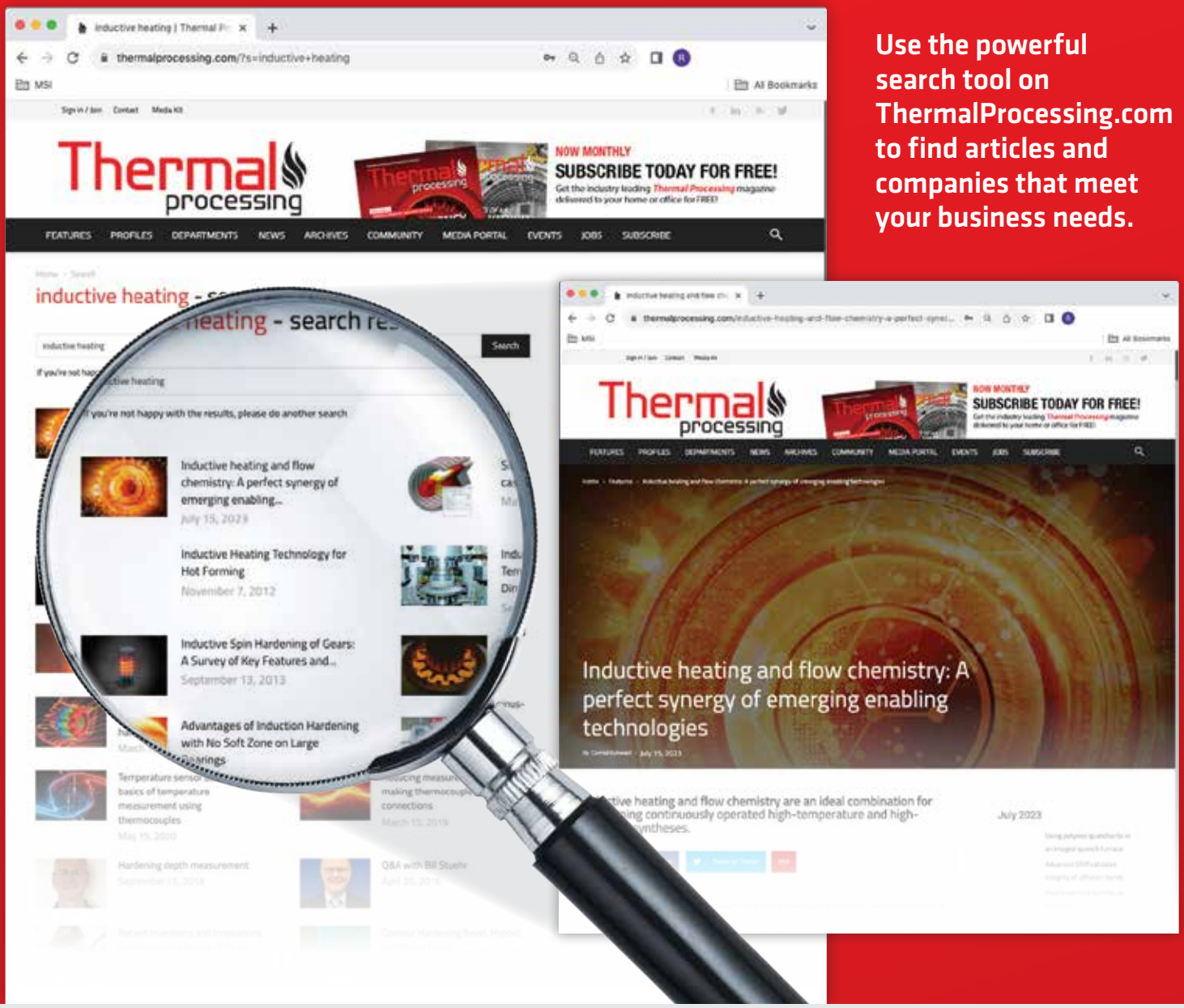

Use the powerful search tool on ThermalProcessing.com to find articles and companies that meet your business needs.

ThermalProcessing.com has a wealth of information about the heat-treat industry. And our search tool gives you access to an extensive range of articles and businesses covering all aspects of heat treating. It's there to help you find the information you need to support the success of your business.

Thermal processing

SUBSCRIBE FOR FREE

Use the QR code or go to www.thermalprocessing.com

ECHT 2024 to focus on processes, tech for sustainable future

ECHT 2024 will deal with all fields of heat treatment and surface engineering, heat treatment of metals, thermochemical treatment of metals, coatings and surface treatments, coatings and surface treatments including dry treatment operations, and wet treatment operations. (Courtesy: Shutterstock)

The ECHT 2024 Conference and the 50th Annual A3TS Congress will be together in Toulouse, France, June 5-7, 2024. The focus will be on processes and technologies for a sustainable future in transport and industry. The conference will deal with all fields of heat treatment and surface engineering, heat treatment of metals (iron and steel, non-ferrous alloys), thermochemical treatment of metals, coatings and surface treatments, coatings and surface treatments including dry treatment operations (PVD, CVD, plasma, thermal spraying, etc.), and wet treatment operations (electrochemistry, etc.). Specific sessions will be devoted to the aerospace industry.

ADDITIONAL FOCUS AREAS

- Contribution of innovative heat and thermochemical treatments to EU climate goals.
- Coatings made from enhanced materials for electrical and thermal conductivity.
- Digital technologies in heat treatment and surface engineering industries.
- Surface engineering to address environmental constraints.
- New needs in tribological properties: An open challenge for heat treatment and surface engineering.

PLANNED KEYNOTE TALKS

- **Laurent Pinto.** Metal technology senior expert, Airbus Group (France): "Metallic and surface technologies development challenges toward a sustainable future."
- **Thomas Ackerson.** Senior metallurgist, Blue Origin (U.S.): "Materials Challenges for Reusable Hardware and Sustainable Processes for Space Travel in the Mid-21st Century."
- **Marcel Somers.** Professor, Dr.ir., Technical University Denmark

(Denmark): "Microstructure Optimization in Additively Manufactured Metals through Heat Treatment and Surface Engineering."

›› **Denis Descheemaeker.** IRT Saint Exupéry (France): "Strategy and Technological Roadmap for Sustainability."

For more information, go to: echt2024.a3ts.org/page/accueil.

MORE CONFERENCE UPDATES

29th IFHTSE World Congress
September 30-October 3, 2024 I Cleveland, Ohio

The ASM Heat Treating Society (HTS) and the International Federation for Heat Treatment and Surface Engineering (IFHTSE) present the highly anticipated 29th IFHTSE World Congress, a premier global event dedicated to advancing the fields of heat treatment and surface engineering. The conference is co-located with ASM's Annual Meeting, IMAT 2024.

The 2024 IFHTSE World Congress revolves around the theme "Innovations in Heat Treatment and Surface Engineering for a Sustainable Future." Emphasizing the critical role of these technologies in shaping a sustainable world, the event will explore the latest developments, breakthroughs, and practices that can enhance the efficiency, performance, and environmental impact of heat treatment and surface engineering processes. In addition, traditional heat-treating topics will be offered.

IMPORTANT DATES

- ›› **First draft of manuscript due:** May 17, 2024.
- ›› **Editor feedback to authors:** June 14, 2024.
- ›› **Final manuscripts due:** June 28, 2024.
- ›› **More info:** www.asminternational.org/ifhtse-congress/

Third International Conference on Quenching and Distortion Engineering
May 6-8, 2025 I Vancouver, Canada

This event will be in conjunction with AeroMat 2025. This is a continuation of the successful Distortion Engineering conference series and the Quenching and Distortion conference series. The first QDE was in Chicago in 2012 and has occurred at approximately five-year intervals. There is a strong focus on the effects of residual stress during manufacturing and methods to control distortion and residual stress. The call for papers is expected in the next few months.

IFHTSE 2024 EVENTS

JUNE 5-7, 2024
ECHT 2024 Conference and the 50th Annual A3TS Congress
Toulouse, France

SEPTEMBER 30-OCTOBER 3, 2024
29th IFHTSE Congress
Cleveland, Ohio I with IMAT and ASM's annual meeting

MAY 6–8, 2025
3rd QDE - International Conference on Quenching and Distortion Engineering
Vancouver, Canada

For details on IFHTSE events, go to www.ifhtse.org/events

IFHTSE LEADERSHIP

EXECUTIVE COMMITTEE

Prof. Massimo Pellizzari I President
University of Trento I Italy

Prof. Masahiro Okumiya I Past President
Toyota Technological Institute I Japan

Dr. Lesley Frame I Vice President
University of Connecticut I USA

Dr. Stefan Hock I Secretary General
IFHTSE I Italy

Dr. Imre Felde I Treasurer
Óbuda University I Hungary

OTHER MEMBERS

Prof. Rafael Colas I Universidad Autónoma de Nueva Leon I Mexico
Prof. Jianfeng Gu I Shanghai Jiao Tong University I China
Dr. Patrick Jacquot I Bodycote Belgium, France, Italy I France
Bernard Kuntzmann I Listemann AG I Switzerland
Dr. Scott Mackenzie I Quaker Houghton Inc I USA
Prof. Larisa Petrova I MADI University I Russia
Prof. Reinhold Schneider I Univ. of Appl. Sciences Upper Austria I Austria
Prof. Marcel Somers I Technical University of Denmark I Denmark
Prof. Mufu Yan I Harbin Institute of Technology I China

ONLINE www.ifhtse.org I **EMAIL** info@ifhtse.org

The journey toward decarbonization

Decarbonization. Sustainability. Carbon neutral. These are definitely the latest buzz words flying around the industrial heating industry, and everywhere else for that matter. The Industrial Heating Equipment Association (IHEA) is dedicated to spearheading critical insights and advancements around the topics of sustainability and decarbonization.

For the past 18 months, IHEA has been developing and delivering a very successful Sustainability webinar series, continuously updating terms and definitions, frequently asked questions (FAQs), and resources for the industry on the IHEA website and — in its biggest step — offering a comprehensive Decarbonization SUMMIT October 28-30, 2024, in Indianapolis, Indiana.

"All IHEA members are continuously being asked about ways to decarbonize their processes," said IHEA President and Sustainability Committee Chair Jeff Rafter. "As the industry association dedicated to all things 'heating,' we feel it is our duty to present an unbiased view of what's happening now and how companies can begin the process of lowering their carbon emissions on their current equipment, while beginning to look at all the alternatives that are coming and how those might fit into their operations. There's no question that change is imminent. We want to be the resource that the industry uses for information on all options to begin to decarbonize operations."

"We are in a unique position," he said. "There has never been an issue like this that has faced our industry. Working together and bringing the industry together at a summit such as this gives everyone a forum to learn, share ideas and best practices, review new technologies, and begin lowering carbon emissions as an industry. No one is going to do this alone."

While not much is going to happen overnight, "Legislation is coming," said IHEA board member Mike Stowe, who is serving on the ISO

Decarbonization Committee.

"The best thing companies can do is begin preparing now," he said. "Take a look at your current operations and start making changes that improve efficiency now. Educate yourself and your staff on technologies that will help you lower carbon emissions. Be ready for what lies ahead."

IHEA is ready to help the industry take the next step by presenting the Industrial Heating Decarbonization SUMMIT. This event is designed to start shaping the future of manufacturing heating processes.

It will include keynote addresses by industry visionaries, ways to begin your decarbonization process now, a look ahead at various technologies that can also help you decarbonize, case histories and a panel discussion on decarbonization collaboration, networking with industry leaders, and a tabletop exhibition that showcases cutting-edge technology.

THEMES RUNNING THROUGHOUT THE SUMMIT

- Low carbon fuels in industrial processes.
- Carbon capture and storage technologies.
- Global benchmarking.
- Economics and business concerns.
- Innovations in clean technologies.
- DOE programs and tools.
- Policy frameworks for decarbonization.
- More.

TARGET AUDIENCE FOR THE SUMMIT

- CEOs and executives from industrial companies.
- Sustainability officers and environmental managers.
- Government officials and policymakers.
- Researchers and academics in clean technology.
- Sustainability engineers and program managers.
- Directors of sustainable manufacturing.
- Utility representatives.

The tabletop exhibits that will accompany the SUMMIT program will allow attendees to explore a wide array of information that will help them in their decarbonization efforts. Those interested in reserving a tabletop should visit summit.ihea.org. Tabletops are expected to sell out quickly.

As IHEA works its way toward the SUMMIT in the fall, the Sustainability webinar series continues with topics that touch all aspects of the journey to decarbonization.

Nearly 1,000 people have tuned in over the past year since the first webinar was launched.

UPCOMING WEBINARS

- **May 16:** Increasing Available Heat to Lower CO2 Emissions.
- **June 20:** Understanding Carbon Credits & Net Zero.
- **July 18:** U.S. Codes & Standards.
- **August 15:** Renewable Fuels.

Additional webinars will be added regularly. IHEA's webinars are free to attend.

You can register by going to IHEA's website (www.ihea.org) and clicking on the Sustainability logo on the home page, then scroll down and click on the "Sustainability Webinar Series" to review and register for the upcoming webinars.

If you have a sustainability topic you would like us to address, please email the topic to anne@goyermgt.com, and IHEA will work to develop a webinar.

IHEA 2024 CALENDAR OF EVENTS

APRIL 8–MAY 19

Fundamentals of Industrial Process Heating Online Course

This course is designed to give the student a fundamental understanding of the mechanisms of heat transfer within an industrial furnace and the associated losses and the operation of a heating source either as fuel combustion or electricity.

Course Fees: $775 IHEA members / $950 non-members

APRIL 18

Sustainability & Decarbonization Webinar Series – Making Decisions: Gas vs. Electric

MAY 16

Sustainability & Decarbonization Webinar Series – Increasing Available Heat to Lower CO_2

This webinar will review the proven methods for heat recovery and emissions reduction and their applicability to processes where fuel savings and/or production increases have not previously justified their implementation.

JUNE 20

Sustainability & Decarbonization Webinar Series – Understanding Carbon Credits & Net Zero

JULY 18

Sustainability & Decarbonization Webinar Series – Industry Adoption: U.S. Codes & Standards

AUGUST 15

Sustainability & Decarbonization Webinar Series – Renewable Fuels

For details on IHEA events, go to www.ihea.org/events

INDUSTRIAL HEATING EQUIPMENT ASSOCIATION

P.O. Box 679 I Independence, KY 41051

859-356-1575 I www.ihea.org

JASON MEYER
MECHANICAL ENGINEER /// DANTE SOLUTIONS

Modeling cyclic loading and the Bauschinger effect to understand plastic deformation in steel.

Metal plasticity in manufacturing

Understanding the plastic behavior of steel plays a crucial role in manufacturing. From raw billet to parts in service, some form of plastic deformation can be found in every step of the manufacturing process, heat treatment not excluded. In fact, I used to joke in Materials and Manufacturing Process class that you should include the words "plastic deformation" in every answer to get full credit. On a macro scale, plastic deformation is simply any permanent shape change to the part. Microstructurally, deformations take the form of atomistic dislocations and planes of slip in the matrix of the base material. Engineers understand plasticity with the classic stress/strain plot from a tension or compression test, Figure 1.

When a tensile sample is pulled in the testing equipment, the resulting strain imparts a stress in the sample. This stress initially increases in a linear relationship to the imparted strain, and the slope of this line, stress over strain ratio, is called Young's Modulus. If the load is released in this region, the elastic range, the sample will return to its original shape, largely unaffected. If the sample continues to be pulled, the stress increases until the sample begins to yield, or plastically deform. The onset of yield is sometimes not as obvious in some materials, so engineers developed the 0.2% offset yield strength, which ensures that the entire macroscopic cross section is yielding, and not just individual regions.

A well-studied phenomenon, called the Bauschinger effect, named after German engineer Johann Bauschinger, states that after a material plastically deforms in one direction, it will be easier to deform in the opposite direction. As an example, tubular steel products are mechanically tested in the hoop direction, and this curvature is often flattened out before machining tensile samples. This can result in a lower yield strength because the coupon has already been deformed. The mechanism behind this effect is easy to understand with the previous definition of plasticity. As the slip-planes are formed, there exists a buildup of dislocations near barriers to movement, such as carbides, precipitates, grain boundaries, etc. These buildups accumulate back stresses, resisting the direction of dislocation, in what is known as cold-working or strain hardening. When the load direction is reversed, these buildups and back stresses now assist the paths of slip and dislocation, reducing the overall yield. Think of it like a game of tug-of-war; the atoms resist slipping much like the teams pulling on each end of the rope. If one team were to suddenly let go, it would be very easy for the other team to "slip" the other direction. This effect is extremely important for modeling the manufacturing process as plastic histories can have a significant effect on the final dimensions of produced parts.

There are several popular constitutive models that are used to simulate plasticity in metals, and two of which that are used in finite element analysis (FEA) are the Johnson-Cook (JC) model and the Baumann-Chiesa-Johnson (BCJ) model. The Johnson-Cook model is a plasticity model based on the von Mises criterion for tensile flow

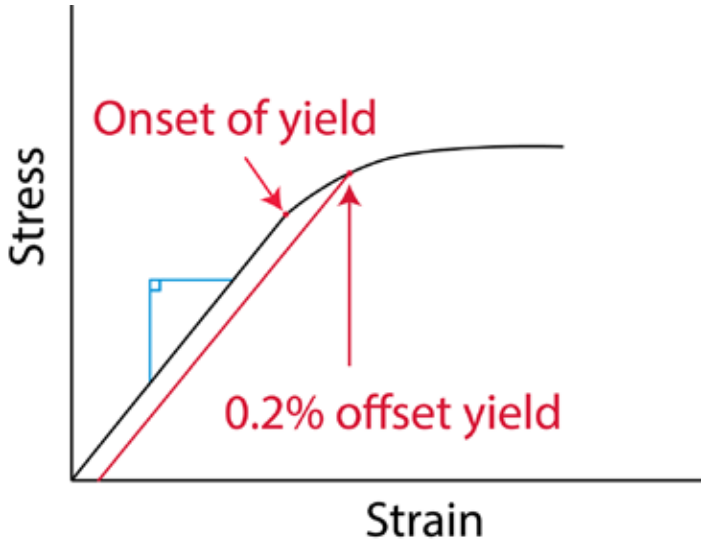

Figure 1: Schematic of a stress/strain plot.

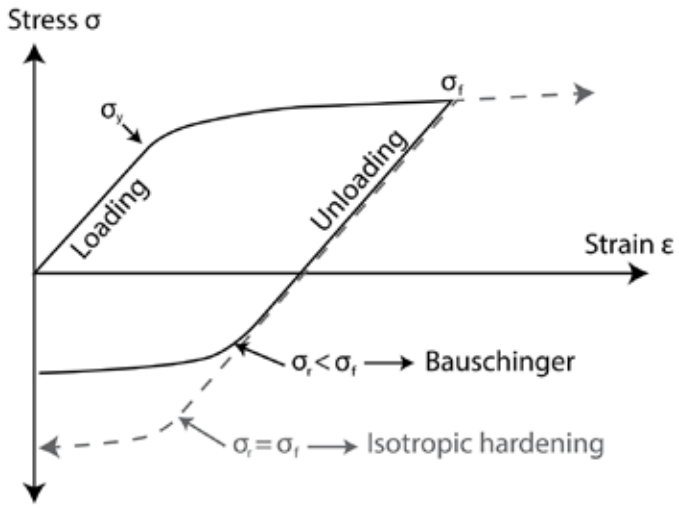

Figure 2: Stress/strain schematic showing reverse loading and the Bauschinger effect.

stress, and the constitutive equation for the model is shown below:

$$\sigma_{JC} = (A + B\varepsilon^n)\left(1 + C\ln\frac{\dot{\varepsilon}}{\dot{\varepsilon}_0}\right)\left(1 - \left(\frac{T - T_r}{T_m - T_r}\right)^m\right)$$

Simply put, the JC stress accounts for the effects of strain hardening, strain rate, and temperature. Engineers use this type of equation by first performing experiments to collect stress/strain data, then adjust the constants A, B, C, n, and m to the best fit for their data.

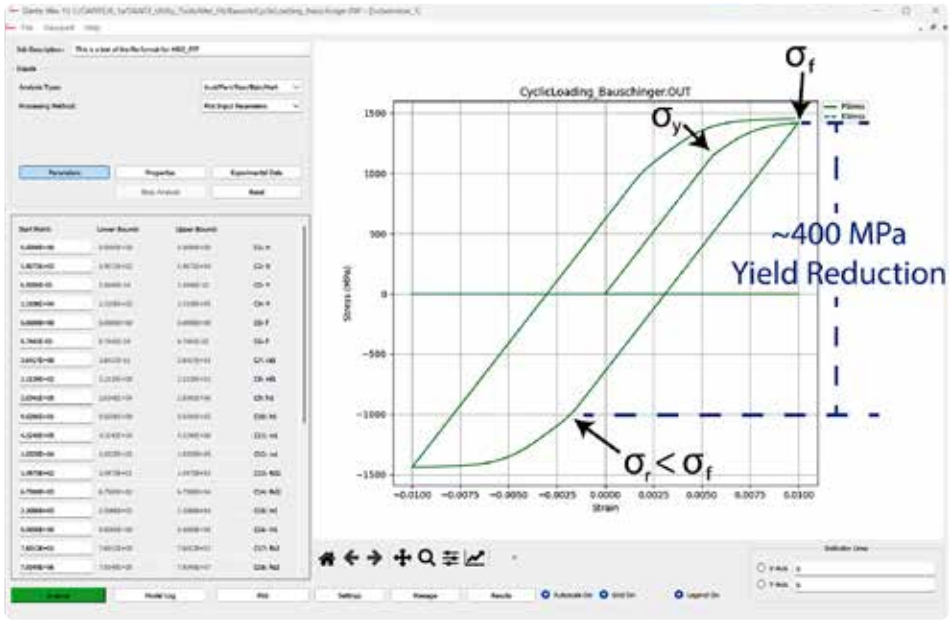

Figure 3: Output of the MecFit utility showing cyclic loading and the Bauschinger effect.

After parameters are solved for a particular material, the model can be used for a wide variety of strain rates, temperatures, and strain values to solve the plastic response. The beauty in the JC equation is the relative simplicity and accuracy for a wide range of materials, temperatures, and strain rates. The drawback is the strain hardening effect has no direction and is purely isotropic. This means that it has no way of tracking the yield in reversed loading as shown with the Bauschinger effect (Figure 2). The JC model would simply yield at the same stress value when the loading is reversed.

The BCJ model, in contrast, accounts for the kinematic and isotropic hardening effects, in addition to the strain, strain rate, and temperature dependance. The BCJ model uses dislocation-based internal state variables to track the material's history and uses a minimum of 18 constants to fit the stress/strain response. While the exact technical form of this model is beyond the scope of this article, a more detailed representation can be found in reference [1]. I would advise those interested to further investigate the applications of this fascinating model. One such use is in modeling the complex effect of stress reversals occurring during heat treatment. For instance, DANTE, a commercial heat-treatment simulation software, uses a modified BCJ plasticity model which accounts for alloy chemical and microstructural changes, adding up to a total of 27 plastic parameters. To fit these parameters from experimental stress-strain test data for use in the Dante materials database, a fitting tool called MecFit was developed. MecFit is frequently used to assist analysts in developing mechanical properties for their own proprietary materials. The tool includes fitting options for individual phases, strain-rate, temperature range, and carbon content. In this example, MecFit is used to simply plot stress/strain response given some parameters from the DANTE material database. Figure 3 shows a marked-up output from MecFit, showing the plot of three tension and compression load reversals on the right, and the model inputs, including the BCJ input parameters, elastic properties, and experimental data tabs on the left.

Initially the simulation starts at the origin where a tensile load is applied, after the initial onset of yield, (about 1150 MPa) the material shows some strain-hardening before stopping at 1% strain (about 1400 MPa). The sample is then loaded in compression until it begins to yield at about -1000 MPa, about 400 MPa lower than the strain-hardened sample in tension. Again, we see some strain hardening before the strain is stopped at -1% (-1440 MPa). The sample is finally loaded in tension until 1% strain, where the initial yield is about 1050 MPa. The Bauschinger effect is clearly shown in the difference from the strain-hardened yield and the onset of yield when the load is reversed. Note: there must be some strain hardening to see this effect as the dislocations need to pile up to contribute to the load reversal.

Plastic deformation will always be an important part of the manufacturing process, which can be better understood these days with the use of advanced methods such as FEA. While the Johnson-Cook model is more simplistic than the Baumann-Chiesa-Johnson model, both have been used to describe the general plasticity of metals. The added simplicity and reduced computational costs of the JC model are good reasons for its popularity in FEA. However, the BCJ model offers a more physics-based approach, with its use of internal state variables, allowing it to better capture material behavior such as the Bauschinger effect. It may be a strain to understand these effects, but don't stress out. Constitutive models can help us to understand and develop new and interesting processes.

REFERENCES

[1] Bammann DJ, Chiesa ML, Johnson GC. Modeling large deformation and failure in manufacturing process. Theory of Applied Mechanics 1996; 359–376.

ABOUT THE AUTHOR

Jason Meyer joined DANTE Solutions full time in May 2021 after receiving his Master's degree in mechanical engineering from Cleveland State University. His main responsibilities include marketing efforts, project work, and support and training services for the DANTE software package and the DANTE utility tools. Contact him at jason.meyer@dante-solutions.com.

D. SCOTT MACKENZIE, PH.D., FASM
SENIOR RESEARCH SCIENTIST–METALLURGY /// QUAKER HOUGHTON INC.

Polymer quenchants are useful for reducing distortion and residual stress in quenched aluminum components, while meeting mechanical property requirements and minimizing susceptibility to IGC.

Polymer quenchants and corrosion of aluminum

When slow quenching 2024 aluminum, this alloy is susceptible to intergranular corrosion. Two common quenchants, water and AMS 3025 PAG type quenchants, are compared.

INTRODUCTION

Heat treating aluminum requires attention to all process parameters to ensure that properties are achieved, without excess distortion or susceptibility to corrosion. Polymer quenchants such as those described by AMS 3025 [1] were developed to accomplish the goal of achieving properties, reducing distortion and residual stresses, while achieving similar corrosion susceptibility as those parts quenched in water. The concentrations of Type I and Type II quenchants, specified by AMS 2770 [2], used for quenching of aluminum, are based on the "zero-delta" concept. In other words, properties of parts quenched in AMS 3025 quenchants will have identical properties as those quenched in water.

Schematically, the heat-treatment process is shown in Figure 1. Of each of these processes, quenching is the most important step to achieving mechanical properties, low residual stresses, and reducing corrosion susceptibility.

As a part is quenched, the solute is held in supersaturation until the part is cooled. Properly quenched, all the solutes will remain in supersaturated solid solution until natural aging commences once the part has cooled to room temperature. This requires a fast quench. If the part is quenched at a rate less than the perfect rate, heterogeneous precipitation will occur, with equilibrium precipitates forming at the grain boundaries. The rate at which precipitation occurs is dependent on the degree of supersaturation, and the diffusion rate. But the diffusion rate increases as a function of temperature. The diffusion rate is greatest at elevated temperature. When either the supersaturation or the diffusion rate is low, the precipitation rate is low. At intermediate temperatures, the amount of supersaturation is relatively high, as is the diffusion rate. Therefore, the heterogeneous precipitation rate is the greatest at intermediate temperatures. The amount of time spent in this critical temperature range is governed by the quench rate.

The amount of precipitation occurring during quenching reduces the amount of subsequent hardening possible. This is because as solute is precipitated from solution during quenching, it is unavailable for any further precipitation reactions. This results in lower tensile strength, yield strength, ductility, and increased corrosion susceptibility.

In aluminum alloy 2024, the inter-granular corrosion susceptibility is driven by the presence of Al_2Cu (θ) and Al_2CuMg equilibrium precipitates at the grain boundaries. The region is surrounded by a precipitate free zone (PFZ) that is essentially pure aluminum and is depleted of solute. This is shown in Figure 2. The difference in electrochemical corrosion potential between the grain boundary and the PFZ creates a galvanic cell, and intergranular corrosion follows this path. Specifically, the copper rich precipitates and grain boundary regions act as local cathodes, which drive anodic dissolution of the precipitate-free zones.

Figure 1: Schematic representation of the aluminum heat-treatment process.

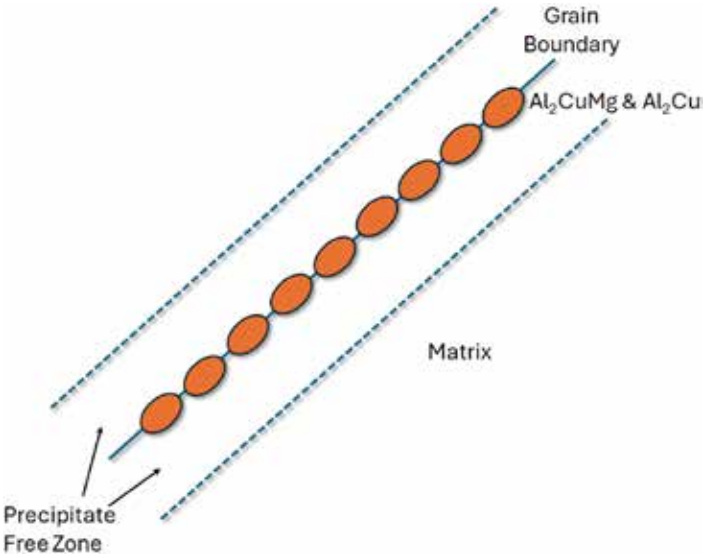

Figure 2: Corrosion mechanism of 2XXX series aluminum alloys (after [1]).

PROCEDURE AND RESULTS

Sixteen 150 x 225 mm panels of 1.8 mm thick 2024 aluminum sheet, consisting of four different heat lots, were solution heat treated at 493°C (935°F) and quenched in either water or 28% AMS 3025 Type I PAG quenchant. Panels were then naturally aged to the -T4 temper for 96 hours. Two panels from each heat lot were quenched in water, and two panels from each heat lot were quenched in 28% AMS 3025 Type I PAG quenchant. The concentration of 28% is the maximum percentage of AMS 3025 [2] permitted for this alloy and thickness per AMS 2770 [3]. The panels were then corrosion tested per ASTM G110 [4], except the immersion period was seven hours. Three 25 x 25 mm samples were sectioned from each panel and examined at 100X through 500X before and after etching with Keller's Etch [5]. The depth of intergranular corrosion was measured and compared to the water quenched panels. The results are tabulated in Table 1.

A comparison of the depth of intergranular corrosion (Figure 3) shows that the recommended maximum concentration for polymer quenchant (28%) produced similar depths of penetration of intergranular corrosion as those that are water quenched. Further, there

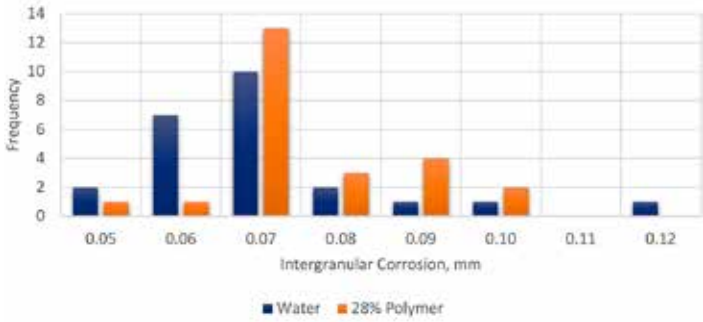

Figure 3: Histogram comparing the depth of intergranular corrosion of 2024-T4 aluminum, quenched in either water or 28% Aqua-Quench™ 260.

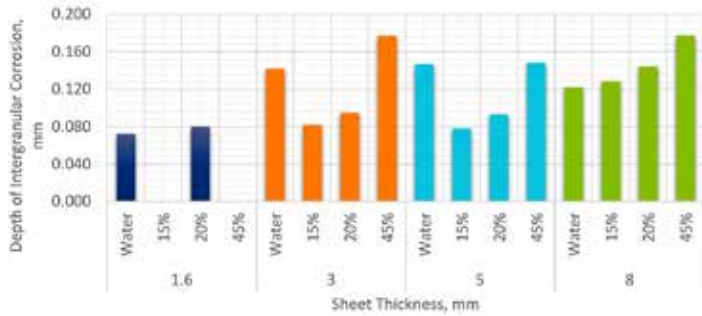

Figure 4: Comparison of the depth of intergranular corrosion of 2024-T4 panels quenched in different quenchants.

Specimen #	Thickness (in.)	Thickness (mm)	% Conc.	Mill	#1	#2	#3	Average (in.)	Average (mm)
24WA1-1	0.063	1.6	0%	Alcoa	0.0023	0.0034	0.0023	0.0027	0.0677
24WA1-2	0.063	1.6	0%		0.0019	0.0023	0.0023	0.0022	0.0550
24WA2-1	0.063	1.6	0%		0.0027	0.0023	0.0023	0.0024	0.0618
24WA2-2	0.063	1.6	0%		0.0034	0.0030	0.0019	0.0028	0.0703
24WK1-1	0.063	1.6	0%	Kaiser	0.0030	0.0027	0.0030	0.0029	0.0737
24WK1-2	0.063	1.6	0%		0.0023	0.0030	0.0028	0.0027	0.0686
24WK2-1	0.063	1.6	0%		0.0030	0.0038	0.0049	0.0039	0.0991
24WK2-2	0.063	1.6	0%		0.0042	0.0027	0.0030	0.0033	0.0838
24GA1-1	0.063	1.6	28%	Alcoa	0.0027	0.0038	0.0027	0.0031	0.0779
24GA1-2	0.063	1.6	28%		0.0042	0.0030	0.0019	0.0030	0.0770
24GA2-1	0.063	1.6	28%		0.0038	0.0038	0.0027	0.0034	0.0872
24GA2-2	0.063	1.6	28%		0.0030	0.0034	0.0030	0.0031	0.0796
24GK1-1	0.063	1.6	28%	Kaiser	0.0034	0.0034	0.0030	0.0033	0.0830
24GK1-2	0.063	1.6	28%		0.0023	0.0030	0.0030	0.0028	0.0703
24GK2-1	0.063	1.6	28%		0.0042	0.0038	0.0030	0.0037	0.0931
24GK2-2	0.063	1.6	28%		0.0030	0.0030	0.0027	0.0029	0.0737
24G50A1-1	0.063	1.6	28%	Alcoa	0.0019	0.0030	0.0030	0.0026	0.0669
24G50A1-2	0.063	1.6	28%		0.0030	0.0030	0.0030	0.0030	0.0762
24G50A2-2	0.063	1.6	28%		0.0027	0.0038	0.0027	0.0031	0.0779
24G50A2-2	0.063	1.6	28%		0.0027	0.0030	0.0034	0.0030	0.0770
24G50K1-1	0.063	1.6	28%	Kaiser	0.0030	0.0030	0.0038	0.0033	0.0830
24G50K1-2	0.063	1.6	28%		0.0030	0.0023	0.0030	0.0028	0.0703
24G50K2-1	0.063	1.6	28%		0.0038	0.0042	0.0046	0.0042	0.1067
24G50K2-2	0.063	1.6	28%		0.0053	0.0034	0.0053	0.0047	0.1185

Table 1: Test results of intergranular corrosion penetration of 2024 aluminum quenched in either water or 28% Aqua-Quench™ 260 and naturally aged to -T4 temper.

Specimen #	Thickness (in.)	Thickness (mm)	% Conc.	Mill	#1	#2	#3	Average (in.)	Average (mm)
24WK1-1	0.118	3.0	0%	Kaiser	0.0038	0.0053	0.0068	0.0053	0.13462
24WK1-2	0.118	3.0	0%		0.0057	0.0066	0.0053	0.0059	0.149013
15GK1-1	0.118	3.0	15%		0.0027	0.0034	0.0038	0.0033	0.08382
15GK1-2	0.118	3.0	15%		0.0030	0.0038	0.0027	0.0032	0.080433
28GK1-1	0.118	3.0	28%		0.0038	0.0038	0.0042	0.0039	0.099007
28GK1-2	0.118	3.0	28%		0.0030	0.0038	0.0038	0.0035	0.089747
45GK1-2	0.118	3.0	45%		0.0076	0.0057	0.0076	0.0070	0.176953
24WA1-1	0.197	5.0	0%	Alcoa	0.0046	0.0061	0.0053	0.0053	0.135467
24WA1-2	0.197	5.0	0%		0.0053	0.0071	0.0061	0.0062	0.15748
15GA1-1	0.197	5.0	15%		0.0030	0.0030	0.0034	0.0031	0.079587
15GA1-2	0.197	5.0	15%		0.0030	0.0030	0.0030	0.0030	0.0762
28GA1-1	0.197	5.0	28%		0.0030	0.0042	0.0034	0.0035	0.089747
28GA1-2	0.197	5.0	28%		0.0038	0.0038	0.0038	0.0038	0.09652
45GA1-1	0.197	5.0	45%		0.0057	0.0046	0.0057	0.0053	0.135467
45GA1-2	0.197	5.0	45%		0.0076	0.0057	0.0057	0.0063	0.160867
24WA1-2	0.315	8.0	0%	Alcoa	0.0046	0.0049	0.0049	0.0048	0.12192
15GA1-1	0.315	8.0	15%		0.0046	0.0049	0.0053	0.0049	0.125307
15GA1-2	0.315	8.0	15%		0.0049	0.0057	0.0049	0.0052	0.131233
28GA1-1	0.315	8.0	28%		0.0053	0.0049	0.0053	0.0052	0.131233
28GA1-2	0.315	8.0	28%		0.0057	0.0057	0.0072	0.0062	0.15748
45GA1-1	0.315	8.0	45%		0.0084	0.0061	0.0072	0.0072	0.183727
45GA1-2	0.315	8.0	45%		0.0072	0.0065	0.0065	0.0067	0.171027

Table 2: Measurements of the penetration of intergranular corrosion of different thickness of 2024, quenched in water and different concentrations of Aqua-Quench™ 260, followed by aging to the -T4 condition.

was less overall scatter in the results of the polymer quenched panels.

Twenty-four additional panels, eight from a single heat of 3.0 mm sheet, eight from one heat of 5.0 mm sheet, and eight from a single heat of 8.0 mm plate, were also solution heated-treated, quenched, and naturally aged. Two panels of each thickness were quenched in cold water. The balance of panels in each thickness was quenched in three different concentrations of Aqua-Quench™ 260 (an AMS 3025 Type I quenchant). These concentrations were 15%, 28%, and 45% respectively. Three 25 x 25 mm samples were sectioned from each panel and examined at 100X through 500X before and after etching with Keller's Etch [5]. The depth of intergranular corrosion was measured and compared to the water-quenched panels. The results are tabulated in Table 2. The resultant data is shown in Figure 4.

CONCLUSIONS

A series of panels of 2024 was heat-treated to the -T4 condition after quenching in water and different concentrations of an AMS 3025 Type I quenchant. In each case, with the exception of the 8 mm thick plate, the depth of intergranular corrosion measured was equal to or less for the polymer quenched panels than the water quenched panels. At lower concentrations, for the 8 mm thick plate, the Type I quenchant exhibited similar intergranular corrosion as the water quenched panels.

The use of polymer quenchants is very useful to reducing distortion and residual stress in quenched aluminum components while meeting mechanical property requirements and minimizing susceptibility to intergranular corrosion.

REFERENCES

[1] SAE, "AMS 3025E Polyalkalene Glycol Heat Treat Quenchant," SAE, Warren, PA, 2018.

[2] SAE International, "Heat Treatment of Wrought Aluminum Alloy Parts," SAE International, Warrendale, 2015.

[3] X. Xiao, Z. Zhou, C. Liu and L. Cao, "Microstructure and Its Effect on the Intergranular Corrosion Properties of 2024-T3 Aluminum," Crystals, vol. 12, p. 395, 2022.

[4] American Society for Testing of Materials, "ASTM G110-92(2015) Standard Practice for Evaluating Intergranular Corrosion Resistance of Heat Treatable Aluminum Alloys by Immersion in Sodium Chloride + Hydrogen Peroxide Solution," ASTM, Conshohocken, PA, 2015.

[5] G. L. Kehl, The Principles of Metallographic Laboratory Practice, New York: McGraw-Hill, 1949.

ABOUT THE AUTHOR

D. Scott MacKenzie, Ph.D., FASM, is senior research scientist-metallurgy at Quaker Houghton. He is the past president of IFHTSE, and a member of the executive council of IFHTSE. For more information, go to www.quakerhoughton.com.

TONY TENAGLIER
QUALITY CONTROL MANAGER ///
HITCHINER MANUFACTURING

Successful heat treating requires all hands on deck – and a well-thought-out process that considers the needs of both production and quality.

The art of leading the heat-treat team

Leadership is about guiding the team toward the best opportunities and taking action toward getting the required task done. But success can come down to whether the process is appropriate for the team to even be able to succeed. Therefore, leaders in engineering, quality, and production must be aware of the relationship of the process and the operators.

For example, if a heat-treat oven is not calibrated, is it really reasonable to expect an acceptable outcome after using it? There is a reason why AMS2750 has guidelines for indicating frequencies of calibration. It is to ensure the quality is upheld such that whatever product runs through can meet the necessary requirements. But in the world of manufacturing, there are always the opposing forces of production and quality. Production wants to do things faster, sometimes at the expense of quality. And quality would prefer to take their time, but can't take forever and find ways to be efficient in meeting the requirements.

Abraham Lincoln once said, "Give me six hours to chop down a tree and I will spend the first four sharpening the ax." Leadership must view this similarly in the given process. Production wants to get product out the door to make the shipments to the customer — but if the "ax" is dull, it will take longer for the team to produce the results. Putting your best employee on the job with a "dull ax" (or unmaintained furnace) will just result in the process taking longer and potentially creating nonconformances. Instead, taking the time to do what is necessary to make all goals must be incorporated into the process.

Sharpening the ax in terms of metallurgical considerations involves reading up on literature papers and ASM handbooks on metallurgical phenomena to properly design heat-treat cycles. Sharpening the ax even for production scheduling comes down to value stream mapping and incorporating concepts such as lean manufacturing into the process. Sharpening the ax in the case of furnace performance is about doing the proper preventative maintenance programs on the furnaces and following through on the correct calibration, system accuracy tests (SATs), and temperature uniformity surveys (TUS).

Because AMS 2750 outlines these critical requirements as necessary, without these being performed the furnace has a potential to not run in accordance with customer requirements. Therefore, the view of "taking time out of the process" for speed must be changed to one of viewing this time as critical for making the process flow smoothly. Hence, the leader must know when to "sharpen the ax." This is not always that simple to convey in the manufacturing environment.

The first step is to clearly realize the goals or modify or even establish them. Without a goal, how does the person cutting the tree even know where to swing the ax? Get clear on AMS2750 and attend the PRI course. Read it multiple times and even attend the PRI conferences hosted around the world to talk to others in the industry about the requirements. ASM courses on heat treat are also great resources to learn about the metallurgical considerations for the "goals" of why transforming the microstructure is favorable depending on the application.

The second step must be about educating and conveying the importance of "why." When the operators know that a sharp ax will result in a faster process of cutting the tree, they will begin to realize that a properly tuned and maintained furnace will produce more consistent results when heat treating. When the instructions are written in such a way that they are clear and meeting requirements, there is less room for error in interpretation. When the process is scheduled and managed to set a cadence of a steady drum beat, the effort can be more consistently maintained. Short bursts of the ax to cut the tree may get you further into the cutting, but might tire out the employee. Thus, having a steadier cadence of performance is better for overall longevity.

"Why" atoms go to their respective crystallographic structures based on equilibrium phase diagrams and time temperature transformation curves is important to understand when troubleshooting. If a furnace is out of calibration and goes to the wrong temperature and a different phase is produced, the phase diagram will tell you. It is "why" meeting requirements to AMS2750 to keep a furnace properly working and consistent with its performance is important — because if the instruments aren't reading correctly, there could be potential escapes of nonconforming product.

However, it has often been my experience over the years that convincing the production team of the importance of quality-related issues is much like convincing a race car driver that speed bumps for safety are a help and not a hindrance. But the racer wants to get to the finish line as quickly as possible, shaving off time anywhere they can. The regular driver wants to get there safely and within the speed limit. Production wants to hurry things along to satisfy the customer in a desire to provide great service. Quality can seem to hold things up in an attempt to maintain the necessary requirements — seemingly "slowing" the process down from meeting the customer demand for fast delivery. This isn't a new concept and happens anywhere in a manufacturing facility.

Instead of thinking of quality as the police and production as a speeding driver, ask when it's time to sharpen the ax and work smarter, not harder. It's a win-win for production and quality as the tree will get cut down more quickly and will still meet the requirements. For companies to stay sharp in the industry, the time to prepare is often more important than the actual time spent doing the work.

ABOUT THE AUTHOR

Tony Tenaglier is the quality control manager at Hitchiner Manufacturing. He earned both a B.S. in material science engineering and an M.A. in psychology. You can contact Tenaglier at tony_tenaglier@hitchiner.com.

YOUR RESOURCE FOR HEAT TREATING SERVICES

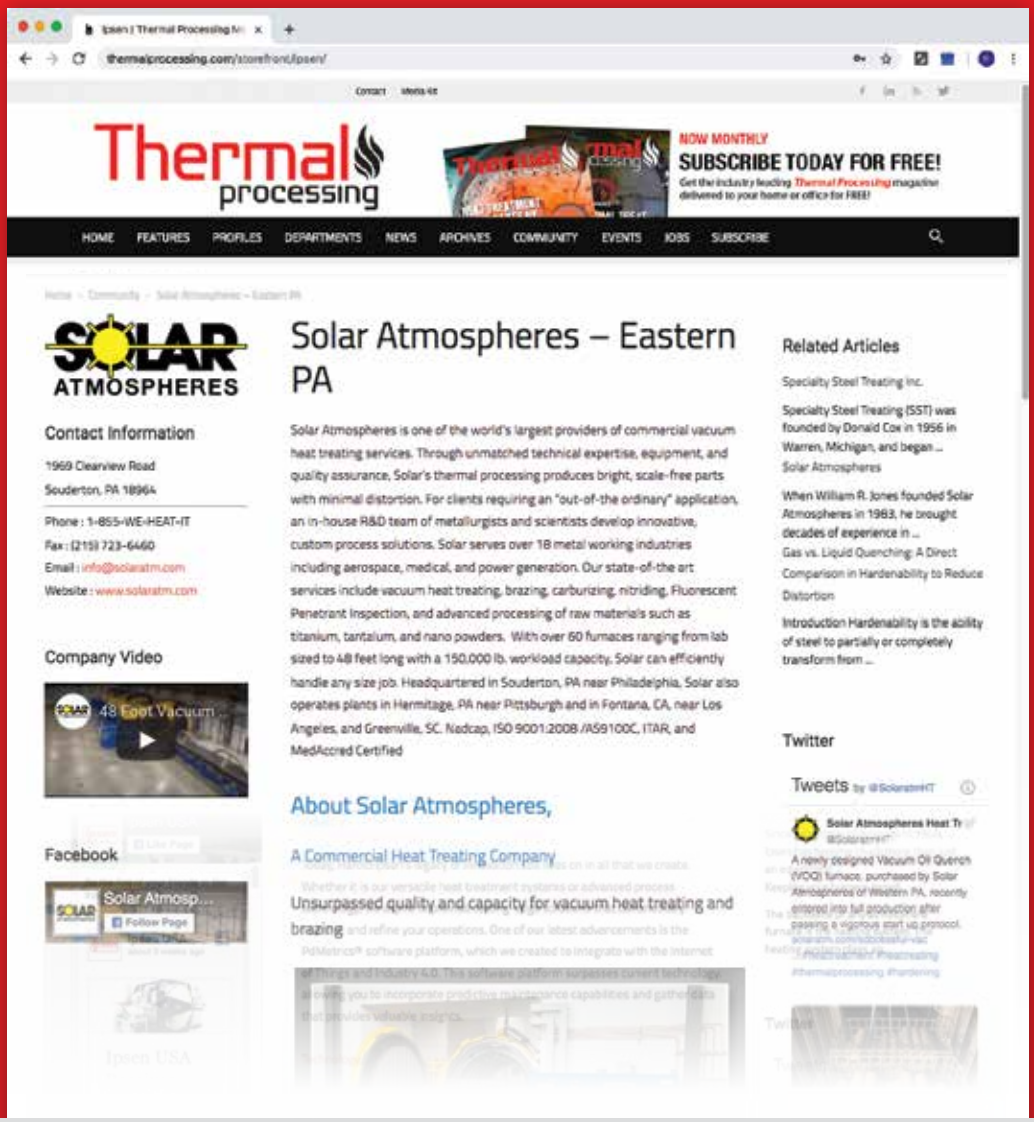

The Thermal Processing Community is your online source for commercial heat treaters, equipment, testing and services.

Search our community for heat treaters by state or services, where you'll find company profiles and contact information.

Our listings are organized so you can easily find companies that meet your heat treating needs.

Find this and more at ThermalProcessing.com.

Not listed in our community storefront? For information on how your company can join and reach more customers, contact

Susan Heinauer – regional sales manager
412.897.0287
susan@thermalprocessing.com

Thermal processing

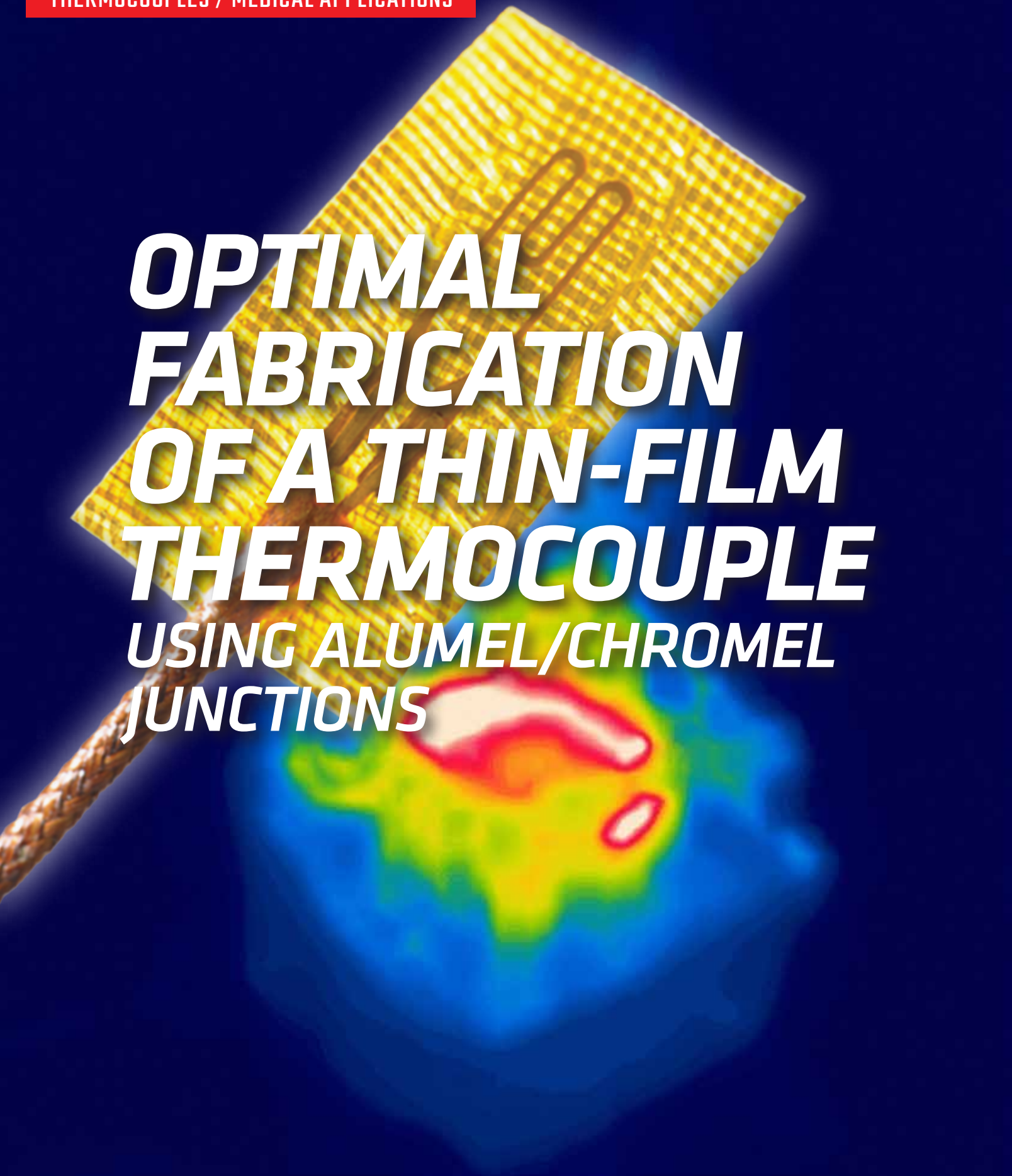

OPTIMAL FABRICATION OF A THIN-FILM THERMOCOUPLE

USING ALUMEL/CHROMEL JUNCTIONS

The TFTC sensor technique can detect temperatures in a unique environment in many cases, and it has potential for measuring cutting temperature.

By DONG MIN KIM, HEE JUNG KWAK, DONG YEOL SHIN, JIN HO PARK, and JUN YOUNG KIM

Thin-film thermocouple (TFTC) technology is a novel measurement method that produces a thermocouple sensor during the deposition process, even though it is a complex surface, to obtain the surface temperature. TFTC is a thin film sensor for measuring temperature by contact methods, consisting of two different metals that can generate thermoelectric forces named "Seebeck effects." In the past decade, there have been many attempts to measure the cutting temperature during machining processes using TFTF sensors. However, research has not yet progressed to optimize the sensor performance or fabrication process. This article studies a preliminary technique for the fabrication of a TFTC sensor on a cutting tool surface and optimizes the deposition conditions, TFTC design, and sensor performance. Chromel and Alumel, which are materials commonly used in K-type thermocouples, were used for the thermal evaporation process. When the Chromel has a nickel-to-chrome ratio of 9:1, low resistivity and minimal variation with increasing temperature were observed. When the contact area of the deposited electrode (+) and (–) poles increased, the resistivity decreased, and the TFTC sensitivity improved. Data acquisition tests using a DAQ system connected to the TFTC sensor show the lowest resistivity in TFTC B and C types are able to measure temperature data. It is expected that the heat generated during the cutting process can be detected using the TFTC sensor with B-type shape and Chromel with a 9:1 nickel-to-chrome ratio.

1 INTRODUCTION

The cutting temperature is a key factor in determining product quality and operation efficiency for machining processes. When a tool contacts the workpiece for the depth of the cut, the result is high-heat generation on the tool, chip, and workpiece. The generated heat energy reaches a temperature of about 1,200°C, depending on the processing conditions. The heat sources are in the frictional, shear, and flank zones at the tool-chip interfaces. The frictional zone has the highest cutting temperature among the heat sources. Frictional heat leads to crater wear, which causes failure, such as tool fracture, shortened tool life, and low-surface integrity. For the reasons presented above, manufacturer and engineer efforts have been made to control cutting temperature generated during the machining process. Up to recently, the cutting temperature has been investigated through experimental measurements and simulation techniques.

Numerical simulation techniques are valuable for predicting cutting temperatures. Tool wear rate can be calculated by the wear model proposed by Usui et al. [1], which is dependent on the contact stress and cutting temperature. Tiffe et al. [2] found optimal cutter edge profiles to reduce tool temperature using the finite element method (FEM) technique. The edge profiles had complex shapes, and the results of their work were beneficial for analyzing the thermal gradient and how it affects tool life. Childs et al. [3] investigated the relationships between temperature, force, and chip geometry for a wide range machining conditions of Ti-alloys using the FEM technique. Elevated temperature influenced the shear failure of Ti64 and the critical strain. The simulated predicted temperature is valuable data for analyzing the cutting mechanisms with changing material properties and failures. Some industries have strict regulations on surface quality; therefore, cutting result predictions are important. Machining temperature is often the main factor that changes material properties, such as microstructure. Imbrogno et al. [4] predicted microstructural and microhardness depending on machining temperature and its effect on surface integrity. As seen in the literature discussed above, machining simulations are useful for assessing the metal-cutting process by predicting cutting temperatures. However, validation is necessary to ascertain the simulation and temperature measurement during machining is required to compare simulated and experimental results.

Many researchers have developed cutting temperature measurement techniques for use during machining operations. These measurement techniques are categorized as contact and non-contact methods. The contact method is applicable in single-point metal cutting processes, such as the turning process. A turning tool does not rotate, unlike tools used in the multi-point metal cutting process. Installing thermocouples onto the cutter is the most typical and easy method for measuring the cutting temperature. Bagherzadeh et al. [5] measured cutting temperature during the cryogenic turning process. The drilled hole of the insert using electrical discharge machining (EDM) is close to the cutting edge. Although using a thermocouple is a stable assessment method, it indirectly measures heat generation from tool-chip interfaces that is transferred through the insert body. Thermal imaging is also a good non-contact technique for determining temperature distributions at tool-chip interfaces. An infrared (IR) camera detects temperature through infrared radiation (IR) during thermal imaging, which has gained significant attention in the machining processes. The IR imagining technique has a constraint of measuring temperature due to cutting fluids [6]. Another non-contact measurement technique involves the use of a two-color fiber pyrometer. This method is analogous to a thermocouple and identifies the data within the spot size (~500 µm). The pyrometer is based on material radiation detection and a predefine term for the emissivity is required [7]. Thermosensitive paints have shown relative variances of temperature but have no way to determine the amount of variation [6]. As indicated in published work, conventional thermal measurement techniques have limitations in obtaining accurate tool-chip interface temperature.

The thin-film thermocouple (TFTC) is a novel technology developed in recent decades and functions as a thermocouple sensor on flat, curved, or any type of surface. Even their small thermal mass allows for significantly faster response times compared to conventional wire sensors [8,9]. Basti et al. [10] deposited TFTCs of Ni-(Ni-Cr) on an alumina cutting tool and fabricated junctions to measure cutting temperatures. TFTC sensor data is suitable for measuring temperature and exhibits a corresponding trend in cutting force variance

Thermocouple layer					Protective layer			References
Deposition Process	Positive (+)		Negative (–)					
	MATERIAL	DESIGN	MATERIAL	DESIGN	DEPOSITION PROCESS	MATERIAL	DESIGN	
DC magnetron sputtering	Ni	Thick 0.5 µm Widths 50–750 µm	Ni–Cr (80:20 ratio in mass %)	Thickness: 0.5 µm Width: ~50–750 µm	DC magnetron sputtering	TiN, TiAlN, or TiAlSiN	Thickness: 3 µm	[10,11]
DC sputtering	WC rhenium (5%)	–	WC rhenum (26%)	–	E-beam evaporation	Al2O3	–	[12–15]
PECVD	NiCr (90:10 ratio)	200 nm	NiSi (97:3 ratio)	200 nm	–	SiNx	1 µm	[16,17]
RF sputtering	Chromel (90:10 ratio)	200 nm	Alumel	200 nm	RF sputtering	Al2O3	435 nm	[18]
Sputtering	Chromel	400 nm	Alumel	400 nm	PECVD	SiNx	800 nm	[19–21]

Table 1: Literature review summary.

[10,11]. Werschmoeller et al. [[12], [13], [14]] attempted fabrication of a micro-arrayed TFTC sensor on a polycrystalline cubic boron nitride (PCBN) cutting tool. The advantage of a micro-arrayed TFTC is the measurement of temperature maps by interpolation. A three-dimensional (3D) map of the data is available instead of thermal imaging data. Li et al. [15] embedded micro-TFTC sensor arrays on a PCBN cutter surface and recorded cutting temperatures. The micro-TFTC has an array design to measure multiple points in the temperature field. TFTC sensors can be used to detect progressive wear. The flank face of the tool is significant to the surface quality. Li et al. [16] and He [17] devised TFTC development process on the flank face of a tool for real-time monitoring of wear progression. The TFTC on the flank face was manufactured in a similar process as that in [15]. The previously mentioned literature indicates the typical TFTC fabrication method is deposition by a sputtering method. The deposited material adheres to the surface. However, high pressures due to the cutting forces damage TFTC sensors.

The strategy for protecting TFTC sensors from extreme friction and temperature is a great challenge because of the damage imparted to the thin-filmed sensor during cutting processes. Kesriklioglu et al. [18] embedded a K-type thermocouple TFTC. In their study, an AlTiN layer coated the upper side on layers of Chromel and Alumel to protect the TFTC sensor. Li et al. [19] suggested a micro-textured tool with a deposited TFTC sensor. The texture of their proposed tool has a depth of about 100 µm via laser beam, while Alumel and Chromel were coated inside the texture using plasma-enhanced chemical vapor deposition (PECVD). Molybdenum disulfide filled in the grooves and acted as a lubricant at the tool-chip interfaces to protect the fabricated TFTC sensors. The micro-textured TFTC sensor exhibited significantly improved performance during the machining process. This design improved the protection of the TFTC sensors under high-pressure and high-temperature environments. However, the preparation process for the fabrication of the grooved tool was inadequate because the complicated procedure was high in cost and time consuming [19, 20, 21].

Table 1 provides a summary of published papers describing TFTC techniques. In the literature, the material combination used for TFTC fabrication was equal to compositions of C- or K-type thermocouples generating electromotive force. The most-used deposition method for the TFTC layer was sputtering. The coating methods used to create the protective layer varied and included methods such as sputtering, e-beam evaporation, and PECVD. Only a few studies have investigated the TFTC fabrication process and design parameter studies for circuit dimensions have been presented only in [10,11]. There is still a lack of knowledge about the effects of circuit design patterns, circuit dimensions, and the ratio of implemented thermocouple materials. The studies are necessary even if they should apply to the cutting-tool surfaces. Still, the circuit design for applying it to the cutting tool surfaces has yet to be discussed. Therefore, a new study is necessary to fabricate an optimal TFTC sensor for measuring cutting temperature.

Materials	Properties		
	Thermal conductivity (W/m/K)	Resistivity (ohm m)	Seebeck coefficient (V/K)
Chromel	19	7.06e– 7	21.7e– 6
Alumel	29.7	2.94e– 7	17.3e– 6

Table 2: Thermal conductivity, resistivity, and Seebeck coefficient values for Chromel and Alumel [27,28].

2 EXPERIMENTAL

2.1 FEM model for thermal-electric potential simulation

This section describes the simulation used to investigate the influence of geometric parameters before fabricating thermoelectric sensors used in machining. The simulation tool is a commercial program that calculates the electromotive force through a thermoelectric module in ANSYS. The boundary condition for the simulated model follows. There are various methods for improving the Seebeck coefficient of materials. Techniques such as hydrazine treatment [22], ionic liquid post-processing [23], alloying [24], control of material alignment [25], and energy filtering through nanoparticle deposition [26] can be employed to enhance the Seebeck coefficient. However, in this work, we focused on creating sensors using commonly available materials from the market without additional processing steps. Alumel and Chromel exhibit a high Seebeck coefficient, enabling sensitive temperature measurements with thermocouples. They also operate reliably in high-temperature environments. Additionally, their suitability for use across a wide temperature range has earned them recognition as industry-standard materials for thermocouples. Therefore, our research concentrated on adjusting the sensor's shape to favor heat conduction without synthesizing new materials through complex processes.

The deposited materials are Chromel and Alumel, which are used in K-type thermocouples, and they were set to (+) and (–) poles, respectively. The initial ambient temperature around the sensor was 25°C. and the other parts in the simulation were set at 50°C. The simulation

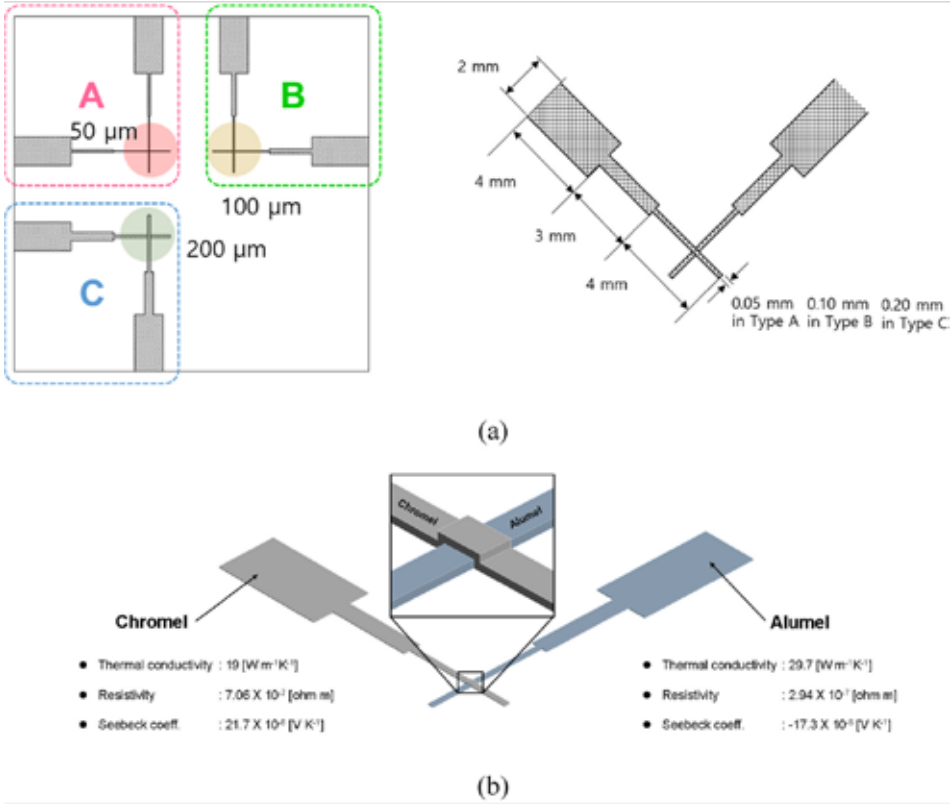

Figure 1: (a) Simulation circuit design for simulation for A, B, and C types; (b) 3D simulation model.

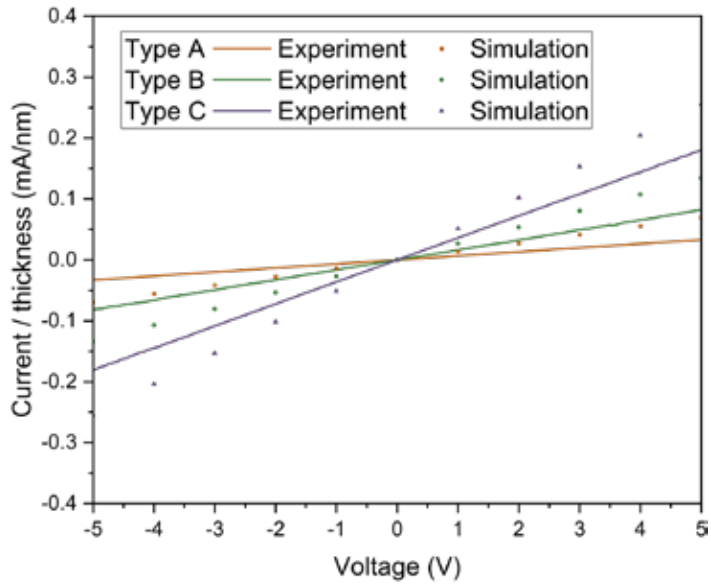

Figure 2: Simulated and experimental data currents for A-, B-, and C-type TFTCs.

model calculated the currents while increasing the potential difference between the Chromel (+) and Alumel (–) electrodes from minus-5 to +5 V. The thermal conductivity, resistivity, and Seebeck coefficients were referred from the literature [27,28], and the coefficient values are represented in Table 2.

We simulated design types A, B, and C, which have 0.05 mm, 0.1 mm, and 0.2 mm of Chromel-Alumel electrode overlap length, respectively. Figure 1a and b show the circuit design used for the simulation. The electro pad dimensions were a width of 2 mm and a length of 4 mm, and the connection two-step lines were 3 mm and 4 mm, respectively. The circuit design was determined by the interferences of the cutting tool clamp and cutting tool surface. The circuit dimension used in this simulation is the case study parameter in the experiment.

Electro pad thermoelements were meshed using hexa type in ANSYS. The minimum mesh size was set to 0.025 mm, and the total number of nodes and elements in the geometry were 104706 and 67787, respectively. The contact element was surface-to-surface contact at the interfaces of the electro pad. Thermal contact behavior is a closed contact type; thermal conduction transfers between two contacting surfaces. The conductive heat-transfer equation is defined by Equation 1 [29]:

$$q = TCC \times (T_t - T_c), \quad \textbf{Equation 1}$$

where q is the heat flux per area, TCC is the thermal contact conductance coefficient, and T_t and T_c are the temperatures of the contact points at target and contact surfaces, respectively.

The electric contact property is implemented with thermal-electric elements, and the solid coupled field element modeled the electric current conduction. The interface definition is determined by equation (2) [29]:

$$J = ECC \times (V_t - V_c), \quad \textbf{Equation 2}$$

where J is the current density for the electric potential degree of freedom (or the electric charge density), ECC is the electric contact conductance for the electric potential degree of freedom (or the electric contact capacitance per unit area), and V_t and V_c are the voltages at the contact points on the target and contact surfaces, respectively.

2.2 Fabrication and performance measurement methods for a thin-film thermocouple (TFTC)

The thermal evaporation method was used to fabricate the K-type TFTC, which included deposition of three materials: Alumel, Chromel, and an insulator. Figure S1 shows the mask used in the experiment. The hot and cold junction in the circuit makes orthogonal contact with the Chromel and Alumel. Four types of junctions, referred to as A, B, C, and D types, were used in this study. A, B, and C junction types have contact areas of 50 µm × 50 µm, 100 µm × 100 µm, and 200 µm × 200 µm, respectively. The electro pad has a width of 2 mm, and this dimension is sufficient to connect the electrode for the DAQ system.

The junction is thin and delicate, which can lead to cracks during deposition. Therefore, we inserted a linked line in the middle of the junction and electrode. Often, a junction crack will be generated during the thermal evaporation process due to the thin linked line. Therefore, first confirmed the influence of the linked line dimension. The D-type junction has an electrode and junction without a step connection line and a square with dimensions of 9 mm × 9 mm to cover the contact and electrode junction. The insulator mask was designed in a 9 mm × 9 mm square shape to cover all junctions.

The thermal deposition method melts the materials using a high current applied to the boat. The initial vacuum pressure was 4.4e 6 Torr. First, we tried to deposit the Alumel material on the flat glass surfaces. The current was ~130-142 A and the deposition rate was 0.03-0.04 nm/s. The boat had a tungsten carbide thickness of 0.5 mm. If the current was set at 100 A, the boat temperature began to increase. Therefore, we set the current to 130 A, and the process

was steady with a deposition rate of 0.03 nm/s. The Chromel material was deposited with a deposition rate of ~0.03-0.05 nm/s with a current of ~134-155 A. The four types of junctions had a deposited Alumel and Chromel thickness of 100 nm, which was measured using an atomic force microscope.

The TFTC will be to measure the temperature at the cutting interface of the tool-chip. Resistivity measurements and scratch tests were carried out to confirm the TFTC performance. Current-voltage (I-V) tests were used to determine the resistivity of the TFTCs, which presented circuit characteristics. The I-V testing process is described as follows: The deposited sample with the four types of TFTC was held on a hot plate. Then, the I-V test cathode and anode (Keithley 2400 in Figure S2b) were connected to the Alumel and Chromel electro pads. The input voltage was swept from minus-5 to +5 V, and the current values were measured while the hot plate temperature was increased from 50°C to 150°C. The connection wires are used in K-type Extension (OMEGA Engineering, Model: EXPP-K-24S-100).

A scratch test was performed after each material was deposited in a 2.5 mm × 1.5 mm area (thickness of 100 nm) on flat glass substrates. The sample was scratched with a probe with strength increasing gradually, from 0 to 14 mN (NST3 nano scratch tester in Figure S2c).

3. RESULTS AND DISCUSSION

3.1 FEM simulation comparison with experimental data

Figure 2 shows the simulated data and experimental data for response currents of A-, B-, and C-type junctions. The experimentally fabricated circuit has a thickness of about 75 nm. However, this circuit is very thin relative to the area. Creating a simulation model at a real scale requires making many meshes to improve the mesh quality. This causes an increase in computational time and requires high computational resources. Reducing the amount of mesh saves computational time but reduces mesh quality. The quality of the mesh plays a significant role in the accuracy and stability of numerical computation. Saving computational time while increasing the mesh quality, we used an arbitrary TFTC thickness of approximately 50 µm.

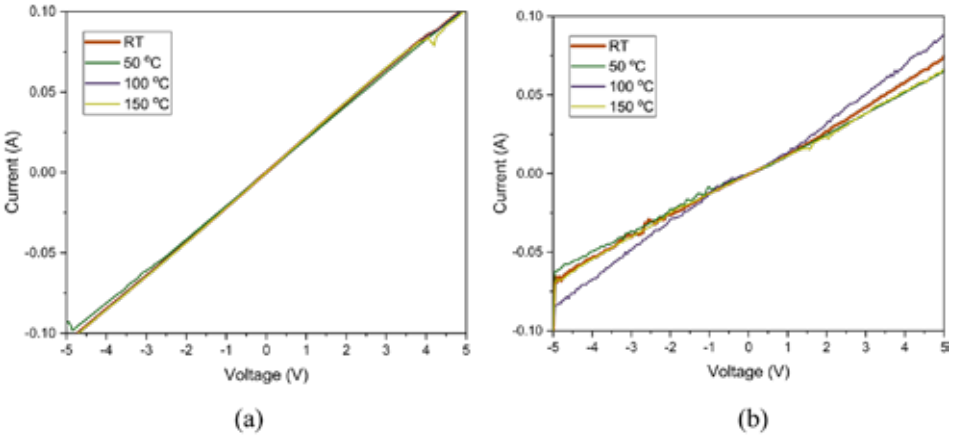

Figure 3: I-V graph of a 1.5 mm × 1.5 mm junction TFTC device using Alumel and Chromel with Ni:Cr ratios of (a) 9:1 and (b) 8:2.

Temperature:	Room Temperature	50 °C	100 °C	150 °C
Chromel with Ni:Cr of 9:1 [ohm-cm]	2.060e−3	2.158e−3	2.060e−3	2.060e−3
Chromel with Ni:Cr of 8:2 [ohm-cm]	3.440e−3	3.754e−3	2.919e−3	3.916e−3

Table 3: Calculated resistivity values of the 1.5 mm × 1.5 mm junction TFTC device.

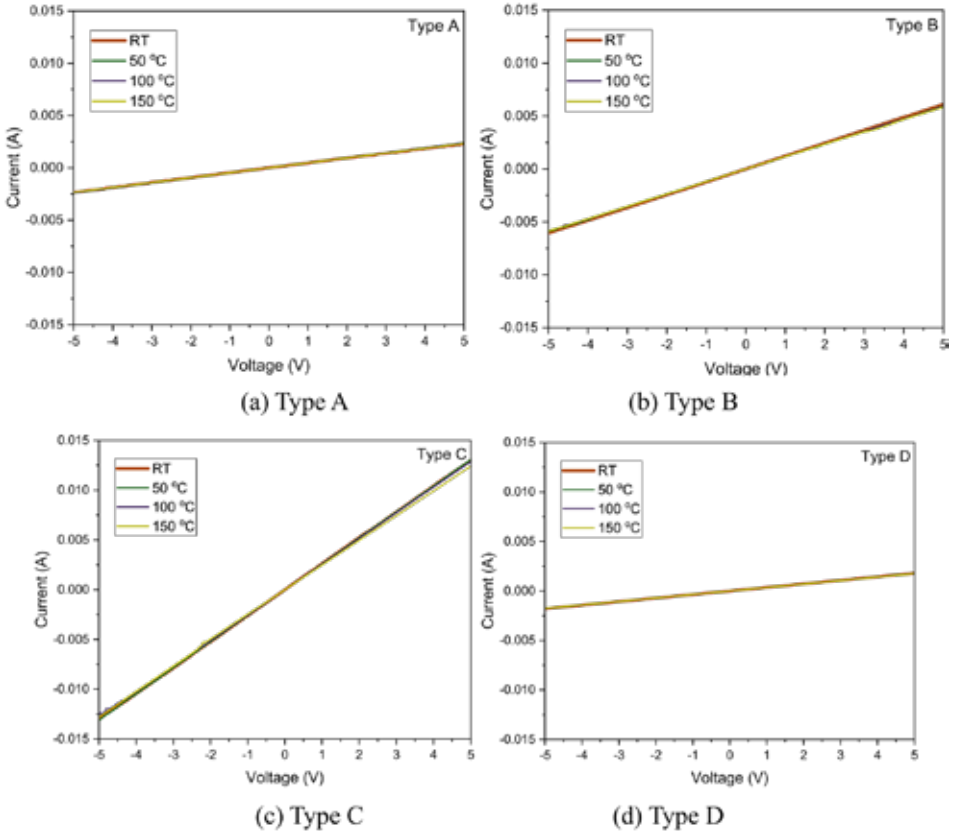

Figure 4: I-V graphs of TFTCs with a Chromel Ni:Cr ratio of 9:1 as a function of temperature. (a) Type A (b) Type B (c) Type C (d) Type D.

The plot comparing experimental and simulated results in Figure 2 is represented with units of current per thickness (mA/nm). The slope of the current per thickness changes; it increases by junction type in the order of A, B, and C types. The C-type has the largest contact area between the Chromel and Alumel electrodes. The reciprocal of the slope provides the resistance value, and resistance and resistivity are proportional; large resistance means large resistivity [30]. This means that the C-type, which has the largest area, has the smallest resistivity. When the contact area is small, the resistance increases because the area in which electrons can move is limited when a thermo-electromotive force is generated by the thermocouple.

In addition, we can determine the thermoelectric characteristics of the thin-film through the measured resistance [31]. Since the performance may be degraded if the resistance of the contact area is high,

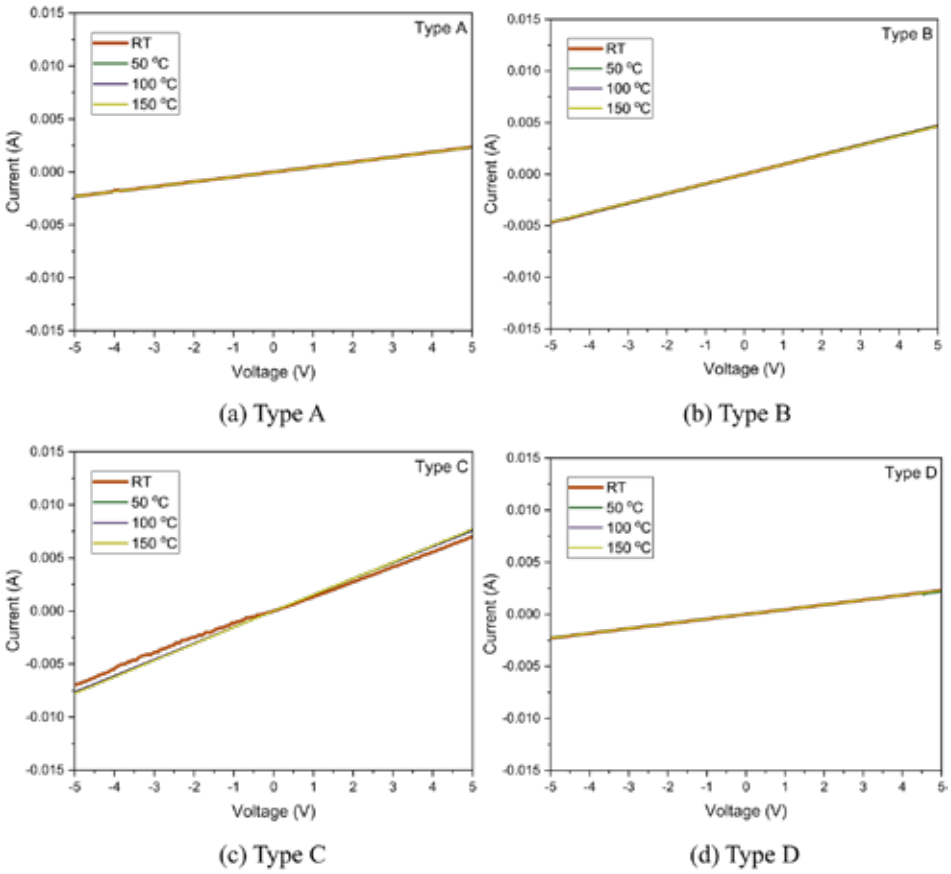

Figure 5: I-V graphs of TFTCs with a Chromel Ni:Cr ratio of 8:2 as a function of temperature. (a) Type A (b) Type B (c) Type C (d) Type D.

the smaller the area, the larger the resistance and possible decrease in thermocouple performance [32]. These results indicate that a large electrode contact area has high sensitivity with respect to the TFTC and the highest performance may be expected in type C.

The simulation model calculated the current density (A/mm^2) on the electrode gap area. The current density values of TFTC A, B, and C types were, on average, 9.4e7 A/mm2, 3.1e8 A/mm2, and 3.3e8 A/mm^2, respectively (Figure S3). The A-type TFTC has the lowest value of current density, which means its relative resistance is higher than the other TFTC types. The A-type TFTC may exhibit low performance compared to the other types. The B- and C-type TFTCs have current density values of more than 3.0e8 A/mm2; the relative resistance is lower than the A-type TFTC. Therefore, this simulation model is a useable model to approximate TFTC performance according to circuit design.

3.2 Principal TFTC analysis

3.2.1 Influence of the chromel Ni to Cr ratio

The TFTC should exhibit stable performance at high temperatures, such as those in the machining process. Even with exposure to extreme cutting temperatures, a single electrode will typically exhibit low sensitivity depending on increasing temperature. This section discusses the resistivity as a function of ratio of nickel (Ni) to chrome (Cr) in the Chromel used for TFTC fabrication.

The two types of raw Chromel materials available in the commercial market have Ni and Cr ratios of 9:1 and 8:2, which consist of Ni-Cr of 90%-10% and Ni-Cr of 80%-20%, respectively. Alumel has consist of Ni-Al-Mn of 95%-2%-2%, respectively. These two types of Chromel were deposited to experimentally determine the influence of the Ni:Cr ratio. Alumel is only available in a single ratio in the market and is therefore excluded from this section. TFTCs composed of Alumel and Chromel with two ratio types were fabricated using a metal mask with a large area of 1.5 mm × 1.5 mm. Figure S4 shows the measurement setup used to observe the I-V performance as a function of Chromel ratio (8:2 and 9:1) with increasing temperature (by heating the hot plate).

Figure 3 shows the I-V graph according to temperature as Chromel ratios of 8:2 and 9:1, presented in Figure 3a and b, respectively. The resistivity of each sample was calculated to compare their electrical properties. The resistivity (ρ) of a thin-film is defined by Equation 3:

$$J = ECC \times (V_t - V_c), \qquad \textbf{Equation 3}$$

where, ρ is a resistivity (ohm-cm), t is the TFTC thickness, and I and V are the current and voltage, respectively.

Table 3 presents the TFTC resistivity calculated using Equation 3. Chromel with a Ni:Cr ratio of 9:1 exhibits minimal sensitivity dependence on temperature, while that at a 8:2 ratio shows a slight change. However, the resistivity variation with increasing temperature is low enough to be ignored. Therefore, the TFTC can be composed of Chromel with Ni:Cr ratios of either 9:1 or 8:2. (Cross Alumel).

3.2.2 Influence of TFTC design type

In this section, the influence of the TFTC design type was analyzed to determine their performance. The TFTC types (A, B, C, and D) were presented in Section 3. Chromel (9:1 Ni:Cr ratio) and Alumel were deposited by the thermal deposition process. The detailed process conditions are described in Section 3.

Figure 4 and Figure S5 show an I-V graph of Alumel and Chromel deposited for A, B, C, and D types (Specified measured data shown in Figure 4 (a to d), respectively). Figure 4 represent the I-V slope results for each TFTC type. The resistivity of each TFTC type shows slight differences. These results suggest the I-V behavior and temperature have no relationship in the same contact area. However, the slope of each TFTC type with the same temperature value exhibits significant differences among the TFTC types (Figure S5). The slope of the graph increases as the junction area is increased, suggesting the resistivity of the TFTC decreases as the junction area increases. In addition, types A and D have calculated resistivity values that are almost the same. This means the linked line has little effect on the electrical characteristics of TFTC and is reasonable to design a three-stage structure for a TFTC that will be applied to an actual tool. Figure 5 and Figure S6 show I-V graphs of TFTCs with Alumel and 8:2 Chromel that also confirmed the resistivity in the same area was almost the same with varying temperature. When comparing the TFTC area at the same temperature, the resistivity decreased as the area increased. These results indicate the TFTC Chromel Ni:Cr ratio has minimal influence on performance.

Table 4 shows the calculated resistivity results for each TFTC type. The highest resistivity of 0.13 Ω-cm was observed in the D-type TFTC. This high resistivity means the flowing current is interrupted and leads to reduced performance. Similar results are observed for the D-type TFTC with Chromel Ni:Cr ratio of 8:2. The lowest calculated resistivity values are ~0.017-0.018 and ~0.03-0.032 Ω-cm, which correspond to C-type TFTCs with Chromel Ni:Cr ratios of 9:1 and 8:2, respectively.

This measurement data means that thermoelectromotive force easily is generated in the C-type design. In section 3.1, C-type design is simulated to have low current density, that means the thermoelectron is a relative easy flow than other designs. No significant change in resistivity is observed with changing temperature. Therefore, the C-type TFTC may be suitable for measuring temperature data during the machining process.

3.2.3 Scratch test results for TFTC adhesion

For the deposited Alumel and Chromel to function properly as sensors, it is important they are well attached to the deposited glass or tool. Therefore, a scratch test was conducted on a sample deposited on a flat glass substrate to determine how much force the materials could withstand. Figure S7 shows an image of the damaged film and the penetration depth. Figure S7- shows the thin Alumel film peeled off at the 0.24-mm point when the applied force was about 6.7 mN. On the other hand, the Chromel thin-film was not wholly peeled off for both Chromel Ni:Cr ratios of 9:1 and 8:2 (Figure S7). However, when looking at the measured image, dig was confirmed to some extent. In addition, when comparing the penetration depth of the two materials, Chromel with a Ni:Cr ratio of 9:1 had a penetration depth of ~300.3 nm while that with 8:2 ratio was ~289.3 nm. It was confirmed the degree of peel off was similar for the two Ni:Cr ratios. Therefore, the Chromel adhesion is better than that of Alumel for glass substrates, and there is little difference in adhesion depending on the Ni:Cr ratio of the Chromel.

3.2.4 The EDS component analysis

Figure S8 shows the SEM images (NOVA NanoSEM 230, FEI, USA) for the surfaces of deposited Chromel/Alumel and their analysis compositions by EDS. The SEM images of the Alumel-Chromel film layer are cleared without defects. The EDS data shows that Alumel consists of a weight percent of 77.3% of Ni, 16.2% of Mn, 2% of Al, and 4% of Si. The standard Alumel compositions are 95% of Ni, 2% of Al, 2% of Mn, and 1% of Si. In Chromel, the compositions of it are 75.3% of Ni and 24.7% of Cr. Chromel is also different from standard composition Chromel (9:1, Ni-Cr). The compositions differ from the standard due to the glass substrate, an insulation material, but both deposited films are useful for measuring the temperature. The acquired temperature is described in the next section.

Chromel Ni:Cr Ratio	Type	At Room Temperature	At 50 °C	At 100 °C	At 150 °C
9:1	A	0.096	0.094	0.095	0.097
	B	0.037	0.038	0.038	0.038
	C	0.017	0.017	0.018	0.018
	D	0.13	0.128	0.13	0.13
8:2	A	0.097	0.097	0.098	0.098
	B	0.048	0.048	0.049	0.049
	C	0.032	0.03	0.03	0.029
	D	0.100	0.100	0.100	0.099

Table 4: Calculated resistivity results for each TFTC type.

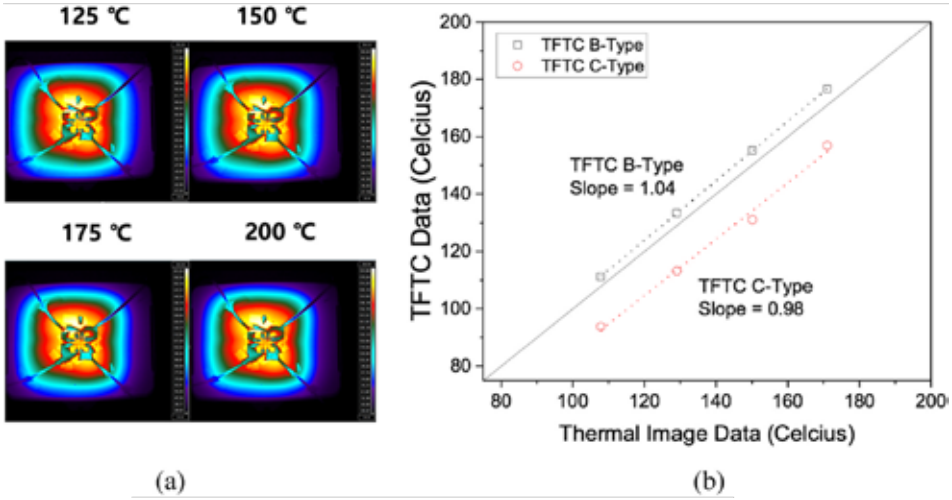

Figure 6: Comparison of (a) thermal imaging and (b) TFTC sensor data (with Chromel having a Ni:Cr ratio of 8:2).

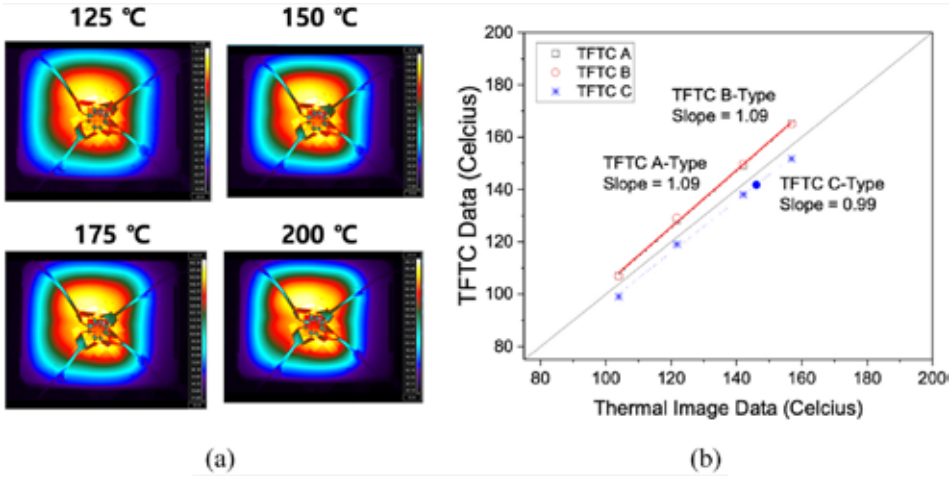

Figure 7: Comparison of (a) thermal imaging and (b) TFTC sensor data (with Chromel having a Ni:Cr ratio of 9:1).

3.3 TFTC performance in acquiring temperature data through data acquisition (DAQ)

In this section, experiments were conducted to obtain TFTC performance. A DAQ system (WebDAQ 904, measurement computing., Inc) was used to collect the TFTC temperature data while increasing the reference temperature (hot plate temperature). The TFTC data was compared with two types of data collected using an IR-thermal imaging camera (A700sc, FLIR., Inc.) and a K-type thermocouple (Omega Eng.). The IR camera has a 1.5-m minimum focus length, and its measuring range is 67.8 mm in width and 50.8 mm in length. The DAQ system saved the temperature data from the TFTC sensors. The hot plate was used to control the temperature as it heated the back of the TFTC sensors from 125 to 200°C. TFTC sensor data were compared

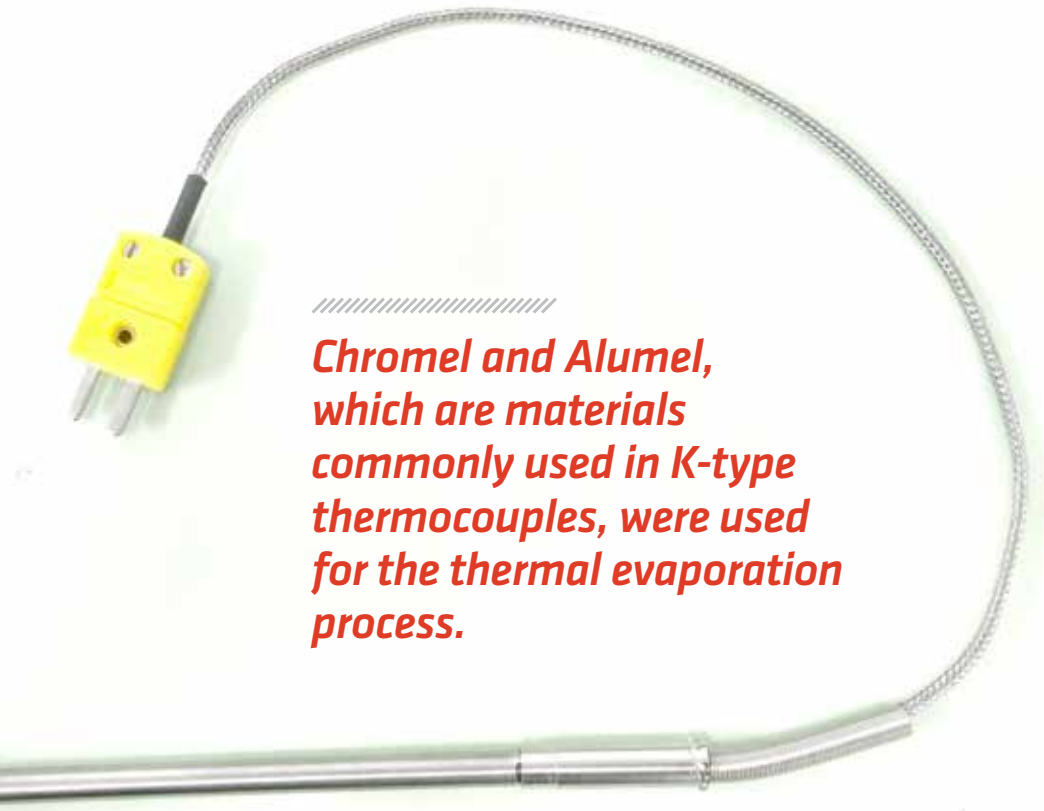

Chromel and Alumel, which are materials commonly used in K-type thermocouples, were used for the thermal evaporation process.

with the IR-imaging data and K-type thermocouple data collected at the same time.

Figure 6 presents the IR-thermal imaging data and a graph comparing the thermal image data to the TFTF sensor data (with an 8:2 Ni:Cr ratio Chromel electrode). The thermal image data is the average of the red rectangular box indicated in the thermal image. Data could not be obtained for the A and D-type TFTCs using the DAQ system. This result is analogous to the trend observed in Table 4 and is due to the small contact area between the (+) and (–) electrode leading to increased resistivity of the TFTC sensor. Slopes of 1.04 and 0.98 were obtained for TFTC B and C types, respectively. Both B and C-type TFTCs have slopes close to a value of one, and their sensitivity is capable of obtaining useable temperature data.

When using Chromel with a Ni:Cr ratio of 9:1 as the TFTC sensor electrode, the DAQ system is able to get data from the A-type TFTC (Figure 7). This Chromel (9:1 Ni:Cr ratio) has low resistivity, as described in the previous section (Figure 3 and Table 3), and the electron flow moves more easily by the electromotive forces. The B and C-type TFTCs have higher sensitivity with this Ni:Cr Chromel ratio. This result is related to the low resistivity of the Chromel with a 9:1 Ni:Cr ratio. Therefore, it is necessary to use the 9:1 Ni:Cr ratio Chromel to obtain electrodes with relatively low resistance and high sensitivity. The high composition of nickel increases the electric forces, improves the performances of the TFTC sensor. The type-B TFTC will be applied to a cutting tool surface for measuring cutting temperatures.

4 SUMMARY AND CONCLUSIONS

The TFTC sensor technique can detect temperatures in a unique environment in many cases, as determined by the literature review, and has potential for measuring cutting temperature. Cutting temperature generation in machining is a significant factor for machining process optimization. This article optimized the TFTC fabrication process for use in the machining field. A simulation model was constructed, using a thermoelectric simulation module in ANSYS to predict the current in different TFTC types. As a result of the simulation, the value of the current responded to increased input voltage similar to that observed in the experiment. This model can be used to predict TFTC sensor performance. TFTC sensor performance was tested for a fundamental TFTC shape with different Chromel raw material ratios (8:2 and 9:1 of nickel and chrome). The TFTC sensor with Chromel, having an 8:2 Ni:Cr ratio, exhibited unstable sensitivity with increasing temperature, while the TFTC sensor with Chromel, having a 9:1 Ni:Cr ratio, exhibited stable sensitivity. A comparison of different TFTC types was made to evaluate their performance. If the electrode contact area of the TFTC sensor is small, its sensitivity was low. The C-type TFTC had the largest electrode contact area and the highest sensitivity. However, no sensitivity variation was observed in the TFTC sensor with increasing temperature. TFTC sensor resistivity was calculated using I-V data; the C-type TFTC had the lowest resistivity due to its largest electrode contact area. When Chromel with a Ni:Cr ratio of 9:1 was used, the resistivity was lower than that with a Ni:Cr ratio of 8:2. The Alumel electrode exhibited lower scratch strength compared to the Chromel electrode, and the Chromel Ni:Cr ratio had no influence on scratch strength. The temperature data was obtained using a DAQ system connected to the TFTC sensors. The B- and C-type TFTCs with an 8:2 Ni:Cr ratio Chromel electrode could sense temperature variation while the other TFTC sensors did not operate under the same conditions. A-, B-, and C-type TFTCs with a 9:1 Ni:Cr ratio Chromel electrode were able to detect the temperature data with the DAQ system. The highest sensitivity was observed for the B-type TFTC with a 9:1 Ni:Cr ratio Chromel electrode.

In conclusion, a TFTC sensor for a DAQ system used during machining operation should be constructed with a large electrode contact area and a Chromel Ni:Cr ratio of 9:1 for high performance. The TFTC sensor with optimized design and fabrication process determined by this study will be integrated on tool rake surfaces similar to those illustrated in Figure S9. This sensor technology will be able to measure the cutting temperature during machining using unique materials (e.g., Inconel, titanium, carbon-fiber reinforced polymer, or biomaterials, such as bone), and will be a useful technology to analyze their cutting principles.

CREDIT AUTHORSHIP CONTRIBUTION STATEMENT

Dong Min Kim: Writing – original draft, Formal analysis, Conceptualization. Hee Jung Kwak: Writing – original draft, Data curation. Dong Yeol Shin: Writing – original draft, Software, Data curation. Jin Ho Park: Data curation. Jun Young Kim: Writing – review & editing, Writing – original draft, Resources, Formal analysis, Conceptualization.

DECLARATION OF COMPETING INTEREST

The authors declare that they have no known competing financial

interests or personal relationships that could have appeared to influence the work reported in this paper.

APPENDIX A: SUPPLEMENTARY DATA

Supplementary data to this article can be found online at https://doi.org/10.1016/j.heliyon.2024.e26128.

ACKNOWLEDGMENTS

This research was supported by the National Research Foundation of Korea (NRF) funded by the Ministry of Science and ICT of Korea (2020R1C1C1008113). Also, this work was supported by the National Research Foundation of Korea (NRF) grant funded by the Korea government (MSIT) (No. RS-2023-00222166). This research was also supported by the GNU-Samsung Display Center.

REFERENCES

[1] E. Usui, T. Shirakashi, T. Kitagawa. Analytical prediction of cutting tool wear. Wear, 100 1–3 (1984), pp. 129-151.

[2] M. Tiffe, R. Aßmuth, J. Saelzer, D. Biermann. Investigation on cutting edge preparation and FEM assisted optimization of the cutting edge micro shape for machining of nickel-base alloy. Prod. Eng. Res. Dev., 13 (2019), pp. 459-467.

[3] T.H.C. Childs, P.J. Arrazola, P. Aristimuno, A. Garay, IrantzuSacristan. Ti6Al4V metal cutting chip formation experiments and modelling over a wide range of cutting speeds. J. Mater. Process. Technol., 255 (2018), pp. 898-913.

[4] S. Imbrogno, S. Rinaldi, D. Umbrello, L. Filice, R. Franchi, A.D. Prete. A physically based constitutive model for predicting the surface integrity in machining of Waspaloy Mater. Des., 152 15 (2018), pp. 140-155.

[5] A. Bagherzadeh, E. Budak. Investigation of machinability in turning of difficult-to-cut materials using a new cryogenic cooling approach. Tribol. Int., 119 (2018), pp. 510-520.

[6] D. Soler, P.X. Aristimuño, M. Saez-de-Buruaga, A. Garay, P.J. Arrazola. New calibration method to measure rake face temperature of the tool during dry orthogonal cutting using thermography. Appl. Therm. Eng., 137 5 (2018), pp. 74-82.

[7] J. Saelzer, S. Berger, I. Iovkov, A. Zabel, D. Biermann. In-situ measurement of rake face temperatures in orthogonal cutting. CIRP Ann-Manuf. Technol., 69 (2020), pp. 61-64.

[8] X. Zhao, K. Yang, Y. Wang, Y. Chen, H. Jiang. Stability and thermoelectric properties of ITON:Pt thin film thermocouples. J. Mater. Sci. Mater. Electron., 27 (2016), pp. 1725-1729.

[9] X. Zhao, H. Li, Y. Chen, H. Jiang. Preparation and thermoelectric characteristics of ITO/Pt thin film thermocouples on Ni-based superalloy substrate. Vacuum, 140 (2017), pp. 116-120.

[10] A. Basti, T. Obikawa, J. Shinozuka. Tools with built-in thin film thermocouple sensors for monitoring cutting temperature. Int. J. Mach. Tools Manuf., 47 5 (2007), pp. 793-798.

[11] J. Shinozuka, A. Basti, T. Obikawa. Development of cutting tool with built-in thin film thermocouples for measuring high temperature fields in metal cutting processes. J. Manuf. Sci. Eng.-Trans. ASME., 130 3 (2008), Article 034501.

[12] D. Werschmoeller, K. I Ehmann, X. Li. Tool embedded thin film microsensors for monitoring thermal phenomena at tool-workpiece interface during machining. J. Manuf. Sci. Eng.-Trans. ASME., 133 2 (2011), Article 021007.

[13] D. Werschmoeller, X. Li. Measurement of tool internal temperatures in the tool–chip contact region by embedded micro thin film thermocouples. J. Manuf. Process., 13 2 (2011), pp. 147-152.

[14] D. Werschmoeller, X. Li, K. Ehmann. Measurement of transient tool-internal temperature fields during hard turning by insert-embedded thin film sensors. J. Manuf. Sci. Eng.-Trans. ASME, 134 6 (2012), Article 061004.

[15] L. Li, B. Li, K.F. Ehmann, X. Li. A thermo-mechanical model of dry orthogonal cutting and its experimental validation through embedded micro-scale thin film thermocouple arrays in PCBN tooling. Int. J. Mach. Tools Manuf., 70 (2013), pp. 70-87.

[16] T. Li, T. Shi, Z. Tang, G. Liao, J. Duan, J. Han, Z. He. Real-time tool wear monitoring using thin-film thermocouple. J. Mater. Process. Technol., 288 (2021), Article 116901.

[17] Z. He, T. Shi, J. Xuan, T. Li. Research on tool wear prediction based on temperature signals and deep learning. Wear, 478–479 (2021), Article 203902.

[18] S. Kesriklioglu, J.D. Morrow, F.E. Pfefferkorn. Tool–chip interface temperature measurement in interrupted and continuous oblique cutting. J. Manuf. Sci. Eng.-Trans. ASME, 140 5 (2018), Article 51013.

[19] J. Li, B. Tao, S. Huang, Z. Yin. Built-in thin film thermocouples in surface textures of cemented carbide tools for cutting temperature measurement. Sens. Actuator A-Phys., 279 15 (2018), pp. 663-670.

[20] J. Li, B. Tao, S. Huang, Z. Yin. Cutting tools embedded with thin film thermocouples vertically to the rake face for temperature measurement. Sens. Actuator A-Phys., 296 (1) (2019), pp. 392-399.

[21] T. Li, T. Shi, Z. Tang, G. Liao, J. Han, J. Duan. Temperature monitoring of the tool-chip interface for PCBN tools using built-in thin-film thermocouples in turning of titanium alloy. J. Mater. Process. Technol., 275 (2020), Article 116376.

[22] T.A. Yemata, Y. Zheng, A.K.K. Kyaw, X. Wang, J. Song, W.S. Chin, J. Xu. Modulation of the doping level of PEDOT: PSS film by treatment with hydrazine to improve the Seebeck coefficient. RSC Adv., 10 (3) (2020), pp. 1786-1792.

[23] Nitin Saxena, et al. Ionic liquids as post-treatment agents for simultaneous improvement of Seebeck coefficient and electrical conductivity in PEDOT: PSS Films ACS Appl. Mater. Interfaces, 11 (8) (2019), pp. 8060-8071.

[24] Z. Huang, D. Wang, C. Li, J. Wang, G. Wang, L.D. Zhao. Improving the thermoelectric performance of p-type PbSe via synergistically enhancing the Seebeck coefficient and reducing electronic thermal conductivity. J. Mater. Chem. A, 8 (9) (2020), pp. 4931-4937.

[25] A. Gunawan, P. Tarakeshwar, V. Mujica, D.A. Buttry, P.E. Phelan. "Improving Seebeck coefficient of thermoelectrochemical cells by controlling ligand complexation at metal redox centers. Appl. Phys. Lett., 118 (2021), p. 25.

[26] Xin Guan, Jianyong Ouyang. Enhancement of the Seebeck coefficient of organic thermoelectric materials via energy filtering of charge carriers. CCS Chem., 3 (10) (2021), pp. 2415-2427.

[27] Concept Alloys Intellectual Property, Concept Alloys (2016).

[28] E. Rathakrishnan. Instrumentation, Measurements and Experiments in Fluids. CRC Press (2007).

[29] ANSYS Contact Technology Guide, Ansys (2004).

[30] M. Naftaly, S. Das, J. Gallop, K. Pan, F. Alkhalil, D. Kariyapperuma, S. Constant, C. Ramsdale L. Hao. Sheet resistance measurements of conductive thin films: a comparison of techniques. Electronics, 10 8 (2021), p. 960.

[31] K.G. Kreider, G. Gillen. High temperature materials for thin-film thermocouples on silicon wafers. Thin Solid Films, 376 (1) (2000), pp. 32-37.

[32] F.I. Igorevich. Thermocouple Condition Monitoring Using Thermocouple Resistance. Experimental Study IEEE (2020), Article 19691094.

ABOUT THE AUTHORS

Dong Min Kim is with the Dongnam Division, Korea Institute of Industrial Technology (KITECH). Hee Jung Kwak, Jin Ho Park, and Jun Young Kim are with the Department of Semiconductor Engineering, Gyeongsang National University. Dong Yeol Shin is with the Autonomous Manufacturing Process R&D Department, Korea Institute of Industrial Technology (KITECH).

THERMAL PROCESSING MEDIA PORTAL

Thermal Processing's online portal is your gateway to social media news and information resources from manufacturers and service providers in the heat-treating industry. You'll find links to social media as well as webinars, blogs and videos.

This quick-and-easy resource is just a click away at thermalprocessing.com.

Thermal processing

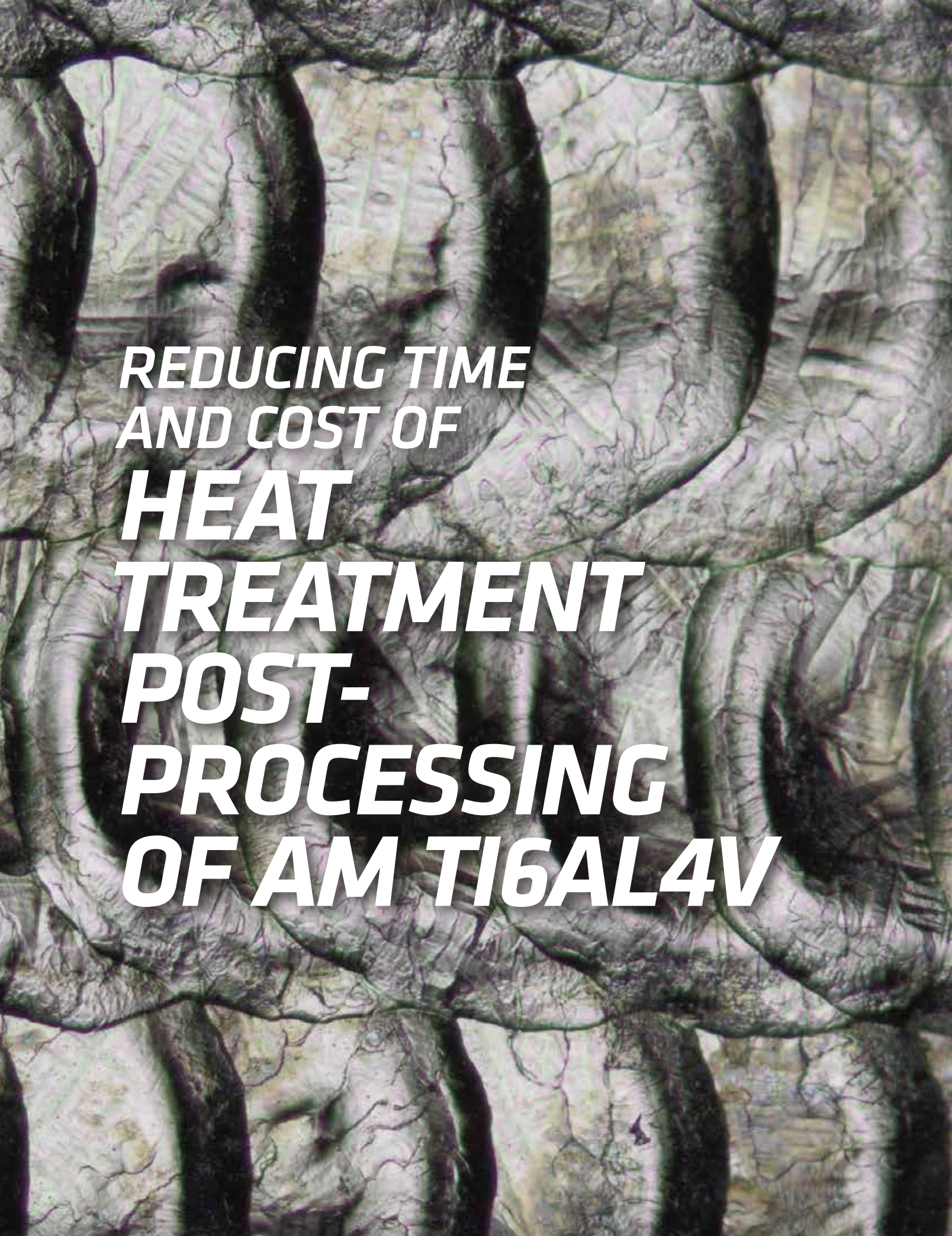

REDUCING TIME AND COST OF HEAT TREATMENT POST-PROCESSING OF AM TI6AL4V

An alternative vacuum heat-treatment cycle, considering all the technical aspects of additive manufacturing, can be used to save time and money.

By DEAN KOUPRIANOFF and WILLIE DU PREEZ

The unique microstructure of Ti6Al4V produced through laser powder bed fusion (LPBF) displays high-tensile strength with low elongation in the as-built state. To obtain desired material properties that comply with standards for Ti6Al4V products, further post-processing is needed. Conventional practice prescribes that the required tensile properties can be achieved with time-consuming post-processing heat treatment of LPBF parts, most of which use air or water quenching that causes surface modification, such as oxidation, when applied to Ti6Al4V. The aim of this work was to develop an alternative heat-treatment process that would retain the benefit of additive manufacturing (AM) but reduce the related processing time and cost, while still complying with the part property specifications. A new heat-treatment cycle was hypothesized and tailored, resulting from a critical analysis of current practice found in literature and practiced in the Centre for Rapid Prototyping and Manufacturing (CRPM) of the Central University of Technology, Free State, based on the need for a quick and cost-effective cycle. By comparing the obtained material properties and microstructure with those of other common heat treatments, the cycle was found to be faster, lasting only four hours in total, and the material properties were superior to those of existing cycles. A high yield stress of 987 MPa was obtained while retaining a good elongation of 16 percent.

1 INTRODUCTION

The additive manufacturing (AM) application market is growing considerably for medical and aerospace applications [1]. Titanium alloys such as Ti6Al4V are especially desired due to the established market, biocompatibility, and high specific strength. Ti6Al4V is an alpha (hcp) + beta (bcc) alloy, which, depending on the processing, can deliver Widmanstätten, equiaxed, and bimodal microstructures with various microstructural parameters, all of which affect the mechanical properties [2]. Martensite formation in Ti6Al4V is based on the formation of an alpha phase supersaturated with substitutional vanadium during rapid cooling. Martensite decomposition generally follows a path of depleting the supersaturated vanadium in the alpha phase through precipitation of the beta phase along the grain boundaries upon heating. The ultra-fine martensitic microstructures with columnar prior-beta grains are unique to laser AM processes and differ for each specific process and parameter set [3]. Therefore, considerable research continues to qualify AM parts made from Ti6Al4V for medical implants and aerospace components. How the AM processes influence the microstructure is an important factor being investigated. More specifically, for certifying AM, many topical standards, including post-processing, are lacking [4], [5], [6]. Aerospace requires good tensile and fatigue properties. Ensuring the material complies with these standards will allow acceptance and safe implementation in safety-critical applications such as aircraft structural components. Many different post-processing heat treatments have been investigated to obtain the desired properties. Not only should these meet the required standards but for implementation in industry, three important factors related to laser powder bed fusion (LPBF) must be considered: residual stress, the feasibility of removing surface contamination resulting from thermal post-processing, and time.

It is important to tailor the microstructure and resulting mechanical properties of LPBF Ti6Al4V parts for specific industrial applications. Conventional heat treatment of Ti6Al4V does not apply for LPBF Ti6Al4V because the microstructure of LPBF parts differs from that of forged and cast Ti6Al4V. One of the important differences is that as-built LPBF Ti6Al4V parts display a very fine martensitic microstructure. This results from the kinetics during LPBF of Ti6Al4V, which differ from conventional forming processes [7]. Due to rapid solidification, various effects arise — among these are the generation of martensitic microstructure, induction of residual stresses, and formation of non-equilibrium phases [8], [9], [10]. The typical as-built yield strength for Ti6Al4V is approximately 1,150 MPa with 6.5% elongation [11]. The Ti6Al4V(ELI) specification for powder bed fusion processes (ASTM F3001–14) specifies that the minimum tensile strength, yield strength (YS) and elongation values for the thermally treated condition are 825 MPa, 760 MPa, and 8%, respectively, for both the horizontal- and vertical-build directions [12]. When comparing the as-built (AB) values of the mechanical properties reported by the authors mentioned above to the ASTM F3001–14 values, the AB exceeds the strength requirement significantly but does not meet the ductility requirement.

As-built LPBF Ti6Al4V parts usually consist of columnar prior-beta grains filled with extremely fine acicular α' martensite. The fine α' martensite obtained during LPBF differs from conventional α' martensite in the sense that the spacing is tight, with many dislocations and twins obstructing dislocation movement and therefore reducing ductility. Columnar prior-beta grain boundaries favor intergranular failure, which decreases ductility along with the negative effects of mechanical anisotropy and limited fatigue life. The cooling rate strongly influences the prior-beta grain size and the morphology of the α phase [13], [14].

Stress relieving to avoid distortion is a critical part of the LPBF process. Residual stress and microstructure greatly influence the fatigue properties and crack growth of titanium alloys. Van Zyl et al. [15] measured residual stress near the top surface of LPBF Ti6Al4V as-built samples attached to the substrate. Residual stresses were tensile and in the range of 200–800 MPa. A stress of 800 MPa is only 30 MPa below the typical YS of annealed Ti6Al4V(ELI). Distortion can occur and cracks can initiate when removing the component from the substrate on which it was produced without prior stress-relieving heat treatment.

Therefore, stress relieving should be applied before removing the parts from the substrate. The standards AMS 2801 and SAE H81200 provide guidance on stress relief. Ter Haar and Becker (2020) found that, for stress-relieving temperatures above 560°C, 90% of the residual stress in LPBF parts was relieved and proposed a higher tempera-

ture of 650°C to give the best ductility. These findings are similar to those found for conventional Ti6Al4V stress-relieving temperatures given by Donachie (2000), who proposed that titanium stress relieving be done at temperatures between 480°C and 650°C for a time of one to four hours, resulting in more than 70% of the residual stress being relieved in the first hour. Ter Haar and Becker [16] also showed these stress-relieving temperatures (427-610°C) with long holding times could lead to the decomposition of martensite, but this resulted in embrittlement of the material due to fine β phase precipitates formed at α/α' grain boundaries.

The temperature at which SR occurs is not as critical as ensuring uniform temperature distribution upon cooling, especially from 480°C to 351°C. Stress relieving can be omitted if high-temperature annealing is carried out [2], [17].

To modify the LPBF microstructure, high-temperature annealing is employed. A well-known work by Vrancken et al. [7], in which many different heat treatments were investigated, found that no significant grain growth occurred for temperatures well below the beta transus. The fine α and β grain interfaces were found to limit grain growth. Only at 850°C did noticeable grain growth effects start to arise. When cooling from 850°C, because of the large fraction of α phase present, no significant change in microstructure was seen with a change in cooling rate. Contrary to conventional Ti6Al4V manufacturing methods, for which an increase in heat-treating temperature decreases the elongation with an increase in YS [2], with LPBF, the elongation values increase with an increase in annealing temperature at the expense of YS. Similarly, time spent below the beta transus had no significant effect on the grain growth, or, rather, no large grains were obtained, and the laminar structure remained. Even after considerable time, the laths were still relatively small, although they might have become less elongated [18], [19].

For LPBF, Yadroitsev et al. [20] showed that a globular microstructure could be obtained at higher temperatures and holding time. In their work, they obtained a globular microstructure by heating to 50°C below the beta transus, followed by a water quench. Ter Haar and Becker [21] suggested the optimal heat treatment for LPBF was a duplex anneal consisting of 910°C for eight hours, followed by a water quench and thereafter 750°C for four hours, followed by furnace cooling. Interestingly, they were able to produce a bi-modal microstructure with ultimate tensile stress (UTS) and elongation above 900 MPa and 15%, respectively. However, these two above-mentioned heat treatments are not feasible solutions for parts that cannot be machined or descaled because they also increase the post-processing time.

Some more recent approaches were from Sabban et al. [22], who obtained a globularized microstructure by cycling at between 975°C and 875°C with slow cooling between the cycles. Another team [23] was able to produce samples with quasi-equiaxed microstructures by using rapid heat treatment above the beta transus. Here, the refinement of prior-beta grain boundaries was reported for the first time.

Name	Ramp rate (°C/h)	Soak temp (°C)	Soak time (h)	Cooling rate (°C/h)
650-SR	200	650	3	Furnace
850-ANN	200	850	2	Furnace
895-ANN	200	895	2	Furnace
940-ANN	200	940	2	Furnace
650-SR&940-ANN	200	650, 940	3,2	Furnace
940-ANNGQ	200	940		
New-cycle	Described below		2	Gas quench

Table 1: Ti6Al4V heat treatment cycle times and temperatures.

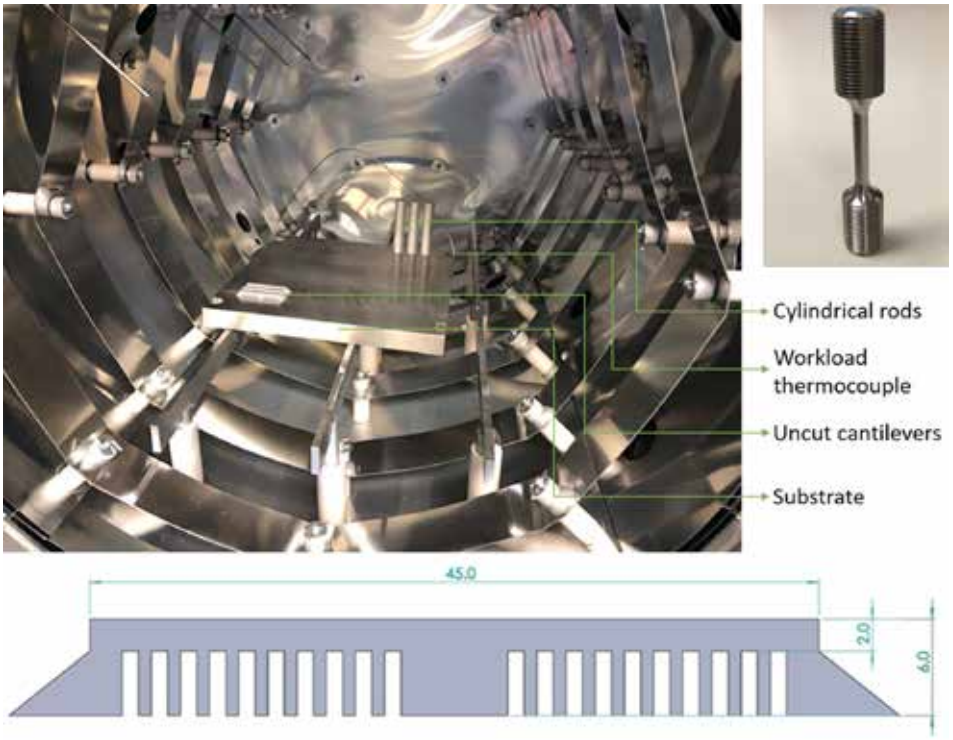

Figure 1: Ti6Al4V substrate with unmachined tensile rods and cantilevers inside the vacuum chamber. A typical machined tensile specimen is shown at the top right, and the cantilever specimen dimensions are at the bottom.

	Al	V	Fe	O	C	N	H
ASTM F 3001–14	5.5–6.5	3.5–4.5	<0.25	<0.13	<0.08	<0.05	<0.012
Current work	6.47	4.12	0.19	0.09	0.01	0.01	0.002

Table 2: Ti6Al4V(ELI) chemical composition and ASTM F 3001–14 requirements.

Baker et al. [24] proposed to the LPBF community that terminology that accurately describes the heat treatment history was needed. The term "high-temperature anneal" was proposed for fully lamellar microstructure. This need for new nomenclature confirmed the development and growth in the field of LPBF post-processing.

To avoid oxygen pick-up, heat treatments can be done in a vacuum. The heat-treatment standard for Ti6Al4V LPBF (ASTM F3301–18a, 4: "Thermal Post-Processing Requirements") specifies that heat treatments should be carried out according to the conventional standard: AMS 2801 "Heat treatment of Titanium Alloy Parts" [25]. In AMS 2801, it is specified that (Notes: 8.5) to avoid surface contamination, parts should not be exposed to air above 204°C. In addition, AMS 2801 requires descaling for parts heated above 538°C in an environment other than an inert atmosphere or vacuum. Consequently, due to the

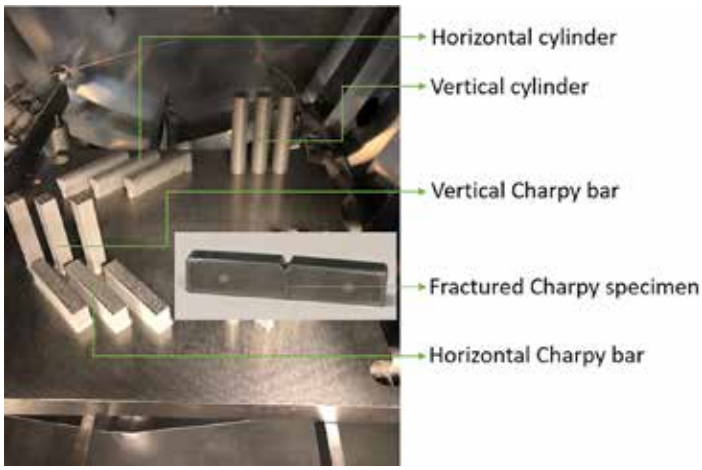

Figure 2: Charpy impact test specimen bars with a typical fractured specimen, as well as tensile test specimen cylinders on the substrate in the furnace chamber.

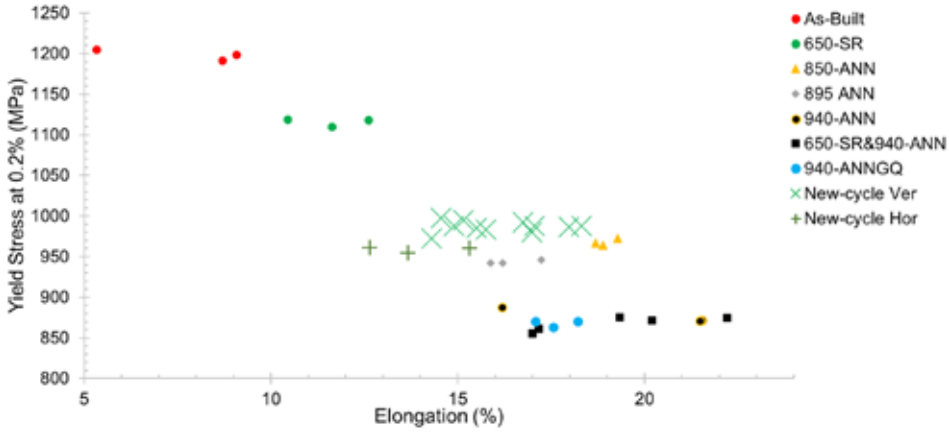

Figure 3: Yield stress vs % elongation for each cycle.

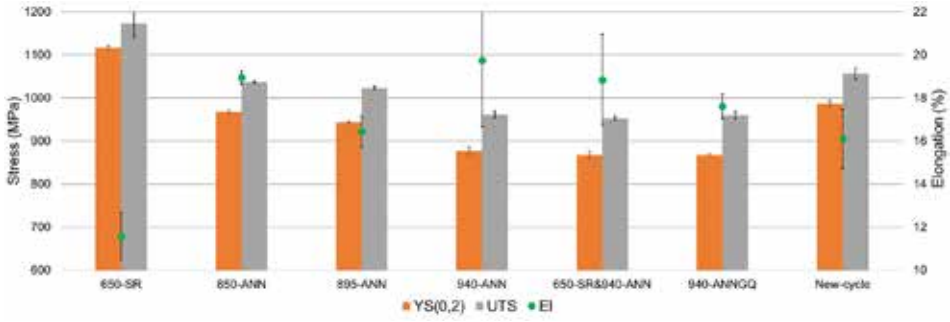

Figure 4: Engineering tensile properties of different heat treatments (stress on primary axis and elongation on secondary axis).

nature of LPBF, which has the advantage of directly delivering the net shape of a final part with complex geometry, conventional removal of surface oxides is normally not a feasible solution. Therefore, many of the suggested post-processes found in literature are not practical solutions for industries such as aerospace. While AMS 2801 specifies that stress relieving (SR) should consist of soaking at 593°C for two hours and annealing at 704°C for two hours, both occur above the temperature where descaling is required in the same standard. This implies that for LPBF of Ti6Al4V, only inert or vacuum atmospheres are suitable. Accordingly, AMS 2801 addresses this point by specifying that parts with net dimensions shall not be heated above 538°C in air or non-inert atmosphere furnaces unless coated with a protective coating, which is not always feasible with LPBF.

From the preceding discussion, vacuum heat treatment of titanium alloys is evidently the best solution because it has the benefits of not only removing contaminants from the atmosphere but also dissociating surface oxides. The use of vacuum heat treatment is also highly recommended by EOS to avoid the formation of alpha case on the surface of the parts [26].

Among the authors, the most common heat treatment that delivers good YS and elongation values (ASTM F3001–14: minimum of 825 MPa and 8%, respectively) seems to be a single-cycle heat treatment at 850-950°C followed by furnace cooling [7], [26], [27], [28], [29].

Despite their general acceptance, these thermal treatment cycles are still time-consuming and dependent on ramping rates, holding time/temperature and the cooling method used. Changes in these parameters result in different material properties; therefore, considerable care must be taken when altering these cycles. Typically, these heat-treatment cycles take more than nine hours to complete, implying that at least one day or night is needed for the parts to be thermally processed.

Therefore, the current study was undertaken to address the need for an alternative heat-treatment cycle that would reduce heat-treatment time and cost for the Centre for Rapid Prototyping and Manufacturing (CRPM) clients while still achieving the required properties. Assuming that the β grain growth is dependent on diffusion through its own grain boundary and that no considerable diffusion takes place below 750°C, a short time above this temperature is needed for the supersaturated elements to travel the length of the minor axis required for martensite to decompose into lamellar $\alpha + \beta$. This will retain the fine microstructure but lead to increased ductility. Yang et al. [14] were the first to show the development of the hierarchical structure of LPBF α' martensite (primary, secondary, ternary and quartic) caused by the thermal history. The hierarchical structure of acicular α' grains has an aspect ratio of between 10 and 20, with the minor axis of the primary α' and quartic α' being ~1-3 µm and 10-20 nm, respectively [14], [21]. The thinnest α martensite (quartic α') is smaller than 20 nm; thus, a very short diffusion path is present for the supersaturated atoms to travel within the grain and form the β phase on its grain boundary. Ti6Al4V has no significant diffusion below 750°C, but at 940°C the diffusion rate is approximately 0.07 µm^2/s and 0.05 µm^2/s for aluminum and vanadium in β titanium, respectively [30]. Even when considering the worst case, for large primary α' of 1 µm width and assuming only bulk diffusion of vanadium, the atoms at the grain center need to travel half the minor axis (0.5 µm). This equates to a rough estimate of ~10 s to traverse this distance. It shows the desired fine lamellar $\alpha + \beta$ morphology can be obtained in a very short time.

This rough calculation is based on bulk diffusion rates and does not consider factors such as the transient non-equilibrium chemical composition, as the supersaturated bulk initially rearranges atoms to precipitate in seed phases. At 882°C, the solubility of vanadium in α-Ti is zero; therefore, rapid rearrangement of atoms and β precipitation on the grain boundaries can be expected. Fine microstructural features like vacancies, high dislocation, and twin density will sig-

nificantly increase the diffusion rate due to grain boundary diffusion. Although the diffusion calculation is a simplified analysis, it shows that even for the slower bulk diffusion mechanism, only short times are needed at this temperature for the transformation, and it can be expected that the actual decomposition will be much faster. These short times reduce grain growth, leading to desirable fine microstructures as it increases material properties and can be particularly beneficial for fatigue and fracture mechanics. Additionally, since the sections of AM parts are generally smaller than industrial Ti6Al4V sections, there is no need for temperature soaking to ensure temperature uniformity. Therefore, the authors propose the use of a very short thermal treatment that would not only save time and money for the clients of the CRPM but would produce exceptional microstructural and material properties. This study compared these properties to those obtained through some of the most common post-heat treatments implemented in the AM industry.

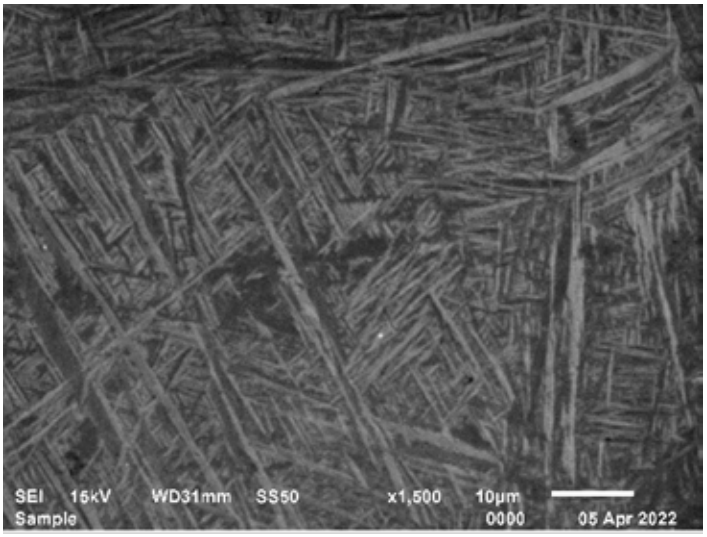

Figure 5: SEM micrograph of a cross-section of an as-built specimen in the XY plane.

2 METHODOLOGY

To compare the hypothesized cycle with conventional annealing (ANN) cycles found in literature, the cycles shown in Table 1 were investigated. Table 1 shows the heating parameters for each investigated cycle, hereafter referred to as 650-SR, 850-ANN, 895-ANN, 940-ANN, 650-SR&940-ANN, 940-ANNGQ and New-cycle, respectively.

The New-cycle consisted of ramping to 600°C at 300 °C/h, then ramping to 940°C at 637.5°C/h, followed by immediately ramping down to 600°C at 637.5°C/h. This was followed by a furnace cool to 400°C. On reaching 400°C, argon gas was introduced and kept stationary until 300°C was reached, whereafter, the quick-cooling fan was turned on for cooling to room temperature.

The vacuum heat treatment was carried out using a T-M Vacuum Products Inc. SS12/24–13MDX vacuum furnace operated consistently at vacuum levels < 0.01 µm Hg, which exceeds the recommended (AMS 2801B) level of 0.1 µm Hg. The vacuum chamber with the platform on which the Ti6Al4V(ELI) test specimens were loaded is shown in Figure 1.

Test specimens of Ti6Al4V(ELI) were produced in an EOS M290 DMLS machine at standard EOS Ti6Al4V process parameters laser power: 280 W, scanning speed: 1,300 m/s, hatch distance: 150 µm and layer thickness: 40 µm from powder with the chemical composition shown in Table 2. The equivalent diameters (by volume) of the powder particles were d10=31 µm, d50=49 µm and d90=75 µm.

For each of the above-mentioned cycles, three cantilever specimens (dimensions shown in the diagram in Figure 1) and three vertical test specimen rods (aligned with the Z-axis of the machine) were manufactured and then heat treated. After each cycle, the T-shaped cantilevers were cut from the baseplate and the deformation was measured to compare the effectiveness of stress relief for each cycle. This measurement indicated the magnitude of residual stress in the material after removal: the cantilever deflection is caused by the stress, which can deform the material after cutting the anchor points from the substrate. The amount of strain was shown to be directly proportional to the residual stress [31], [32], [33]. The cylindrical rods

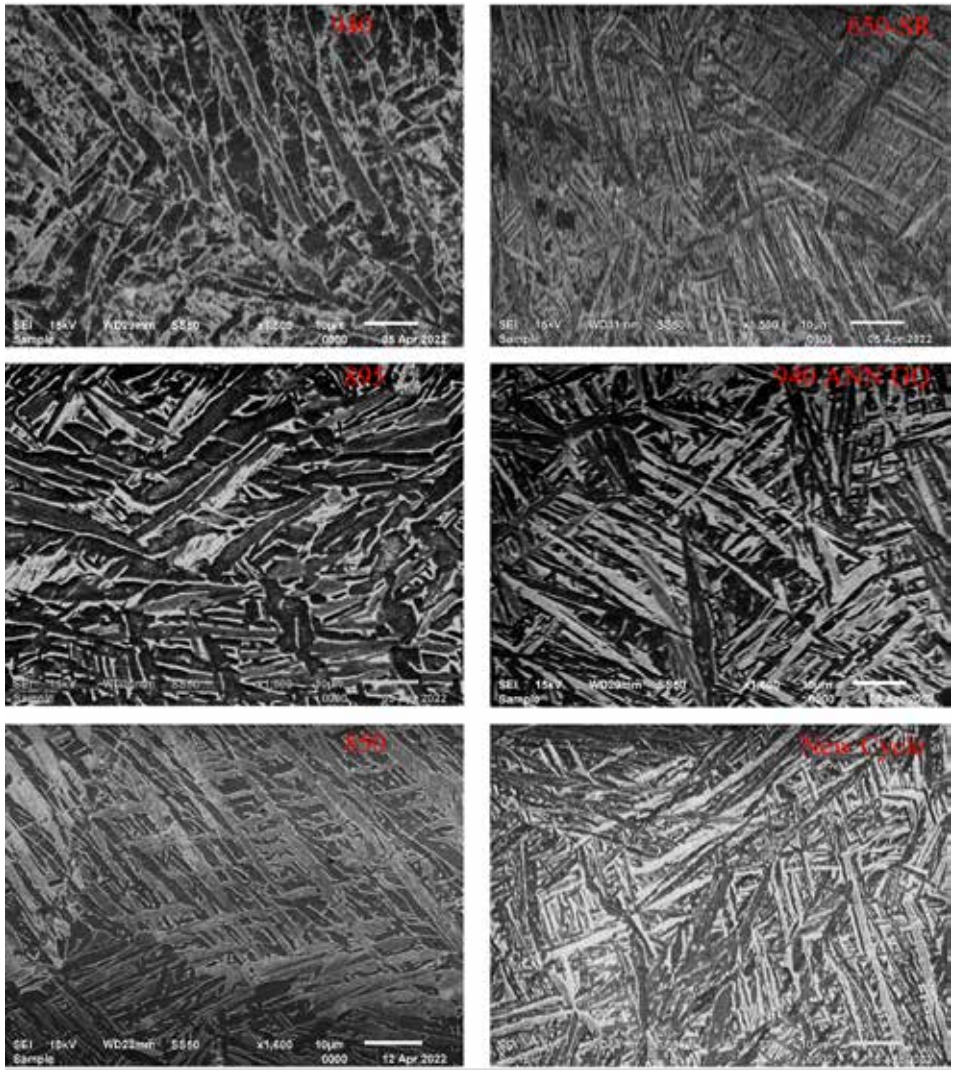

Figure 6: SEM micrographs of horizontal cross-sections (X-Y plane) showing the microstructures resulting from the corresponding heat treatment cycles.

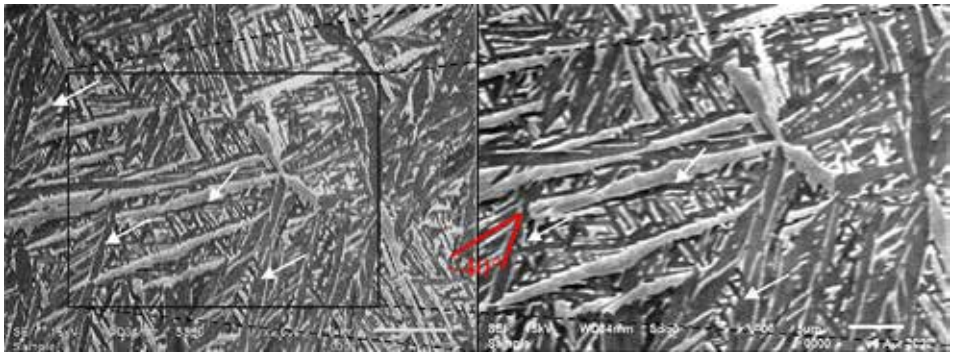

Figure 7: SEM micrographs of New-cycle showing alpha twin fragmentation indicated by arrows (left) and higher magnification of the square region (right).

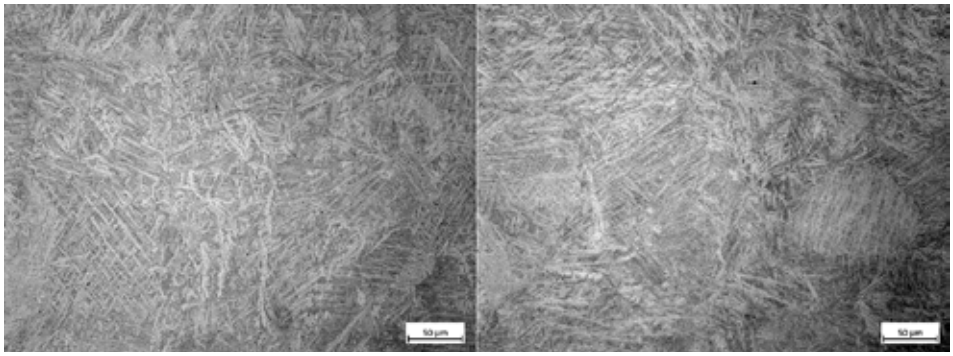

Figure 8: OM micrographs of 850-ANN (left) and New-cycle (right).

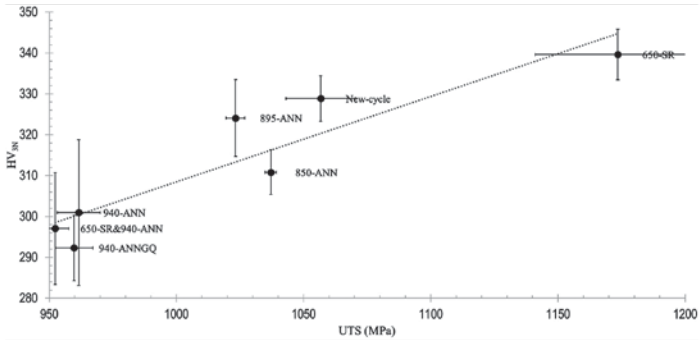

Figure 9: Microhardness vs UTS in the X-Y plane of the different cycles.

were machined according to ASTM E8 to produce tensile specimens with a gauge length of 16 mm. For microstructural analysis, the threaded ends of the tensile specimens were cut, polished, and etched with Kroll's reagent. A JEOL JSM-7800 F was used for scanning electron microscopy (SEM) and backscattered electron (BSE) imaging of the microstructure and fracture surfaces. The grain width of the lathes in the microstructures was measured with ImageJ software. To compare the impact of microstructural features of the different cycles, Vickers microhardness measurements were done at 3 N for 10 s on representative specimens from each type of heat treatment cycle.

Charpy impact testing was also done for the New-cycle, along with more tensile tests, resulting in 12 vertical tensile specimens from three different build orientations and treatments. Both the Charpy impact and tensile testing were performed on test specimens orientated in the vertical and horizontal building directions. The impact specimens were 100 × 10×10 mm with machined v-notches (see Figure 2). The 650-SR&940-ANN data was also obtained from five specimens, implying that the tensile properties and standard deviation data for the New-cycle and 650-SR&940-ANN were statistically more reliable.

3 RESULTS

None of the cantilevers used in the different heat-treatment cycles showed any deflection, confirming that all the cycles sufficiently relieved residual stresses. Figure 3 shows the yield stress versus the % elongation for each cycle.

Figure 3 shows the New-cycle performed well with 16.1% elongation and the highest yield stress of all the HTA specimens. For the 650-SR&940-ANN specimens, the additional stress-relieving cycle seemed to have no impact on the final material properties, which were very similar to those of the single 940-ANNGQ. This is shown more clearly in Figure 4, with the property values and standard deviations being similar for 940-ANN and 650-SR&940-ANN.

For the different HTA cycles, both the YS and UTS decrease with an increase in temperature. A significant increase in elongation is seen in the temperature range of 895-940°C, while a drop in elongation is seen between 850°C and 895°C, which has the same temperature range. This will be discussed in more detail later. The elongation of the 650-SR is the lowest because the alloy still has a martensitic microstructure (see Figure 5, Figure 6). On the other hand, the 650-SR specimens have the highest UTS, being 140 MPa above that of the 850-ANN specimens. For the 940-ANNGQ, the gas quench from the high temperature seemed to have had no impact on the strength when compared to furnace cooling from the same temperature. However, the 940-ANNGQ specimens did have slightly lower average elongation than the 940-ANN specimens.

Figure 5 shows the well-known, as-built fine martensite structure obtained by the LPBF process.

The corresponding microstructures of the other heat-treatment cycles can be seen in Figure 6. The AB and 650-SR microstructures are similar (Figure 5, Figure 6) in the sense that the fine needle-like microstructure is retained.

For the 940-ANNGQ cycle, the gas quench reintroduced high cooling rates, and its microstructure in Figure 6 shows that the 940°C anneal, followed by the higher cooling rate (gas quench), compared to the 940-ANN with furnace cool, did exhibit the same size of laths, but with sharper needle-like martensite shape.

For the New-cycle, some hierarchical α' substructures were still present, as shown in Figure 7. Here the smaller laths are clearly orientated to the larger ones indicating that the shape of the starting grain structure has been retained.

Figure 8 shows optical microscopy (OM) micrographs of cross-sections of the 850-ANN and the New-cycle specimens, which both display a fine $\alpha + \beta$ microstructure, although the 850-ANN is coarser due to the longer annealing time, which allowed the finer laths to be dissolved into adjacent grains (also compare the SEM images of 850-ANN and New-cycle in Figure 6). This New-cycle microstructure correlates with the EOS Titanium Ti64 Grade 23 material data sheet, which specifies that for a heat treatment of "120 min (±30 min) at 800°C (±10°C) measured from the part in vacuum (1.3×10^{-3} –1.3×10^{-5} mbar) followed by cooling under vacuum" the microstructure will consist of "fine alpha + beta ($\alpha+\beta$) phase" [26].

Heat treatment, which resulted in martensite decomposition into a fine alpha +beta microstructure, was between 800°C and 850°C. This is consistent with other findings [34], [35], [36]. It confirms that the fine microstructure obtained during the New-cycle was similar, although finer, than that of the other studies that used heat treatments between 800°C and 850°C. The finer $\alpha+\beta$ structure of the New-cycle promoted grain boundary strengthening and, hence, led to a higher yield stress than that of the 850-ANN. This was confirmed by the increased microhardness shown in Figure 9. The mean widths of the α laths in the microstructures obtained with the different heat treatments are given in Table 3.

The LPBF microstructure of Ti6Al4V(ELI) seemed to follow a Hall-Petch relationship in the sense that the fine martensitic grain structures showed the highest UTS, and as the size of the grains increased (as seen in Figure 6), the UTS and hardness decreased.

The microhardness trend seen in Figure 9 is similar to that reported by Malka-Markovitz et al. (2016), who reported that the hardness decreased as the martensite decomposed to α between the temperatures of 650°C (SR) and 850°C, but then from 850°C upward, the hardness increased as the α evolved into a bi-phasic $\alpha+\beta$ microstructure. Subsequently, a drop in hardness follows again with an increase in temperature as observed between 895°C and 940°C, which is due to the fine $\alpha+\beta$ microstructure that coarsened, resulting in a drop in hardness.

BSE images of the cross-sections of the specimens that have undergone the three annealing temperatures and the New-cycle are shown in Figure 10. A clear difference can be seen in the width and length of the laths resulting from the different cycles. The 940-ANN developed very long laths, with one long one clearly visible in the middle of the micrograph.

The microstructure in the XZ plane retains the columnar prior-beta grain morphology after the New-cycle heat treatment, as shown in Figure 11. The measured microhardness values were constant across the cross-section of the threaded section of a tensile specimen, as shown in Figure 11.

The New-cycle specimens had good impact toughness, as shown in Table 4. The lower impact toughness in the horizontal direction can be attributed to the directionality of the prior-beta columns leading to preferential crack propagation. It should be noted that, although the horizontal property values were lower than the vertical values for both the tensile and impact toughness, they exceeded the requirements of the Aerospace Specification Material for annealed Ti6Al4V(ELI) [37].

Fracture surfaces for both the vertical and horizontal impact specimens were the same. The fracture surfaces were flat and very smooth, with shear lips, as shown in Figure 12.

Similar to the grains' size reduction seen in the micrographs between the 940-ANN, 850-ANN and the New-cycle, the fractography of the tensile specimens showed the dimple sizes decreasing with temperature, as depicted in Figure 12. All specimens fractured in a ductile mode, and the fracture surface of the New-cycle showed the smallest dimples with a very uniform topography.

		850-ANN	895-ANN	940-ANN	New-Cycle
A lath width (µm)	mean	1.4	1.2	2.5	0.5
	stdev	0.6	0.5	0.8	0.3

Table 3: Width of alpha laths for 940-ANN, 895-ANN, 850-ANN and New-cycle.

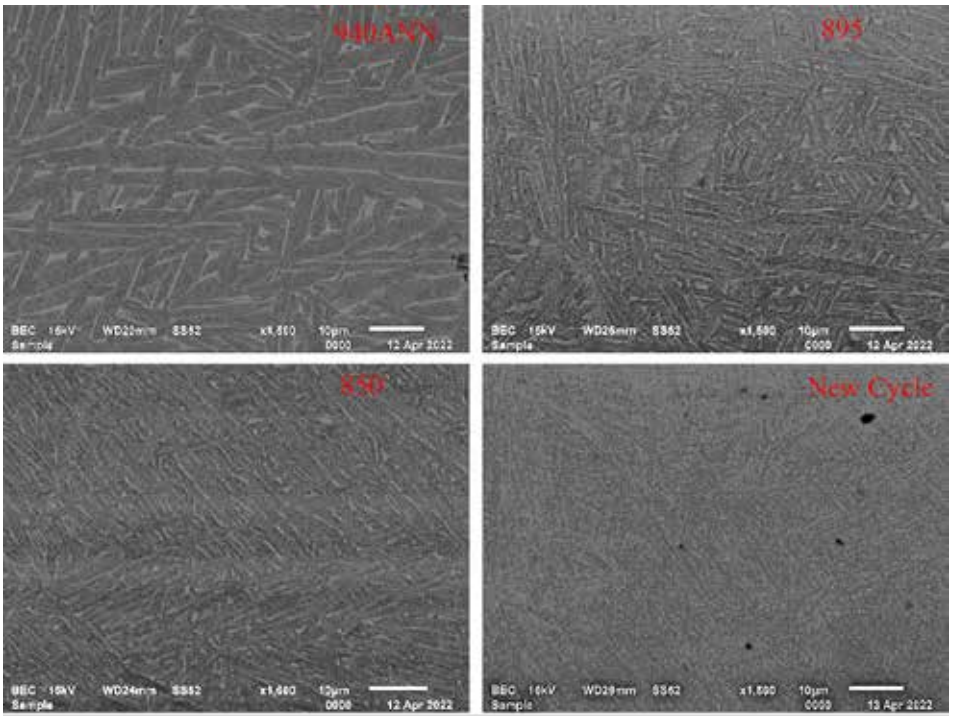

Figure 10: X-Y plane BSE images of 940-ANN, 895-ANN, 850-ANN and New-cycle (alpha = dark grey; beta = white).

Figure 11: Vertical (XZ plane) cross-section and microhardness across the threaded section of a New-cycle tensile specimen.

	Horizontal	Vertical
		
Impact toughness (J)	26.0 ± 2.0	33.3 ± 2.3

Table 4: V-notch impact toughness at 22°C of a specimen submitted to the New-cycle heat treatment.

4 DISCUSSION

4.1 Material properties

For the New-cycle, the vertically orientated specimens performed slightly better than the horizontally orientated ones, which had lower

elongation. This anisotropic nature of the tensile properties agrees with other findings [26], [35], [38], [39].

The vertical tensile properties reported by EOS for HTA at 800 for two hours are 980 MPa, 1050 MPa and 15% for $YS_{0.2}$, UTS, and elongation, respectively [26]. When considering the tensile results of the different heat treatments in Figure 4, the tensile properties resulting from New-cycle compare or exceed those reported by EOS and others [7], [21], [23], [26]. The 850-ANN shows an even higher elongation value with a slightly lower yield point, as shown in Figure 4. In general, all cycles showed good elongation, with the AB being 7.7%; an attributing factor can be the short interlayer time. All specimens were not built on one substrate but over multiple prints, i.e. for each different heat treatment, only three vertical rods were manufactured on the substrate. This results in a very short interlayer time, which has been shown to increase elongation due to coarsening of the α laths [40].

Ter Haar and Becker [21] showed that α-grain fragmentation during high-temperature annealing formed at twinning locations. During the New-cycle, fragmentation of α at twins occurred (see Figure 7), which, considering that the New-cycle was only kept at high temperatures for a brief time, confirmed that the fragmentation occurred rapidly at high temperatures. Some of the smaller ternary and quartic α had dissolved into the larger primary and secondary α grains. These laths, when compared to the AB microstructure shown in Figure 5, are larger and not as needle-like.

The grain structure of the New-cycle is considerably finer (submicron) compared to the other cycles and shows compositional contrast (Figure 10), verifying that the short holding time is sufficient for the supersaturated α' to decompose into a fine α+β phase. This agrees with Cao et al. [19], who showed that above 900°C, a time shorter than 0.5 h was needed to decompose the martensite. The alpha lath widths for 850-ANN and 895-ANN are very similar, explaining the similarities in tensile stresses (Figure 4), but the 895-ANN has reduced elongation as noted in the increase of hardness (Figure 9) when α evolved into a bi-phasic α+β microstructure [36]. Figure 11 shows good microstructural uniformity in the thick 12.5 mm sections. Although it is challenging to successfully build LPBF parts with large cross-sections due to residual stress, it was decided to simulate the New-cycle heat-treatment process to calculate the maximum temperature

difference for a 100 mm cube on the substrate. In a SolidWorks 2020 thermal study, the temperature vs. time profile was simulated while assuming that, for the vacuum heat treatment, the surface of the part was equal to the temperature measured by the thermocouples, and no conduction or convection occurred. For a simplified 100 mm cube, it was found that the maximum temperature difference would be ~40°C lower at the core, i.e. a maximum temperature of 900°C. However, this was not a concern, bearing in mind that the lower temperature anneals (895-ANN and 850-ANN) and 650-SR do give good tensile properties. It was noted that the microhardness measured on the cross-sections in the XZ plane was ~10 HV lower than that obtained in the XY plane. The New-cycle XY microhardness (329 HV) was below those of AB and 650-SR specimens of 352 HV and 340 HV, respectively, indicating that microstructural changes had occurred.

The New-cycle showed good impact toughness, with the values of the vertical specimens being considerably higher than other LPBF work in heat-treated conditions [41], [42], [43], [44]. This is an exciting finding and an area for further research, which might hold promising benefits for fatigue and fracture toughness.

Yonemura et al. [45], Cerda et al. [46] and De Knijf et al. [47] showed that, for rapid heating of 0.1 % C steel, the high dislocation density and carbon concentration of the initial ferrite was retained upon transformation to austenite. Higher dislocation density increases the work-hardening effect. Although the New-cycle can possibly lead to retention of the favorable high dislocation density and greater strength, none of the cycles showed any significant difference in the work-hardening rate. A significant change in dislocation density was found between AB and heat-treated specimens built in a similar EOS M280 machine at the CRPM by Muiruri et al. [47]. They reported dislocation densities for the AB, SR (650 3 h FC) and annealed (800 2.5 h FC) of 3.82×10^{-15}, 1.02×10^{-15} and 5.73×10^{-14} m^{-2}, respectively [48].

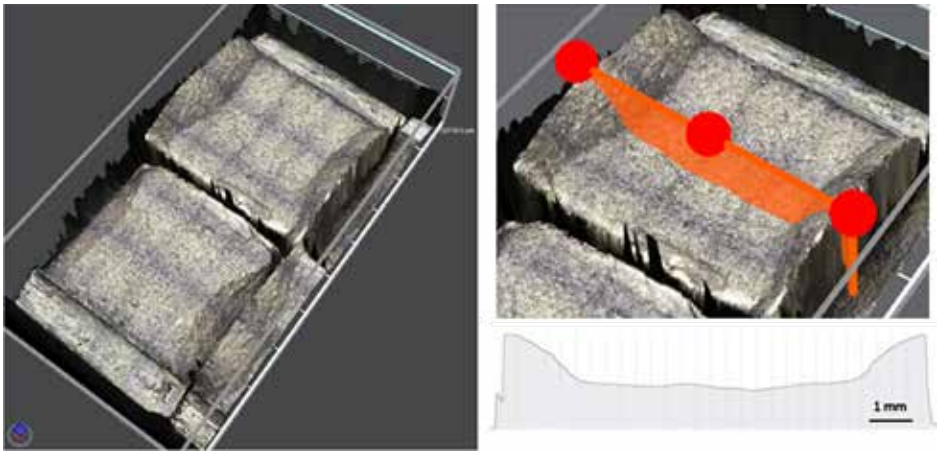

Figure 12: Fracture surfaces of vertical V-notch impact specimen (left) and corresponding depth profile (right).

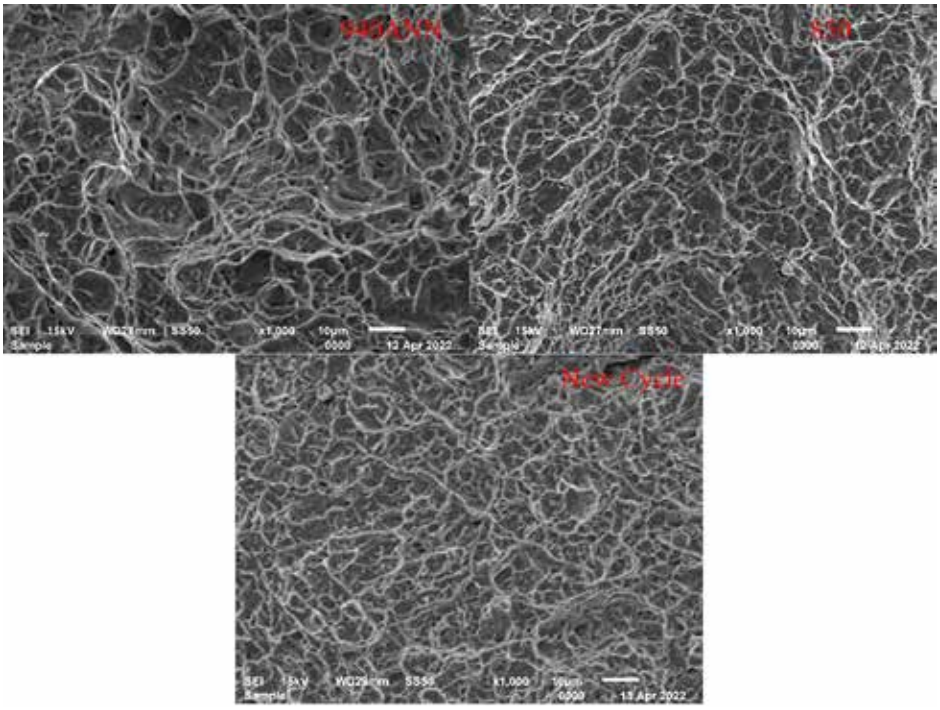

Figure 13: SEM fractographs of vertical tensile specimens heat treated at 940-ANN, 850-ANN, and New-cycle.

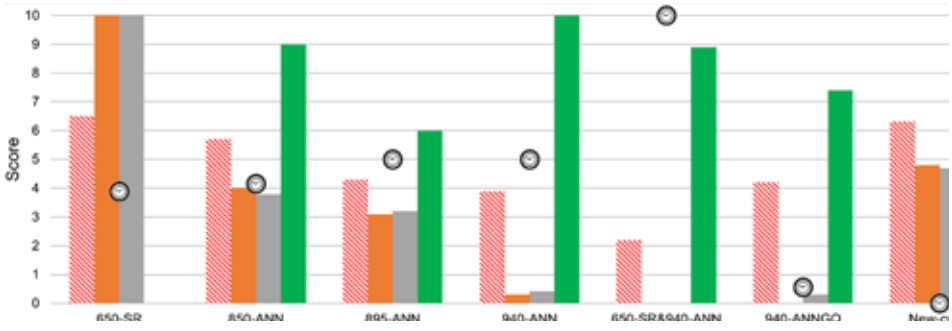

Figure 14: Calculated scores for each cycle.

4.2 Practical considerations: cycle

The New-cycle consisted of slow ramping to 600°C then more rapid heating to 940°C. No hold was present upon reaching 940°C. The initial ramp was slow to allow for stress relief and prevention of deformation. After the component had reached a temperature of 600°C after two hours, the slow ramp had also allowed for temperature uniformity and stress relief, which agrees with the cantilevers having shown no visible deformation and with the findings of Ter Haar and Becker [16], who showed that above 610°C almost all residual stress was relieved within the first five minutes. An additional contribution to this is the relatively small thicknesses of AM parts when compared to industrial parts. After the components had slowly reached temperatures of 600°C and above, the temperature distribution was uniform, and the temperature-dependent yield stress had been lowered so that subsequent rapid heating would not lead

to distortion. The ramp down was controlled and slowed to allow for more time in the temperature range where diffusion can occur (above 750°C) to ensure a more uniform temperature, irrespective of the furnace load. This results in consistency across different-sized builds, with consequent lower induced thermal stress and distortion. Since no air or water cooling is introduced, no descaling or machining is needed to remove oxides. To obtain better statistical reliability of the tensile properties of specimens submitted to the New-cycle, multiple LPBF builds were combined with multiple heat treatment cycles with a total of 15 tensile specimens.

4.3 Practical considerations: time, cost, and performance

Although most of these heat-treatment cycles produced excellent mechanical properties when compared to wrought Ti6Al4V (as found in [2]) and are all above the requirements of ASTM F3001–14, from a practical point of view, reduced cycle time and cost are of major importance. Therefore, each cycle was scored based on a very simple calculation: the maximum value of each property scored 10 points, while the lowest scored zero points, and anything in between was interpolated linearly between the maximum and minimum points. The scores and actual times of the cycles are shown in Figure 13.

In this scoring system, the 650-SR cycle only just beat the New-cycle and scored 0.2 more on average than the New-cycle, which is in second place, with the 850-ANN cycle in third place. Although the 650-SR cycle is in the first place, its low elongation should be noted, which is not clearly represented by this scoring system. Performing only a stress-relieving heat treatment does not optimize the mechanical properties for improved fatigue life performance. From a time-saving point of view, the New-cycle has a considerably lower cycle time of only four hours, with the 940-ANNGQ close on its heels. However, the latter has the disadvantage of creating larger grain structures and considerably lower yield stress and UTS. Therefore, because of the application of the New-cycle, parts for heat treatment can be received and delivered in half a working day, which has significant time- and cost-saving advantages.

5 CONCLUSION

The purpose of this article was to show that an alternative vacuum heat treatment cycle, considering all the technical aspects of AM, can be used to save time and money. The New-cycle offers a significant reduction in time (from 40 to 4 h), making it cost-effective to maximize the advantages of AM by offering parts that need no further descaling or machining. A yield stress of 987 MPa, higher than all other conventional treatments, was obtained while still having an elongation of 16%. This cycle delivered exceptional tensile and impact properties and sufficiently decomposed the as-built martensite into an $\alpha+\beta$ phase while retaining a very fine microstructure conducive to improved fatigue properties. In this case, the saying "less is more" rings true.

CREDIT AUTHORSHIP CONTRIBUTION STATEMENT

Dean Kouprianoff: Conceptualization, Methodology, Writing-Original draft preparation Willie du Preez: Conceptualization, Reviewing and Editing.

DECLARATION OF COMPETING INTEREST

The authors declare that they have no known competing financial interests or personal relationships that could have appeared to influence the work reported in this article.

ACKNOWLEDGEMENTS

The Collaborative Program in Additive Manufacturing (CPAM), (CSIR-NLC-CPAM-21-MOA-CUT-01), funded by the South African Department of Science and Innovation, is acknowledged for financial support. The Centre for Rapid Prototyping and Manufacturing (CRPM) is acknowledged for assistance and financial support.

REFERENCES

[1] T. Wohlers. Wohlers Report 2019. Additive Manufacturing and 3D Printing State of the Industry, Annual Worldwide Progress Report (2019).

[2] M.J. Donachie. Titanium: a technical guide ASM International (2000).

[3] M. Motyka. Martensite formation and decomposition during traditional and AM processing of two-phase titanium alloys–an overview. Metals, 11 (3) (2021), p. 481, 10.3390/met11030481.

[4] ASTM, 2022. Committee F42 on Additive Manufacturing Technologies. (Online) Available from: https://www.astm.org/COMMITTEE/F42.htm (Accessed on 29 March 2022).

[5] B. Blakey-Milner, P. Gradl, G. Snedden, M. Brooks, J. Pitot, E. Lopez, M. Leary, F. Berto, A. du Plessis. Metal additive manufacturing in aerospace: a review. Mater. Des., 209 (2021), Article 110008, 10.1016/j.matdes.2021.110008.

[6] ISO, 2022. Technical committees ISO/TC 261 Additive Manufacturing. (Online) Available from: https://committee.iso.org/home/tc261 (Accessed on 18 June 2022).

[7] B. Vrancken, L. Thijs, J.P. Kruth, J. Van Humbeeck. Heat treatment of Ti6Al4V produced by selective laser melting: microstructure and mechanical properties. J. Alloy. Compd., 541 (2012), pp. 177-185, 10.1016/j.jallcom.2012.07.022.

[8] P. Krakhmalev, G. Fredriksson, I. Yadroitsava, N. Kazantseva, A. du Plessis, I. Yadroitsev. Deformation behavior and microstructure of Ti6Al4V manufactured by SLM. Phys. Procedia, 83 (2016), pp. 778-788, 10.1016/j.phpro.2016.08.080.

[9] J.P. Kruth, M. Badrossamay, E. Yasa, J. Deckers, L. Thijs, J. Van Humbeeck. Part and material properties in selective laser melting of metals 16th International Symposium on Electromachining (ISEM XVI) edition:16, Shanghai, China (2010), pp. 19-23.

[10] I. Yadroitsev, I. Yadroitsava. Evaluation of residual stress in stainless steel 316L and Ti6Al4V samples produced by selective laser melting. Virtual Phys. Prototyp., 10 (2) (2015), pp. 67-76, 10.1080/17452759.2015.1026045.

[11] D. Agius, K.I. Kourousis, C. Wallbrink. A review of the as-built SLM Ti-6Al-4V mechanical properties towards achieving fatigue resistant designs. Metals, 8 (1) (2018), p. 75, 10.3390/met8010075.

[12] ASTM F3001–14, Standard Specification for Additive Manufacturing Titanium-6 Aluminum-4 Vanadium ELI (Extra Low Interstitial) with Powder Bed Fusion, ASTM International, West Conshohocken, PA, 2014, www.astm.org DOI: 10.1520/F3001–14.

[13] T.F. Broderick, A.G. Jackson, H. Jones, F.H. Froes. The effect of cooling conditions on the microstructure of rapidly solidified Ti-6Al-4V Metall. Trans. A, 16 (11) (1985), pp. 1951-1959.

[14] J. Yang, H. Yu, J. Yin, M. Gao, Z. Wang, X. Zeng. Formation and control of martensite in Ti-6Al-4V alloy produced by selective laser melting. Mater. Des., 108 (2016), pp. 308-318, 10.1016/J.MATDES.2016.06.117.

[15] I. Van Zyl, I. Yadroitsava, I. Yadroitsev. Residual stress in Ti6Al4V objects produced by direct metal laser sintering. South Afr. J. Ind. Eng., 27 (4) (2016), pp. 134-141, 10.7166/27-4-1468.

[16] G. Ter Haar, T. Becker. Low temperature stress relief and martensitic decomposition in selective laser melting produced Ti6Al4V. Mat. Des. Process Comm. (2020), 10.1002/mdp2.138.

[17] S. Leuders, M. Thöne, A. Riemer, T. Niendorf, T. Tröster, H.A. Richard, H.J. Maier. On the mechanical behaviour of titanium alloy TiAl6V4 manufactured by selective laser melting: fatigue resistance and crack growth performance. Int. J. Fatigue, 48 (2013), pp. 300-307, 10.1016/j.ijfatigue.2012.11.011.

[18] S. Cao, R. Chu, X. Zhou, K. Yang, Q. Jia, C. Voon, S. Lim, A. Huang, X. Wu. Role of martensite decomposition in tensile properties of selective laser melted

Ti-6Al-4V. J. Alloy. Compd., 744 (2018) (2018), pp. 357-363, 10.1016/j.jallcom.2018.02.111.

[19] S. Cao, Q. Hu, A. Huang, Z. Chen, M. Sun, J. Zhang, C. Fu, Q. Jia, C. Voon, S. Lim, R. Boyer, Y. Yang, X. Wu. Static coarsening behaviour of lamellar microstructure in selective laser melted Ti–6Al–4V. J. Mater. Sci. Technol., 35 (8) (2019), pp. 1578-1586, 10.1016/j.jmst.2019.04.008.

[20] I. Yadroitsev, P. Krakhmalev, I. Yadroitsava. Selective laser melting of Ti6Al4V alloy for biomedical applications: Temperature monitoring and microstructural evolution. J. Alloy. Compd., 583 (2014), pp. 404-409, 10.1016/j.jallcom.2013.08.183.

[21] G. Ter Haar, T. Becker. Selective laser melting produced Ti-6Al-4V: Post-process heat treatments to achieve superior tensile properties. Materials, 11 (1) (2018), 10.3390/ma11010146.

[22] R. Sabban, S. Bahl, K. Chatterjee, S. Suwas. Globularization using heat treatment in additively manufactured Ti-6Al-4V for high strength and toughness. Acta Mater., 162 (2019), pp. 239-254, 10.1016/J.ACTAMAT.2018.09.064.

[23] Z. Zou, M. Simonelli, J. Katrib, G. Dimitrakis, R. Hague. Refinement of the grain structure of additive manufactured titanium alloys via epitaxial recrystallization enabled by rapid heat treatment. Scr. Mater., 180 (2020), pp. 66-70, 10.1016/j.scriptamat.2020.01.027.

[24] A. Baker, P. Collins, J. Williams. New nomenclatures for heat treatments of additively manufactured titanium alloys. JOM, 69 (7) (2017), pp. 1221-1227, 10.1007/s11837-017-2358-y.

[25] ASTM F3301-18a, Standard for Additive Manufacturing – Post Processing Methods – Standard Specification for Thermal Post-Processing Metal Parts Made Via Powder Bed Fusion, ASTM International, West Conshohocken, PA, 2018, www.astm.org DOI: 10.1520/F3301-18A.

[26] EOS, 2022. EOS Titanium Ti64 Grade 23 Material Data Sheet. (Online) Available from: https://www.eos.info/03_system-related-assets/material-related-contents/metal-materials-and-examples/metal-material-datasheet/titan/ti64/material_datasheet_eos_titanium_ti64_grade23_premium_en_web.pdf (Accessed on 24 May 2022).

[27] D. Hollander, M. von Walter, T. Wirtz, R. Sellei, B. Schmidt-Rohlfing, O. Paar, H. Erli. Structural, mechanical and in vitro characterization of individually structured Ti–6Al–4V produced by direct laser forming. Biomaterials, 27 (7) (2006), pp. 955-963, 10.1016/j.biomaterials.2005.07.041.

[28] G. Kasperovich, J. Hausmann. Improvement of fatigue resistance and ductility of TiAl6V4 processed by selective laser melting. J. Mater. Process. Technol., 220 (2015), pp. 202-214, 10.1016/j.jmatprotec.2015.01.025.

[29] G. Longhitano, M. Arenas, A. Conde, M. Larosa, A. Jardini, C. de Carvalho Zavaglia, J. Damborenea. Heat treatments effects on functionalization and corrosion behavior of Ti-6Al-4V ELI alloy made by additive manufacturing. J. Alloy. Compd., 765 (2018), pp. 961-968, 10.1016/j.jallcom.2018.06.319.

[30] S. Semiatin, T. Brown, T. Goff, P. Fagin, R. Turne, J. Murry, D. Barker, J. Miller, F. Zhang. Diffusion coefficients for modeling the heat treatment of Ti-6Al-4V. Met. Mater. Trans. A, 35 (2004), pp. 3015-3018, 10.1007/s11661-004-0250-1.

[31] J.P. Kruth, J. Deckers, E. Yasa, R. Wauthlé. Assessing and comparing influencing factors of residual stresses in selective laser melting using a novel analysis method. Proc. Inst. Mech. Eng., Part B: J. Eng. Manuf., 226 (6) (2012), pp. 980-999, 10.1177/0954405412437085.

[32] Vrancken, B., Wauthle, R., Kruth, J.P., Van Humbeeck, J., 2013. Study of the influence of material properties on residual stress in selective laser melting. 24th International SFF Symposium – An Additive Manufacturing Conference, SFF 2013. p.393–407.

[33] D. Buchbinder, W. Meiners, N. Pirch, K. Wissenbach, J. Schrage. Investigation on reducing distortion by preheating during manufacture of aluminum components using selective laser melting. J. Laser Appl., 26 (1) (2014), 10.2351/1.4828755.

[34] J. Lee, M. Lee, S. Yeon, D. Kang, T. Jun. Influence of heat treatment and loading direction on compressive deformation behaviour of Ti–6Al–4V ELI fabricated by powder bed fusion additive manufacturing. Mater. Sci. Eng.: A (2022), p. 831, 10.1016/j.msea.2021.142258.

[35] Y. Liu, H. Xu, B. Peng, X. Wang, S. Li, Q. Wang, Z. Li, Y. Wang. Effect of heating treatment on the microstructural evolution and dynamic tensile properties of Ti-6Al-4V alloy produced by selective laser melting. J. Manuf. Process., 74 (2022), pp. 244-255, 10.1016/j.jmapro.2021.12.035.

[36] D. Malka-Markovitz, A. Katsman, A. Shirizly, M. Bamberger. Microstructure and mechanical properties of heat treated selective laser melting manufactured Ti-6Al-4V. J. Int. Sci. Publ. Mater. Methods Technol. (Online), 10 (2016), pp. 495-505.

[37] ASM Aerospace Specification Metals Inc. Titanium Ti6Al4V (Grade 5), ELI, Annealed. Available online: https://asm.matweb.com/search/SpecificMaterial.asp?bassnum=MTP643 (accessed on 27 May 2022).

[38] G. Ter Haar, T. Becker. The influence of microstructural texture and prior beta grain recrystallisation on the deformation behaviour of laser powder bed fusion produced Ti–6Al–4V. Mater. Sci. Eng.: A, 814 (2021), Article 141185, 10.1016/j.msea.2021.141185.

[39] T. Voisin, N. Calta, S. Khairallah, J.P. Forien, L. Balogh, R. Cunningham, A. Rollett, Y. Wang. Defects-dictated tensile properties of selective laser melted Ti-6Al-4V. Mater. Des., 158 (2018), pp. 113-126, 10.1016/j.matdes.2018.08.004.

[40] W. Xu, E.W. Lui, A. Pateras, M. Qian, M. Brandt. In situ tailoring microstructure in additively manufactured Ti-6Al-4V for superior mechanical performance. Acta Mater., 125 (2017), pp. 390-400, 10.1016/j.actamat.2016.12.027.

[41] A. Singh, F. Yang, R. Torrens, B. Gabbitas. Heat treatment, impact properties, and fracture behaviour of Ti-6Al-4V alloy produced by powder compact extrusion. Materials, 12 (23) (2019), p. 3824, 10.3390/ma12233824.

[42] L. Monaheng, W. du Preez, C. Polese. Towards qualification in the aviation industry: impact toughness of Ti6Al4V(ELI) specimens produced through laser powder bed fusion followed by two-stage heat treatment. Metals, 11 (11) (2021), p. 1736, 10.3390/met11111736.

[43] P. Manikandan, V.A. Kumar, P.I. Pradeep, R. Vivek, K. Sushant, G. Sudarshan, S.V.S. Narayana Murthy, D. Sivakumar, P. Ramesh Narayanan. On the anisotropy in room-temperature mechanical properties of laser powder bed fusion processed Ti6Al4V-ELI alloy for aerospace applications. J. Mater. Sci., 57 (2022), pp. 9599-9618, 10.1007/s10853-022-07032-y.

[44] A. Muiruri, M. Maringa, W. du Preez. Effects of stress-relieving heat treatment on impact toughness of direct metal laser sintering (DMLS)-produced Ti6Al4V (ELI) parts. JOM, 72 (2020), pp. 1175-1185, 10.1007/s11837-019-03862-5.

[45] M. Yonemura, H. Nishibata, T. Nishiura, N. Ooura, Y. Yoshimoto, K. Fujiwara, K. Kawano, T. Terai, Y. Inubushi, I. Inoue, K. Tono, M. Yabashi. Fine microstructure formation in steel under ultrafast heating. Sci. Rep., 9 (2019), p. 11241, 10.1038/s41598-019-47668-6.

[46] F. Cerda, C. Goulas, I. Sabirov, S. Papaefthymiou, A. Monsalve, R. Petrov. Microstructure, texture and mechanical properties in a low carbon steel after ultrafast heating. Mater. Sci. Eng., 672 (2016), pp. 108-120, 10.1016/j.msea.2016.06.056.

[47] D. De Knijf, A. Puype, C. Föjer, R. Petrov. The influence of ultra-fast annealing prior to quenching and partitioning on the microstructure and mechanical properties. Mater. Sci. Eng., 627 (2015), pp. 182-190, 10.1016/j.msea.2014.12.118.

[48] A. Muiruri, M. Maringa, W. du Preez. Evaluation of dislocation densities in various microstructures of additively manufactured Ti6Al4V (ELI) by the method of X-ray diffraction Materials, 13 (2020), p. 5355, 10.3390/ma13235355.

ABOUT THE AUTHORS

Dean Kouprianoff and Willie du Preez are with the Centre for Rapid Prototyping and Manufacturing, Faculty of Engineering, Built Environment and Information Technology, Central University of Technology, Free State, South Africa.

SHARE YOUR EXPERTISE WITH OUR READERS

Have a technical paper or other work with an educational angle? Let Thermal Processing publish it.

Each issue, Thermal Processing offers its readers the latest, most valuable content available from companies and institutions, as well as critical thoughts on what this information means for the future of the heat-treat industry.

Our readers want your expertise and we want to share it.

Thermal Processing is your trusted source for information and technical knowledge about the heat-treat industry.

Contact the editor, Kenneth Carter, at editor@thermalprocessing.com for how you can share your expertise with our readers.

Thermal processing

COMPANY PROFILE ///

ALGAS-SDI

APPLYING RELIABLE CLEAN-ENERGY SYSTEMS

FOR COMMERCIAL, INDUSTRIAL, AND UTILITY CUSTOMERS

Algas-SDI makes products and systems for the deployment of clean fuels worldwide, as well as designing and manufacturing LP-gas vaporizers, industrial process heating burners, synthetic natural gas systems, and more.

By KENNETH CARTER, Thermal Processing editor

What would you do if supply chain issues during a pandemic kept you from shipping your product because one final, crucial part wasn't available? If you're Algas-SDI, then you make that crucial part yourself.

The natural gas replacement systems and vaporizers that Algas-SDI had been producing for years use packaged burners to heat their process, but COVID created an enormous supply chain constraint in 2021, according to Ad de Pijper, director of the combustion products value stream division, at Algas-SDI.

"We could not get burners, so we had a lot of equipment sitting on our shop floor — basically, everything was ready except there was a hole in the product where a burner should go," he said. "So, in 2021, we decided to make our own burners. That's how we started our journey in the burner industry. Once we started making burners for ourselves, other people — since we're very close to many players in the industry — they said, 'Hey, you want to sell your burners to us?' And we said to ourselves, 'Well, if there is a need, let's start a business to fill this need, so that's what we did.' So, from a burner perspective, we've been at it about two and a half years. But the company itself has more than a 90-year background."

MAJOR ACHIEVEMENT

To put that monumental business change into focus, Algas-SDI went from deciding to add a brand-new product to their catalog to shipping it in eight months, according to de Pijper.

"We literally had nothing," he said. "We had no designs; we had no supply chain; we had no team to support the burner business. We received our first order late 2021, and we shipped 36 burners in April of the following year. We went from nothing to shipping our first order for 36 burners in eight months. To put that in perspective: Other companies that are more established, some with more than 100 years of experience building and selling burners, had a lead time of nine to 12 months."

Part of Algas-SDI's journey back into the heat-treat industry stemmed from the company's desire for others in the sector to not have to go through the same struggles where people couldn't get product or those products took an exorbitant amount of time to get, according to de Pijper.

"We are very focused on short lead times and customer service, and that's really because of the pain that we felt ourselves," he said. "We were trying to get burners for our own equipment. The lead time was too long, but we also would not get good customer service because these other companies, they were struggling getting product out the door. And again, because of our long history and experience with Eclipse, which now, of course, is owned by Honeywell, it was a no-brainer for us to also go into the heat-treat industry."

DIRECT-FIRED BURNERS

Algas-SDI's current focus is on direct-fired burners — with and without integral blowers for combustion air — for medium- to high-temperature processes, according to de Pijper.

"That's what we offer," he said. "The smallest burner we have has a capacity of 150,000 BTU/hr. The largest standard burner we sell is 7.5 million BTU/hr. Those are the products that we're offering right now, but our development team is working on a radiant tube fired burner we plan to release later this year."

Algas-SDI's TRUXX CNG/RNG decompression unit for pipeline injection with a heating system that includes the Phoenix SH burner. (Courtesy: Algas-SDI)

'SIMPLE AND EASY-TO-USE'

Adding burners to its catalog is just one of the ways Algas-SDI strives to take some of the complications out of how its customers run their operations, according to de Pijper.

"Everything we do is about making products that are simple and easy-to-use for our commercial, industrial, and utility customers," he said. "That's driven by supplying high-quality products with dependable lead times. Not necessarily just short lead times, because some

"We listen to customers and by doing that well, we evolve with the industry. We're not trendsetters. We do not lead with the latest technology, but to make sure we're offering the right product and service, we are customer focused."

Algas-SDI's new facility is dedicated to its future growth and expansion. (Courtesy: Algas-SDI)

people don't want it quickly. They just want to know that they get the product when they need it."

Being approachable to customers is a point that de Pijper is particularly proud to emphasize.

"We listen to customers and by doing that well, we evolve with the industry," he said. "We're not trendsetters. We do not lead with the latest technology, but to make sure we're offering the right product and service, we are customer focused. We do this by having a lot of in-person interactions with our customers. One way to do that is by providing training. We train end users; we train operators; we train engineers. In-person training does two things: One, is it'll help improve brand loyalty, because our customers know us personally. But it also allows us, by listening, to get customer feedback on our products. This allows us to renew and improve our products continuously and quickly. We're just built that way."

Listening to feedback is important because it pushes the company to continuously improve its product in a meaningful way, according to de Pijper.

"All feedback is a gift, good and bad, because it's feedback that you get that you can use to make the product better, so customers have a better experience next time," he said.

Algas-SDI's Simple Heat (SH) packaged burner can be configured for just about any application. (Courtesy: Algas-SDI)

DEVELOPING CUSTOMER RELATIONSHIPS

Asking for feedback is also important when developing a new customer relationship. It starts with the goal to make it as easy as possible for Algas-SDI's customers to choose a product that works best for them, according to de Pijper.

"Making things easier for our customers is our goal — even when we quote," he said. "Instead of asking a lot of questions, we listen to the customer's needs, and we say, 'OK, we heard you. We think this is what you need, and these are the assumptions that we made.' We get it right most of the time, but if we don't, customers comment on the assumption, and we send them a new quote right away."

"When we hire new people, I always say, 'Just realize this: This is a manufactured product, so stuff is not always going to work the way you expect," de Pijper said. "It could be a supplier issue. It could be an assembly issue. It could even be that the customer is not using the product the way we expected them to, but whatever happens, if the customer has an issue, it will be our priority to solve the problem and have them up and running as quickly as possible. That means you're asking questions that help you decide what the next action is to help the customer. If we must replace the product, then replace the

product. We can do our investigations later, and that is when we are going to learn from this situation and make our product even better, but we cannot let that get in the way of having the customer get back to run their process."

SMALL CATALOG

Part of what makes the Algas-SDI Combustion Products team good at what it does is because it keeps the catalog of products small, according to de Pijper.

"We have a very small catalog, and we did that on purpose because focus is critical when customers expect short response times." he said. "When I started my career in the combustion industry in the early '90s, lead times for most products was four to six weeks, and personable customer service was the norm. I want to go back to that time. I do not want people to get used to long lead times. I don't want people to get used to customer service not picking up the phone. I want to go back to that time because I truly believe that's what customers and end users want and need."

Although Algas-SDI has only recently been more directly involved in the heat-treat industry, the company has been manufacturing products and systems to deploy clean fuels globally since 1932.

In that vein, de Pijper said he expects the company will continue to do this as the use of fuel gases for commercial, industrial, and utility applications changes.

"Natural gas is not going away, at least not for the foreseeable future," he said. "For now, Algas-SDI will continue to supply our equipment for fossil fuel applications, but there are obviously environmental concerns, so I expect that there will be a transition to renewable and non-carbon-based fuels — likely renewable natural gas, propane, ammonia, and hydrogen. This switch to new fuels cannot be done immediately; it'll be a transition."

Algas-SDI's Velocity Heat (VH) direct fired burners are perfect for medium- to high-temperature furnace applications. (Courtesy: Algas-SDI)

And with that transition, the burners that use that gas will also need to adapt as well, according to de Pijper.

"When the molecule changes, the combustion properties change, and so does the burner and fuel supply and control components." he said. "My vision is that Algas-SDI will be the company that can provide the products to support this transition to renewable fuels."

MORE INFO algas-sdi.com

ADVERTISER INDEX ///

Q&A /// INTERVIEW WITH AN INDUSTRY INSIDER

JAMES P. ADAMS /// EXECUTIVE DIRECTOR/CEO /// METAL POWDER INDUSTRIES FEDERATION AND APMI INTERNATIONAL

"PowderMet and AMPM will bridge together the industries as we come together under one roof to advance the industry."

PowderMet2024, in Pittsburgh, Pennsylvania, June 16-19, will be a hub of technology transfer for professionals from every part of the powder metallurgy and metal additive manufacturing industry. James P. Adams, executive director and CEO of Metal Powder Industries Federation and APMI International, recently discussed with Thermal Processing what attendees can expect from this popular conference.

What about the Pittsburgh venue made it ideal for the 2024 show?

It has been 30 years since we last held our conference in the "Steel City." Pittsburgh is within driving distance to the majority of powder metallurgy (PM) and metal additive manufacturing (AM) component manufacturers, material suppliers, equipment manufacturers, and service providers, allowing even more professionals access to this premier event. The region is also a hub for carbide manufacturing. As the hundreds of bridges connect the city, PowderMet and AMPM will bridge together the industries as we come together under one roof to advance the industry.

How will this year's show differ from what attendees experienced in Las Vegas last year?

For this year's conference, we took the PowderMet and AMPM conferences, put everything into a big box, shook it up, and made some great changes to this year's program.

The Design Experience general session has been opened to all conference delegates, providing more visibility to these award-winning parts. The objectives of the conferences are to explore materials advances, assist in the transfer of technology, and investigate new developments to continue growth. For the first time, daily tutorials focused on press and sinter, metal injection molding (MIM), and metal additive manufacturing will be offered to encourage cross training and introduction of these exciting technologies. A Carbide Forum is offered for delegates to explore and learn more about these niche materials.

We have implemented more ways to allow for networking and collaboration among delegates through all areas of the conference, including our usual opening night reception, the PM Evening Alehouse, and the Consolidation Celebration: "Take me out to the ballgame." For more details on the program, schedule, and sessions, visit our website below.

If I were a first-time attendee, what should I expect from this year's show?

As a first-time attendee, you should expect to be surrounded by like-minded individuals who share the common goal of continuing to advance the PM and AM industries through education, networking, and collaboration.

What subjects should I expect presenters to address?

The technical program was developed and organized by industry experts. Professionals in both PM and AM joined forces to collaborate and compile the individual sessions. With 200 presentations by industry experts from around the world, topics will cover all aspects of the technology. Additionally, conference proceedings will capture the technology transfer for future reference.

Programming is aligned to provide an excellent experience for first timers and seasoned attendees alike. Numerous networking opportunities are intentionally designed for interaction with other attendees, speakers, and exhibitors. For 2024, we have over 40 future engineers with us courtesy of student conference grants from the National Science Foundation (NSF), and Center for Powder Metallurgy Technology (CPMT).

What kind of networking opportunities will be available for attendees?

PowderMet provides networking at every corner. From the time you arrive, you will meet with old friends and make new acquaintances at the opening reception. Once the conference kicks off, there are a plethora of opportunities to network and make those meaningful connections. From the exhibit hall to the luncheons, to the Consolidation Celebration and everything in between, the contacts you make will become lifelong friends.

What about the conference will make it feel unique to the Pittsburgh location?

Pittsburgh is such an amazing city, and we are excited to bring our delegates back. We will be submerged in the culture of Pittsburgh throughout the conference. You will get a taste of Pittsburgh through our food and beverage events. We will get a true Pittsburgh experience during our Consolidation Celebration as we head to PNC Park for a major league baseball game, where the group will cheer on the Pittsburgh Pirates as they take on the Cincinnati Reds.

What are you personally looking forward to at this year's show?

As always, I look forward to meeting face-to-face with the industry and having the group together under one roof. The energy that you can get from meeting with your colleagues and peers in the same room is unmatched. I'm also very excited about some new elements that we will be introducing into the conference this year that will continue to build and harvest those networking opportunities and engagement among delegates.

MORE INFO PowderMet2024.org

DMP CryoSystems®

DMP Cryosystems offers several types of cryogenic processors. The **CryoFurnace** is the first and only cryogenic processor available with a temperature range of +1200˚F to –300˚F. The **CryoTemper** which has a temperature range of +550°F to –300°F, continues to set the standard for which all other systems are judged. It remains the most efficient and versatile cryogenic tempering processor available in today's market. The **CryoFreezer**, offers a temperature range of ambient to –300°F. Each temperature range/model can be built as a front load swing, front load guillotine, or top load chest style chamber. We have placed equipment around the world, so various incoming main power preferences are also available.

MULTIPLE TEMPERS. ONE CYCLE.

+1200°F to -300°F

CRYOFURNANCE

CRYOTEMPER

CRYOFREEZER

INQUIRE TODAY!

Phone
1(800)851-7302

Website
www.cryosystems.com

Our leading edge vacuum technology provides precise control and repeatability for consistently superior parts.

Vacuum Heat Treating & Brazing Services

Annealing • Aging • Carburizing • Nitriding • Stress Relieving • Degassing • Brazing • Harden and Temper
Sintering • Solution Treat and Age (STA) • Homogenizing • Creep Forming • Hydriding / Dehydriding

Solve your toughest thermal processing challenges by utilizing our brain-trust of metallurgists, chemists and engineers.

- Over 70 vacuum furnaces – lab-sized to 48 feet long
- Argon, nitrogen and helium quenching up to 20 bar
- Operating range of -320°F to +3,600°F
- On-site metallurgical testing lab
- 24/7 Operations

SOLAR ATMOSPHERES
Celebrating 40 YEARS

1-855-WE-HEAT-IT
solaratm.com

Nadcap Administered by PRI ACCREDITED HEAT TREATING NONDESTRUCTIVE TESTING
ISO9001 AS9100 Registered
MedAccred Heat Treating

Eastern PA • Western PA • California • South Carolina • Michigan